Summer 8-4-2011

The Effect of Tool Rotation Speed and Clamping on Deformation in Friction Stir Welded 6061-T6511 Aluminum Extrusions

Travis Lee Smith
University of New Orleans, tsmith2@uno.edu

The Effect of Tool Rotation Speed and Clamping on Deformation in Friction Stir Welded 6061-T6511 Aluminum Extrusions

A Thesis

Submitted to the Graduate Faculty of the
University of New Orleans
in partial Fulfillment of the
requirements for the degree of

Master of Science
in
Engineering
Mechanical Engineering

by

Travis Lee Smith

B.S. University of California at Berkeley, 2003

August 2011

Acknowledgement

I would like to primarily thank Professor Paul Schilling for supporting the testing, providing guidance, and editing the manuscript. Professors Paul Herrington and Melody Verges were further members of my thesis committee.

The Friction Stir Welding and measurements would not have been possible without Duy Pham's assistance, Dr. Tim Li's guidance, and Randy Brown's support.

Members of Dr. Schilling's lab - Will, Daniel, and George – performed all of the microstructure testing.

Table of Contents

List of Figures

List of Tables

ABSTRACT

Friction Stir Welding (FSW) was used to perform Bead on Plate (BOP) welds on 6061-T6511 aluminum extrusions. Using a DOE approach, tool rotation speed, clamp spacing, and clamping force were altered to ascertain their effects on distortion in the welded panels. Mechanical forces were monitored during the weld process. Both linear and out of plane distortion were measured on the welded extrusions. The Vickers hardness of the weld nugget was measured. The effect of each parameter on weld distortion was discovered and the mechanism of this link was suggested.

Keywords: Friction Stir Welding - Distortion – Shrinkage - Welding Parameters – Clamping – DOE – Aluminum – 6061 T-6511 – Extrusions - Hardness – Weld Power

1.0 Introduction

The aerospace – and increasingly – the naval industries, manufacture structures from thin sectioned aluminum (1), (2). Although the aerospace industry has long used thin aluminum sections, they are typically joined with rivets. Next generation naval vessels are turning to aluminum for faster, more fuel efficient vessels. Thin walled structures can be made from uniform plate, onto which are subsequently added stiffening members, as shown in figure 1.0.1. Thusly, high performance structures can be made both lightweight and of high strength, and stiffness.

Figure 1.0.1: High performance thin walled structure – single thin plate with subsequently joined stiffeners

Stiffening members can be integral to thin walled structures by incorporating them into extrusions which are joined together to form the structure (3).

Figure 1.0.2: High performance thin walled structure – integrally extruded stiffeners

Although the use of extrusion stiffened panels can create novel design opportunities, the practical limit in the cross sectional area of extrusions requires many extrusions to be joined together to make a large structure. If the joining technique is to be welding, careful consideration must be paid to distortion. This is easily surmountable if say, only the finished dimension of the structure is required to be precise, but many structures have multiple geometric precision requirements (for example, each stiffening extrusion element may interface with a secondary structure).

This study seeks to understand the effects of Friction Stir Welding (FSW) tool rotation speeds and clamping schemes on distortion in thin sectioned aluminum extrusions. A Design of Experiments (DOE) approach will be used to determine this link. Microstructural analysis will help to strengthen this understanding.

2.0 Literature Review

2.1 Friction Stir Welding

FSW is a solid state welding process, used to join metallic and thermoplastic solids, that was invented at The Weld Institute in 1991 (4). FSW uses a rotating tool (pin tool) plunged into and then traversed across a joint to fuse two or more members together. A combination of rotation speed and axial force directed into the weld joint (termed forge force) creates frictional heat, which plasticizes the material around the tool. With rising temperature, the material strength of the metal around the pin tool decreases until the shear stress applied by the pin is sufficient to plastically deform the metal. Thus the total energy requirement of a FSW is the combination of friction and deformation heat. After plunging, and once suitable heat has built up, the pin tool (basic cross section in figure 2.1.1) is traversed along the weld.

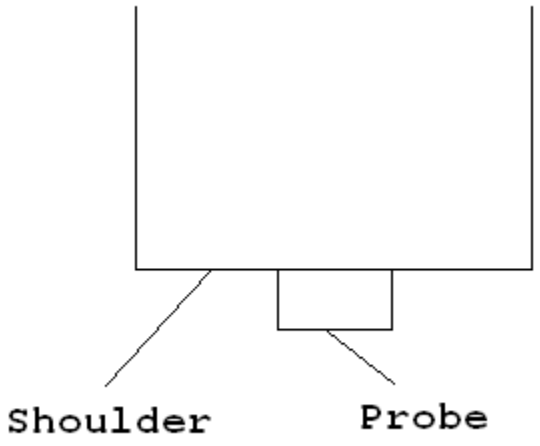

Figure 2.1.1: Basic FSW pin tool terminology

The forge force acting over the area of the shoulder serves to compress and consolidate the weld nugget. The rotating probe serves to break up the interface and mix the two parts together (5). Basic FSW geometry and terminology are shown in figure 2.1.2.

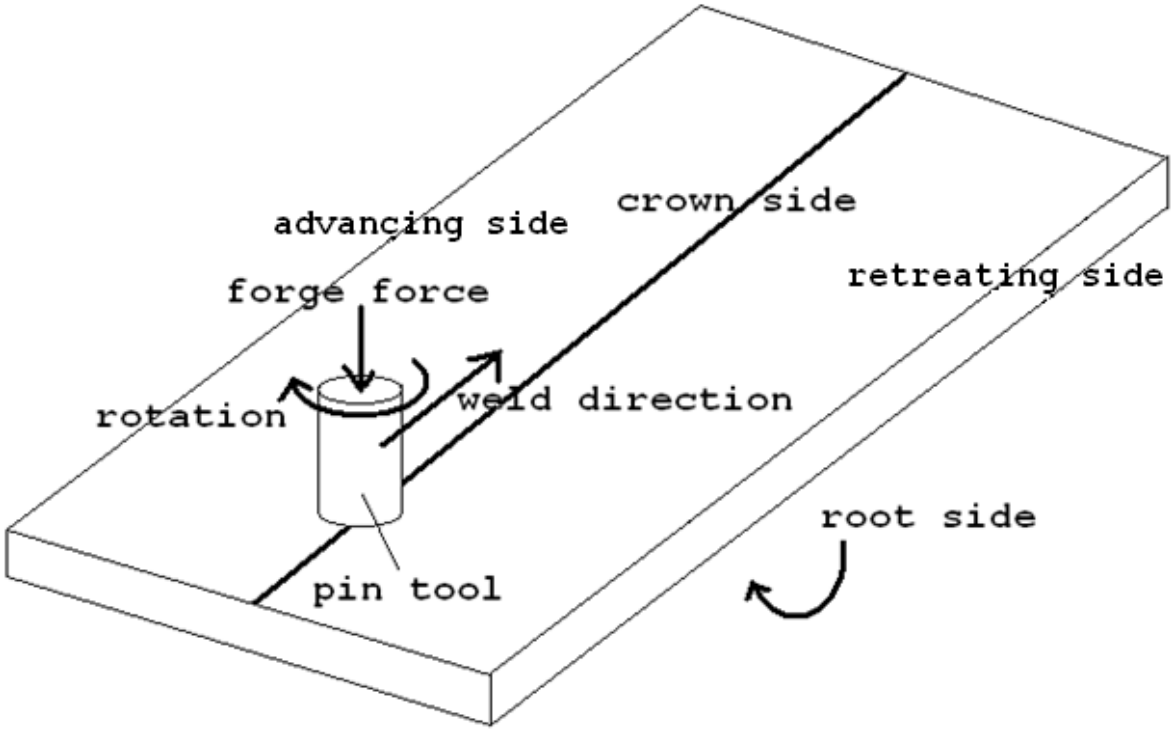

Figure 2.1.2: FSW terminology

The side of the weld facing the pin tool is the crown side; the opposite is the root side. Since the tool rotates, there is an asymmetry in the surface speed of the tool. The side on which the travel speed and rotation speed are additive is the advancing side; the side they are subtractive is the retreating side.

FSW is used extensively for joining aluminum in aerospace and other applications where weight is a primary concern. As fuel efficiency and high speed capabilities become of increasing concern in the naval industry, vessels such as the US Navy

Littoral Combat ship are increasingly turning to aluminum super structures. Here especially, high strength and high corrosion resistance are desired. High strength, low corrosion aluminum alloys (7000 series), considered un-weldable with traditional fusion welding techniques (TIG etc.), are easy to weld using FSW (6). Since FSW plasticizes – not melts – the welded material, the maximum temperature seen in FSW is lower than in fusion welding. For heat treatable alloys (the predominant case for high strength alloys), this lower temperature causes less damage to the metal's temper, yielding stronger welds (7). Fusion welding requires the addition of a filler material to the weld joint to aid in the joining process. As this introduces a dissimilar metal, it can hasten corrosion. The lack of filler material and the lower maximum temperature seen in FSW over MIG/TIG welding leads to an increased corrosion resistance (8).

FSW produces welded structures with smaller, but extant distortions than fusion welding (9), (10). If many extruded members are joined with FSW, this small per weld distortion can add up across the finished part. This can lead to dimensional tolerance mismatch of the finished part, as well as fitting and interference issues during the later stages of the manufacturing process.

The most often studied parameters that affect FSW properties are pin tool geometry, tool rotation speed, forge force, and travel speed (11), (12). These four factors interact to dictate the coupled thermo-mechanical environment around a pin tool during a FSW (13). For a set pin tool design, a 3-d space can be imagined consisting of rotation speed, travel speed, and forge force. Within this space exists a volume of arbitrary largeness inside of which suitable FSW can occur. A rotation speed of 1rpm and travel speed of 500ipm would simply drag the pin through the material (or likely result in a broken pin); just as inappropriate, a 10,000rpm/0.1imp weld would likely eject over worked material from below the tool, leading to collapse of the weld nugget. Research on high speed FSW (>2000rpm tool rotation speed) is in its infancy, mostly due to limitations of available FSW machine tools (14). Thus, an upper bound on suitable FSW tool rotation speed has yet to be found, leading to an arbitrarily large parameter space. Since much FSW research is

still being performed on milling machines, forge force is not always a strictly controlled parameter. Unpublished studies within Lockheed Martin indicate that tool rotation is often the dominant parameter, and this has been the lone controlled variable in much testing (15).

Heat plays a critical role in FSW. The temperature of a weld affects both the process window (the material needs to be sufficiently hot to be plastic), and the properties of the finished weld (excessive time at high temperatures can damage the temper). Table 2.1.1 shows the general techniques to control the heat in a FSW (16).

	Decrease Heat	Increase Heat
rotation speed	decrease	increase
travel speed	increase	decrease
forge force	decrease	increase
pin tool design	decrease size, features	increase size, features
clamping design	increase area, force, thermal conductivity	decrease area, force, thermal conductivity

Table 2.1.1: FSW parameter effects on heat

2.2 Microstructure

The general form of a FSW nugget and terminology are shown in figure 2.2.1.

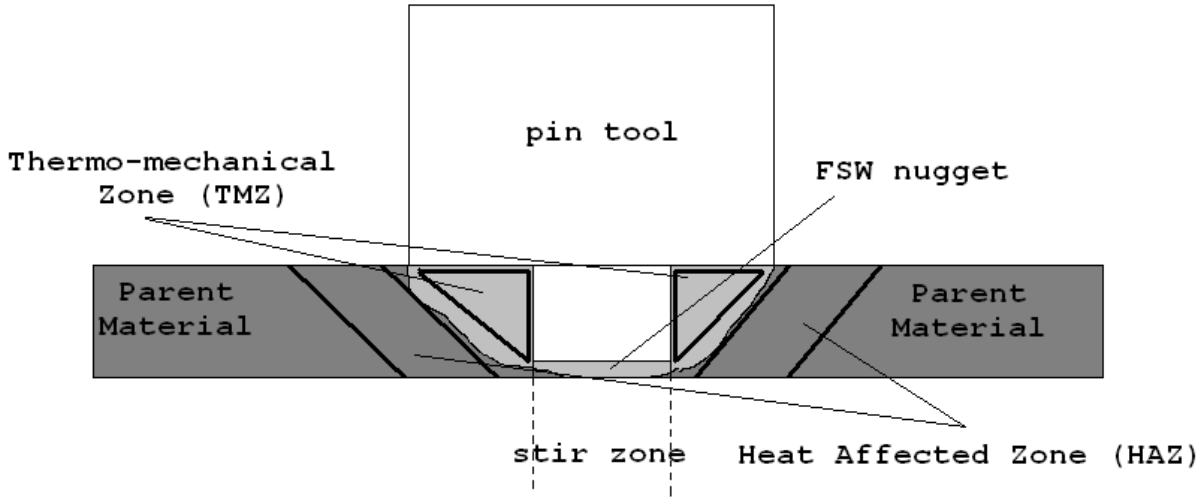

Figure 2.2.1: FSW nugget terminology

The FSW nugget is the region of the weld that has undergone dynamic recyrstallization (17). The width of the nugget is typically slightly wider than the pin tool shoulder at the crown side of the weld, gradually tapering to slightly wider than the probe at the root side. The stir zone is the region of the nugget through which the probe traveled – the entirety of this region having undergone plastic deformation from the tool. The remainder of the nugget is the Thermo-Mechanical Zone (TMZ), which has experienced a decreasing amount of work the further from the shoulder and probe, but still characterized by equiaxial, dynamically recrystallized grains. The Heat Affected Zone (HAZ) was heated via conduction from the nugget, but experienced no hot work from the pin tool. Outside of the HAZ, temperatures were insufficient to alter the parent metal microstructure, and the un-welded properties exist (18).

Hand in hand with the microstructural variation, the material properties also differ across a FSW weld (19). Figure 2.2.2 shows the general distribution of properties across a weld nugget.

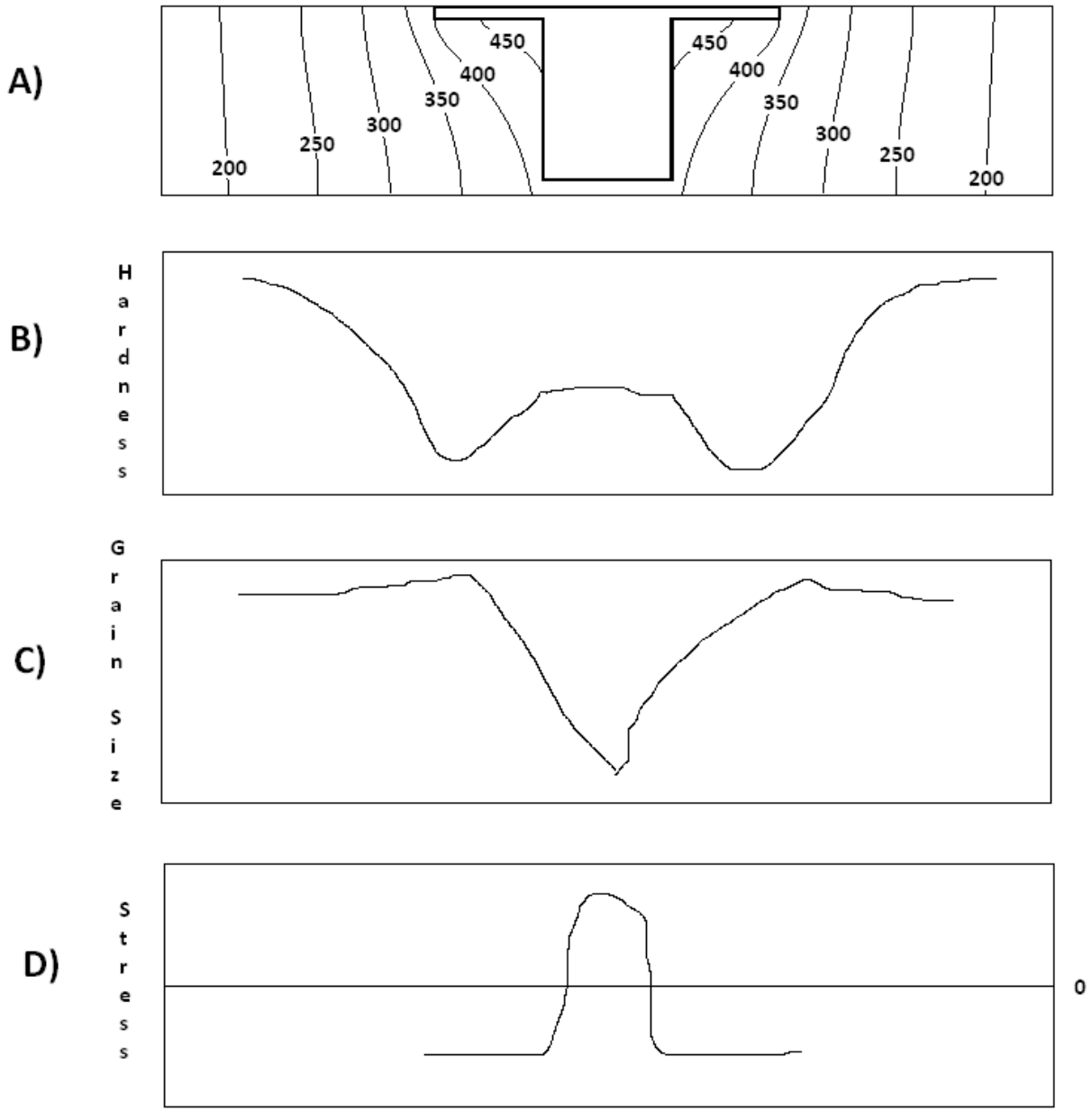

Figure: 2.2.2: Nugget property variation, (18), (19), (20)

A) shows the temperature variation (18), B) the Hardness (19), C) the grain size (19), and D) the transverse residual stress (20). These plots are obviously from separate welds, but the general trends hold and can generally be correlated to the temperature distribution.

Many aluminum alloys (including the 6061 used in this study) derive their strength from hardening precipitates. After

solution heat treating, the distribution of these precipitates is optimized through artificial aging, i.e. controlled heating and cooling. The strengthening precipitates in 6061-T6 are needle-like Mg_xSi β'' phase structures that are finely and uniformly distributed. These precipitates hinder dislocation movement, and a disruption of their distribution can lead to decreased strength. The temperature in the stir zone is high enough to bring these precipitates into solution, though re-precipitation during the cooling phase can lead to moderate strength (21), (22). The "heat treatment" generated by FSW on aluminum yields a microstructure and material properties very similar to the –T4 temper (22). In figure 2.2.2b this is displayed by the lower hardness in the stir zone than the parent hardness at the edges. This is the case for T6 temper alloys, tempers softer than T4 can yield FSW stir zones that are harder than the base metal. As the temperature decreases away from the stir zone, a threshold is crossed where instead of re-entering solution, the precipitates grow in size and decrease in number. This is akin to over aging the metal during the heat treatment process (23). This reordering of the ideal precipitate structure is worst in the HAZ, corresponding to the hardness minima seen in 2.2.2b (24). In defect free welds, the HAZ is the predominant location of failure (25).

Reynolds has shown (26) that the temperature history and distribution of a FSW can be inferred from a hardness traverse through the T/2 line of a 7050 FSW. A further link exists between the torque required to rotate the pin tool and the temperature history. Using the torque and hardness (both being responses to the weld parameters) a link can be made (through peak temperature) to residual stresses (27) and therefore, distortion.

2.3 Welding Distortion

In this study, two deviations from nominal weldment geometry are investigated: linear deviation (measured transversely and longitudinally with respect to the FSW), and out of plane deviation from flat. Both factors can have cumulative effects leading to geometric mismatch during manufacture and to out of tolerance finished parts. Rotational distortion as seen in

figure 2.3.1, is eliminated from this study by using BOP welds instead of butt welds (28).

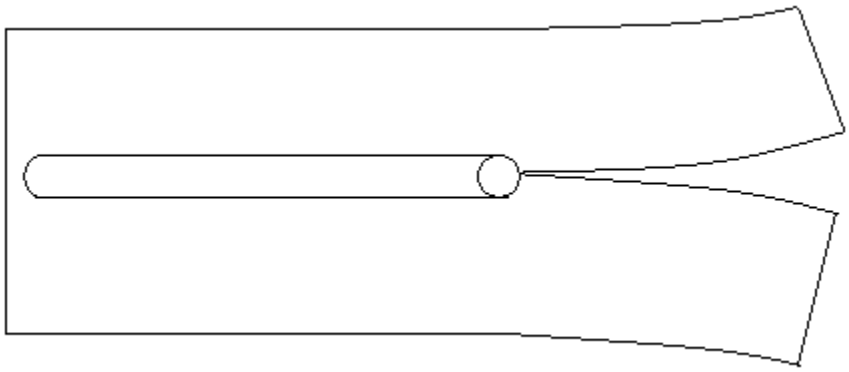

Figure 2.3.1: Rotational distortion ahead of FSW pin tool in a butt weld

With increasingly affordable computing power, detailed models are becoming possible (29), that can predict distortion in welded structures, the study of which comprising a great deal of the literature. Integrally stiffened thin walled structures with FSW for aerospace applications have been successfully modeled (30).

It has been shown by Shi (31) that FSW weldments, when viewed from the crown side, have convex longitudinal bowing, and concave transverse bowing, both being opposite compared to fusion welds. Shi also showed that tool rotation speed affected distortion, while the effect of weld travel speed was not clear. For the panels tested, Shi found transverse out of plane distortion to be ~1% of panel width and longitudinal distortion to be 1-3% of panel length. It was also shown that lower tool rotation speed led to lower distortion.

In FSW weldments, 99% of the impetus for buckling in stiffened structures is the residual stress level. The finished weld strength contributes only 0.1% (32).

2.4 Residual Stress

Residual stress from welding is the primary source of deformation in welded panels. Especially in thin sections, when

the residual stress level exceeds the buckling limit of the weldment, out of plane distortion occurs (33). The total stress on a part is the stress from in-service loads combined with the residual stress (34). Residual stress also contributes to diminished fracture resistance (35). To control both geometric tolerances and material properties it is desirable to mitigate residual stress by control of the welding parameters.

The localized heating from welding causes compressive stresses in accordance with temperature and the thermal expansion coefficient of the material. The elevated temperature additionally decreases the material strength (in a fusion weld, the weld center is temporarily a stregnthless liquid) and at sufficient conditions, the thermal compressive forces plastically deform the weld region. Plastic deformation of the weld nugget relieves the compressive stresses at the weld line, but the temperature gradient -- and the subsequent strength gradient -- cause a tensile stress at the edges of the panel to statically counteract the compressive stresses at the weld line. As the weld cools, the material strength returns, eventually to the point that plastic deformation is halted. Once room temperature is reached, full strength has returned. The plasticized region near the weld center equilibrates with tensile residual stress, and the weld edges have compressive stresses (33). In FSW weldments, longitudinal residual stress is greater than transverse stress (36).

Residual stress can be controlled by decreasing the maximum temperature induced in the weld (37) and by improving the mechanical restraint of the panel during the weld (35).

Density changes in the weld nugget can also contribute to residual stress formation in the same mechanism as thermal expansion. The nugget in a fusion weld undergoes a liquid to solid phase transition as it cools, with a subsequent density change. FSW temperatures are below the melting temperature for aluminum. The grain processing in FSW is isochoric, and does not produce residual stresses from large density fluctuations (38).

2.5 Heat

Much academic research on FSW is focused on modeling the heat characteristics. FEM models have proven capable of describing the effects of weld material properties (39), convection effects (40), and torque response (41) on temperature distributions and histories in FSW.

Experimental measurement of FSW temperature distribution can be problematic. The high temperature gradients require precision location of temperature sensors. Imbedding thermocouples through the panel thickness requires arduous machining and installation techniques with moderate uncertainty in placement. The thermal expansion and plastic deformation experienced during welding leads to further location uncertainty. Machining required for thermocouple installation can furthermore alter the thermal environment from the un-instrumented weld (26). Because of these problems, thermal models relating temperature distributions to more measureable welding parameters and responses have been sought.

Fully instrumented FSW machine spindles operate in a speed control feedback loop. This leaves the torque reacted by the spindle (through the pin tool) a response to a set of weld parameters. On the PDS and other hydraulic spindle FSW machines, this torque can be ascertained by the pressure differential across the spindle motor. In contrast to temperature monitoring, torque data is easily collected and can be used to determine weld power (42).

The energy input from the spindle in an FSW is the sum of the energy dissipation from friction heating, and from plastic deformation of the weld nugget. Based on the material properties of the welded material and the geometry of the pin tool, equation 3.5.1 describes the frictional contribution to torque (43).

$$T = 2\pi\tau \left[\frac{r_0^3}{3} + hr_i^2\right] = 2\mu F \left[\frac{r_0}{3} + \frac{hr_i^2}{r_0^2}\right]$$

Where:

r_0 is the pin tool shoulder radius

r_i is the probe radius

h is the probe height

F is the forge force

τ is the shear stress

μ is the coefficient of friction between the pin tool and the welded material

Equation 2.5.1: Torque in FSW

Hamilton (43) suggests using μ=0.5 for steel pin tools in aluminum welds (the material combination used in this study). Since the material properties of aluminum (including μ) are temperature dependent, this is not universally applicable. Regardless, the lone source of power for FSW is that delivered by the spindle, so the easy to monitor spindle torque is a sound way to at least rank temperatures seen in different welds (22).

Heat sinks in FSW include: conduction into the spindle through the pin tool, conduction into the machine bed through the clamping fixture, and convection to the atmosphere through air exposed surfaces. The convection environment for this testing will be held constant. It has been shown that only 4% of the heat in an FSW butt weld travels back through the pin tool (44), and the pin tool tooling will remain constant. Thus, the only source of heat loss from the weld will be conduction into the weld fixture.

Su characterized the differing heat fluxes into spot FSW fixtures (45). Clamping fixtures made from steel (with a high thermal conductivity) and ceramic (with a low thermal conductivity) were compared. The ceramic fixture conducted away 10% of the weld input power, while the steel fixture removed 50%. For butt welds in 2195 aluminum with standard metallic tooling, approximately 20% of the input power is conducted into the tooling (46).

2.6 Clamping

Clamping fixtures for FSW have the built in requirement to react the forces generated by the welding machine, which can be thousands of pounds both axial to the pin tool and wildly varying (in magnitude and sign) in the plane of the weld (47). Since fusion welding involves comparatively miniscule physical forces, the clamping used is typically less robust, and can be designed solely for optimal distortion mitigation (48). This much larger minimum clamping requirement for FSW may be part of the reason the friction stir welds are lower in distortion than fusion welds.

Clamping plays a key role in counteracting welding induced distortions. Moving the clamps closer to the weld centerline increases this effect (49). Increasing clamping force will limit distortion, but above a certain threshold, has diminishing returns (50). Mechanical constraints must be left in place until after the part has cooled to room temperature to realize their full benefit (51).

Work to date has mainly been on modeling, and almost exclusively on fusion welding. The study of clamping frequency (and its coupled effects with welding parameters) based on FSW experimental results are deficient in the literature.

2.7 Design of Experiments

Design of experiments (DOE) is a statistical method for experimental design that increases understanding of the effects of variables on outputs, while decreasing the required number of tests. DOE was invented by Ronald Fisher in the 1920s in support of agricultural experiments (52). Since the 1940s, industry has used DOE, and the advent of modern quality control techniques, such as Six Sigma, has seen an increase in the application of DOE in industrial research (53).

DOE compares with One At a Time (OAT) experimentation. An experiment consists of factors (the variables that affect the outcome), which can have multiple levels (the numerical value of the factor), and the generated responses. The design of a one

factor, two level experiment is obvious, and the application of DOE is unnecessary. DOE quickly shows its utility as the scope of experimentation expands. The OAT design for any experiment involves altering one factor between levels while holding all other factors constant. This isolates the effect of the chosen factor on the response. Linear regression is then used to determine the functional effect of the altered factor on the system response. To understand all single factor effects (and to even have a chance at understanding combined effects), n^k experiments need be run, where n is the number of levels, and k is the number of factors (i.e. a full factorial experiment). This exponentially growing number of experiments, and the required resources to perform them, quickly becomes unmanageable.

DOE systematically alters multiple factors simultaneously. In this way, factor interactions are tested, and tests can be eliminated. A three factor two level experiment is represented in figure 2.7.1.

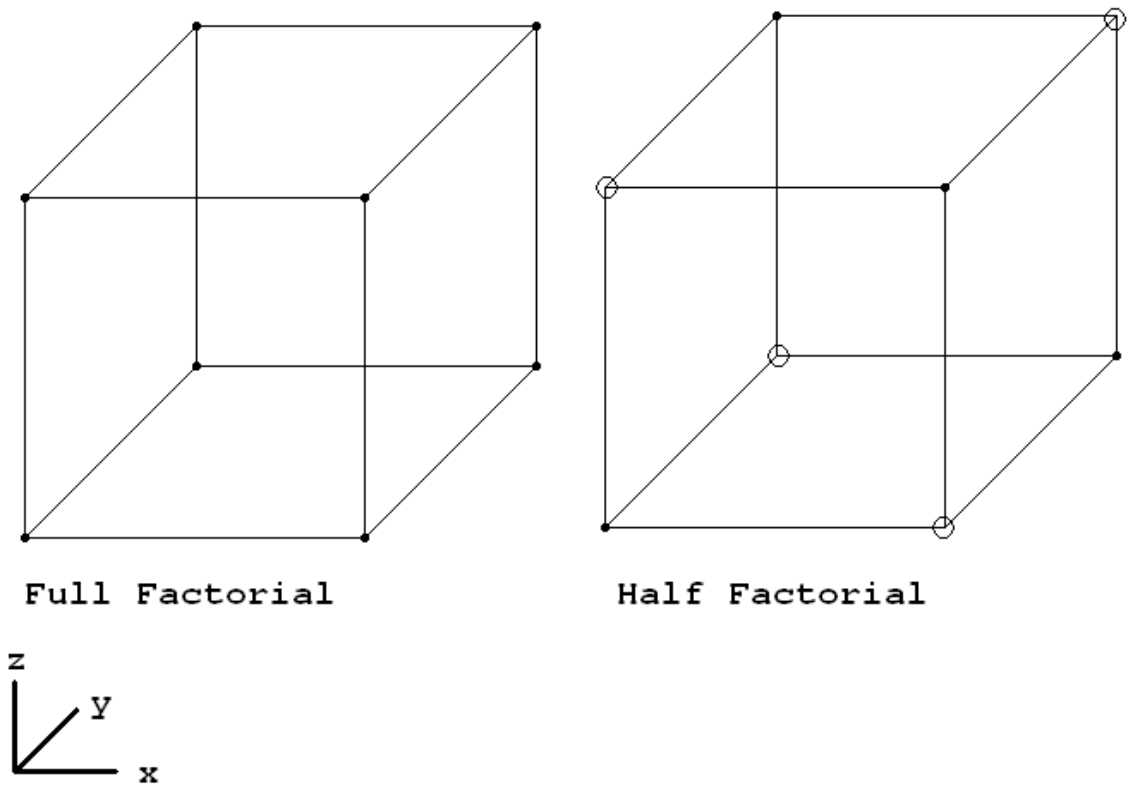

Figure 2.7.1: Three factor (x,y,z) two level design

Here the factors x, y, and z are tested at arbitrary levels (low and high for each). The full factorial design on the left requires eight tests. For each factor, the level is altered from low to high four times. The half factorial design can find the same information using four tests (either the dots or the circles). For each factor here, the level is altered from low to high twice. This represents a decrease in fidelity of the data, but it will be less than the decrease in the resources required running the experiment.

The goal of DOE (for the 3 factor 3 level design in this study) is to determine equation 2.7.1.

$$Y = \beta_0 + \sum_{i=1}^{p} \beta_i X_i + \sum_{i=1 \neq j}^{p} \sum_{j=1 \neq i}^{p} \beta_{ij} X_i X_j + \beta_{ijk} X_i X_j X_k + \sum_{i=1}^{p} \beta_{ii} X_i^2$$

Where:
Y = the response variable
X_x = the factors
β_0 = the overall mean response
β_i = the main effect
β_{ij} = the two way interactions
β_{ijk} = the three way interaction
β_{ii} = the quadratic interactions
p = the number of levels

Equation 2.7.1: Polynomial form of DOE model (54)

The sparsity of effects principle states that higher order terms are less likely than lower order terms to affect the response variable. Equation 2.7.1 represents all interactions tested by the DOE software in this study (55).

By comparing the mean response to each of the single and combined factor interactions, DOE can determine which factors are affecting the response variable, to what extent, and can identify the factors that are not affecting the response. Using iterative linear regression, a model fitting the experimental data can be constructed, which can predict the results on

heretofore untested combinations of factors. By performing these suggested tests, the DOE model can be further validated.

3.0 Experimental Details

This research was performed in collaboration with industrial partners. To ensure the free distribution of this thesis, certain details of the welding have been omitted, specifically a detailed description of the pin tool design, the welding parameters other than tool rotation speed, the CNC program used to execute the welds, and the full suite of data collected during welding.

3.1 Weld Configuration

All welds in this study were Bead on Plate (BOP). A butt weld is run down the interface of two plates butted together edge to edge. In a BOP weld, the weld is simply run down the middle of a single plate or extrusion. BOP welds have been shown to display residual stress distributions similar to butt welds (56). Butt welds require additional edge constraints to prevent the separate pieces from being forced apart by the pin tool, and the non-uniform heat distribution caused by it (28). By studying BOP welds, the procedure was simplified, and more importantly, a further experimental variable was eliminated (e.g. the configuration of the edge clamps). Using BOP also eliminated the effects of rotational distortion, described in section 2.3.

The FSW technique used in this study was the conventional type. Conventional FSW refers to the pin tool design. Various designs include multipart pin tools with articulated features. Conventional FSW pin tools are a single monolithic part.

The end view of the clamping fixture is seen in figure 3.1.1.

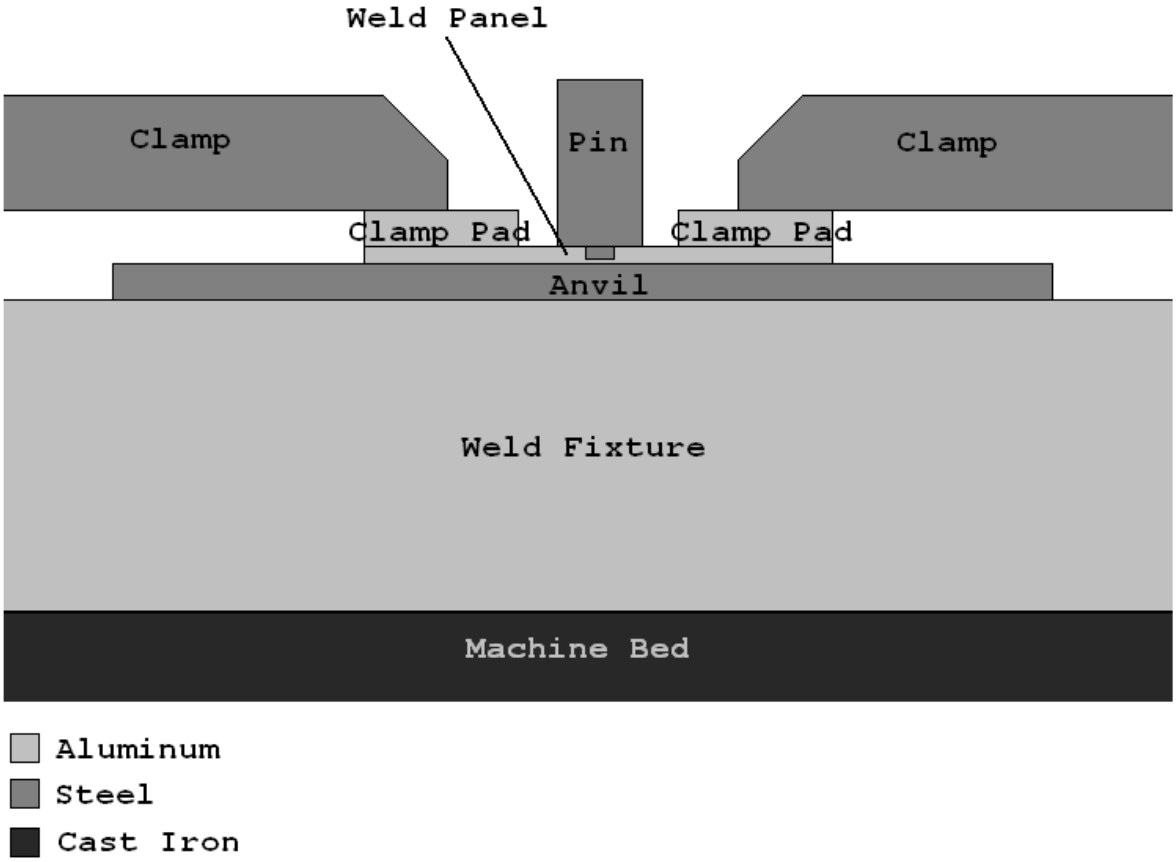

Figure 3.1.1: End view (in weld direction) of tooling

The clamp pads are ~1”x1/4” 6061-T6 aluminum bars used to distribute the clamping force, and prevent the clamps from digging into the weld panel. The anvil is a 6” wide 1/4” thick plate made from 404 stainless steel. The clamp pads, weld panel, and anvil are all free floating (with no fasteners) and held in place only with the clamping force. They are all aligned to marks on the weld fixture prior to each weld. The weld fixture is a 2219-T8 aluminum plate bolted to the ductile cast iron machine table. The weld fixture has studs used to tighten the clamps. The pin tool is made from hardened H-13 tool steel. A series of various tool holders adapt the pin tool to the machine spindle and are made from H-13 tool steel and 404 stainless steel.

The weld panels are made from 6060-T6511 aluminum extrusions with a 0.125”x4” cross section. Eight foot long extrusions were

cut into 24” weld panels. A 20” long weld was run down the center of the panel, starting and stopping 2” from each edge.

The varied parameters in this study were clamp spacing (pitch), clamp tightening torque, and the rotation speed of the pin tool. Figure 3.1.2 shows the weld fixture with the three used clamp pitches, loaded with a weld panel.

Figure 3.1.2: Three clamp configurations used in this study

3.2 Pin Tool Design

The pin tool used in this study is of the conventional design. The lack of moving parts simplifies its manufacture and use. A conventional FSW pin tool has two main geometries: the shoulder and the probe.

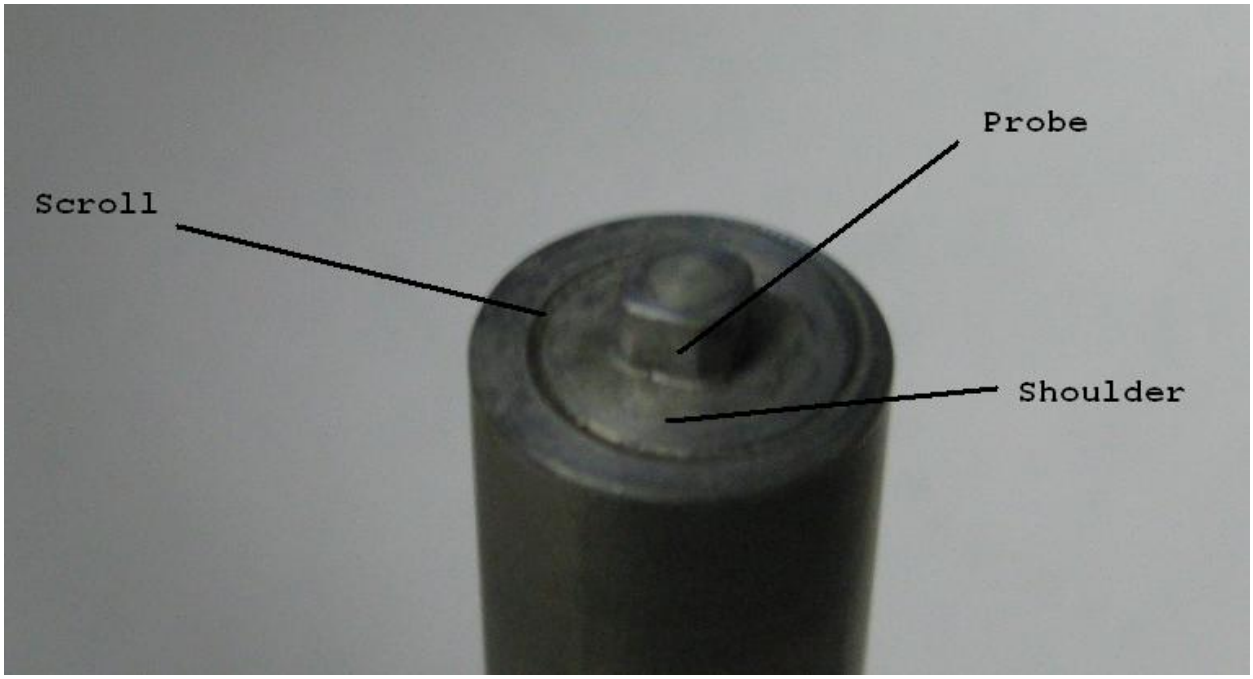

Figure 3.2.1: FSW pin tool used in this study

The shoulder rides along the top surface of the weld. The shoulder may have features to aide in weld consolidation, alter the heat input, or affect the weld surface finish. The pin in figure 3.2.1 has a spiral scroll machined with a ball end mill. The handedness of the spiral is such that it draws material toward the center of the tool. If constraining features, such as a scroll, were not present, the plasticized material under the pin could be extruded out from under the shoulder, eventually resulting in collapse of the weld (57).

The probe provides the mixing action that consolidates the weld nugget. For some designs, the probe can generate a significant portion of the heat, but for most designs, the shoulder generates most of the heat. In a butt weld, the pin serves to break up the interface. Features on the pin such as threads,

flutes, and as seen above, flats, increase pin tool performance, and can widen the process window (11).

FSW pin tools require high hardness to survive the initial cold plunge into the weld, high toughness to prevent fracture from highly cyclic bending loads, and the ability to maintain sufficient properties at high temperatures (~900°F for aluminum welds). FSW pin tools for aerospace manufacturing are typically made from exotic high temperature alloys. If a pin were to break in the middle of a weld, a multimillion dollar part could be ruined. These materials pose two hurdles to university research: they are expensive and they are difficult to machine. For example, a commonly used alloy is MP-159, a nickel cobalt super alloy with excellent wear resistance and strength at FSW temperatures. MP-159 is a work hardening alloy and thus must be machined in its hardened state (working the machined pin tool being an impossible feat). Developing pin tool manufacturing capability at UNO was a desired side effect of this study, and since the machine tools at UNO are incapable of working hardened metal, use of these high performance materials was infeasible.

H-13 tool steel is widely used in university FSW pin tool manufacture (12). In the hardened condition, H-13 exhibits an acceptable level of hardness and toughness for FSW, properties it maintains at aluminum FSW temperatures. H-13 was developed as a hot working die steel, and is commonly used in aluminum extrusion dies. The FSW process involves the forging of plasticized metal, and thus is very similar to the extrusion process (indeed, the temper produced by FSW on heat treatable aluminum alloys closely approximates that from extrusion). The properties of H-13 can be sufficiently manipulated using only heat treatment. It can be annealed to a soft state, machined, and subsequently hardened, all with good dimensional stability (58).

H-13 drill rod was used to manufacture the pin tools used in this study. The diameter was selected to be the largest that would fit through the spindle bore of the available CNC lathe. The H-13 was supplied in the hardened state, and was therefore annealed prior to machining. The drill rod was annealed as follows: placed in a preheated 200°C oven, increased to 850°C at

50°C/hr, held at 850°C for 2 hours, furnace cooled to 300°C, then removed to cool in still air. The pins were annealed under a nitrogen atmosphere to prevent the formation of oxide scale.

The softened pins were machine on an Emco Concept Turn 55 CNC lathe, seen in figure 3.2.3.

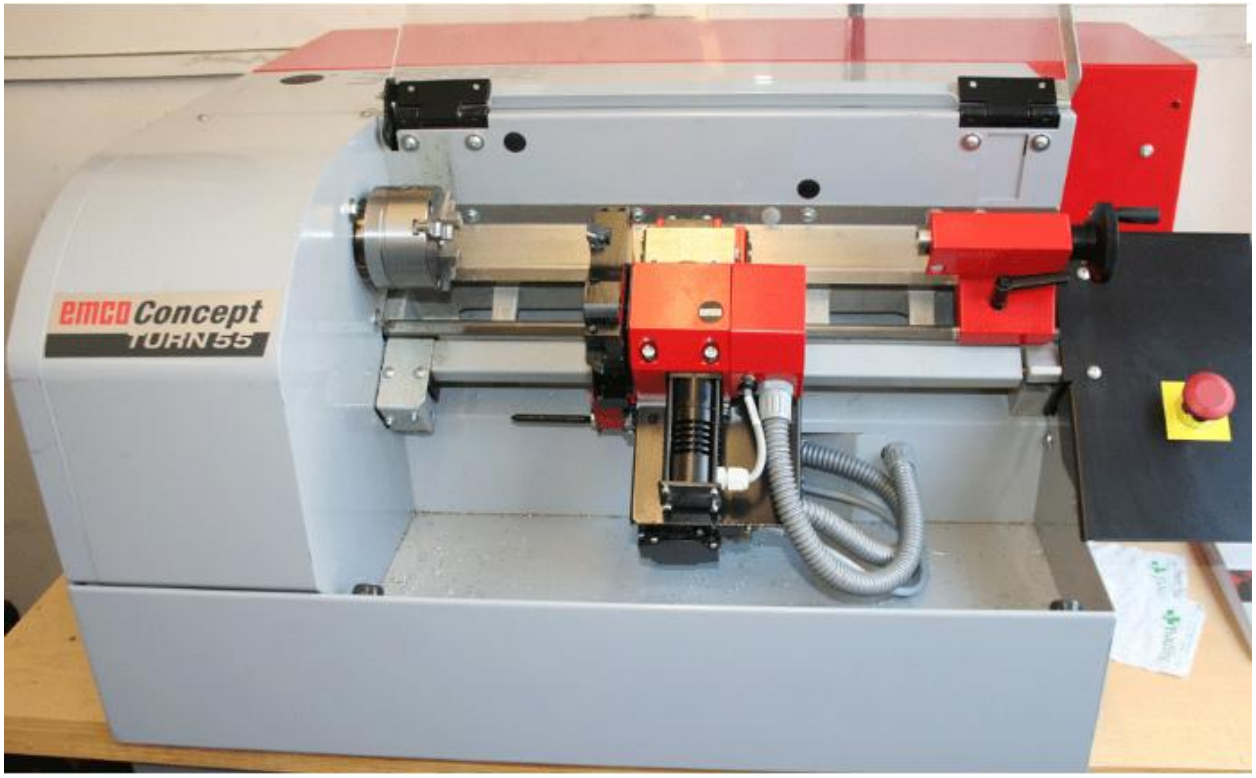

Figure 3.2.3: CNC lathe used to machine the pin tools

After the shoulder and rough shape of the probe were machined on the CNC lathe, the pins were held in a vertical fixture for subsequent milling. The milling was performed on the MTS Production Development System (PDS) seen in figure 3.2.4. With this machine, the square flats were cut onto the sides of the probe, and the scrolls were added.

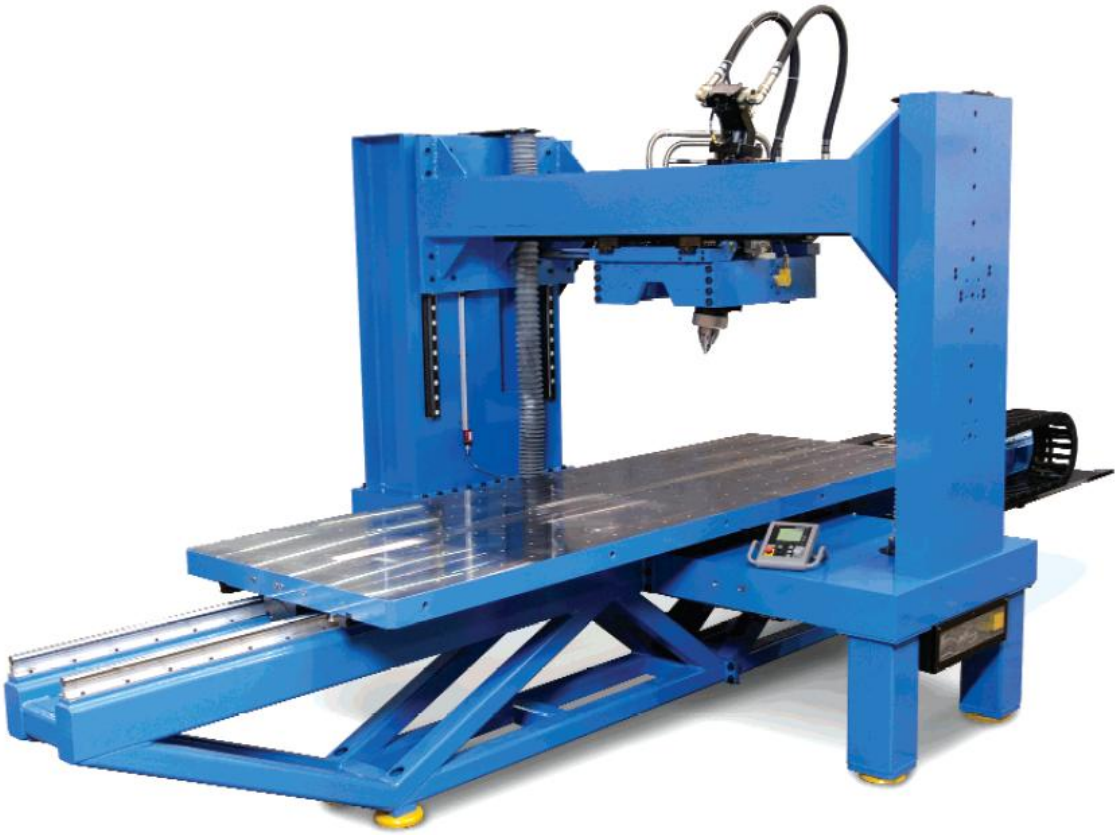

Figure 3.2.4: MTS Production Development System (PDS)

The PDS is the servo-hydraulic FSW machine used to perform the welds in this study. Its open source programming environment (allowing customizable spiral path generation) and adaptable spindle allows it to also be used as a milling machine.

After turning and milling, all sharp corners were broken by hand and the pins were hardened and tempered. Since H-13 is an air quenching tool steel, it must be exposed to atmospheric oxygen at high temperature, which can lead to oxide scale formation. To mitigate scaling, the pin tools were heat treated in 309 stainless steel tool bags. This allowed all heat treatment steps to occur in atmospheric conditions as the tools were protected from oxidizing conditions by the tool bag. The complete heat treatment cycle for the machined pins was: placed in preheated 1050°C hardening furnace, held for 45 minutes, removed to air cool to 55°C, placed in 550°C tempering furnace, held for 2 hours, furnace cooled to room temperature.

The heat treatment was chosen for its optimal combination of hardness and toughness, and is similar to that suggested for H-13 aluminum extrusion dies (58). Witness samples were measured as Vickers hardness 550. This was the predicted hardness based on the reference, but slightly harder than FSW pin recommendations in the literature (RHC52 vs RHC45-50). It was initially feared that this indicated too low of a fracture toughness, but the same pin was used for all welding in this study - approximately 75 linear feet with no breakage or excessive wear.

The initial pin tool design consisted of a square probe with a scrolled convex shoulder. More complex pins can serve to open the FSW processing window, leading to better performing welds (11). This pin tool design was selected as being the most highly featured pin that was still within the available manufacturing capabilities.

A priori design of a FSW pin tool for a new weld configuration can be difficult as a full understanding of transport phenomena around FSW pins is still being developed (59). The convex shoulder was chosen to help mitigate uncertainty in the pin design. The contact area of a spherical shoulder can be increased by pushing it farther into the weld. If insufficient heat was being generated, the plunge depth could be increased, leading to a larger effective shoulder diameter (11). It was hoped that this adjustable nature would yield a pin tool with a wide range of acceptable rotation speeds.

There is a delicate balance in the interaction of shoulder diameter, pin length, and material thickness. The backing anvil used in FSW tooling is typically hardened stainless steel. If the shoulder provides insufficient resistance to the forge force, the pin tool can be pushed too far into the weld, eventually causing the probe tip to plunge into the anvil. These anvil strikes typically ruin the weld, the tool, and the anvil. During the bounding welds for the convex shoulder pin, one anvil strike was so severe that the aluminum panel was permanently lap welded to the stainless steel anvil. At the other extreme is Lack of Penetration (LOP). In an LOP weld, the probe tip was not deep enough into the weld, and some thickness

of material under the probe tip is left un-welded. This crack-like defect along the length of a part (in the case of a butt weld), at the most highly stressed region of the structure is also disastrous. Typically, the probe length that prevents both anvil strikes and LOP is around 90% of the weld thickness (12). At roughly this length, the tip of the probe induces sufficient mixing beneath it to ensure the entire weld land thickness is processed. The exact pin tool length for a convex shoulder is not fixed, as the adjustable nature of this pin tool can lead to different effective probe lengths.

The PDS allows the user to manually trim many controlled parameters live during a weld. For the initial welds, a nominal CNC program was executed and during the welding, the visual appearance of the weld surface was monitored. If the weld appeared too cold as in figure 3.2.6, the forge force was increased to increase heat input.

Figure 3.2.6: Excessively cold weld appearance

An overly cold weld typically has insufficient shoulder contact, and thus not enough heat input to plasticize the weld nugget. The tool begins to act like a dull endmill and cuts a jagged channel instead of a consolidated weld.

Conversely, an overly hot weld is typically caused by excessive forge force, which causes the shoulder to plunge below the top surface of the panel as in figure 3.7.

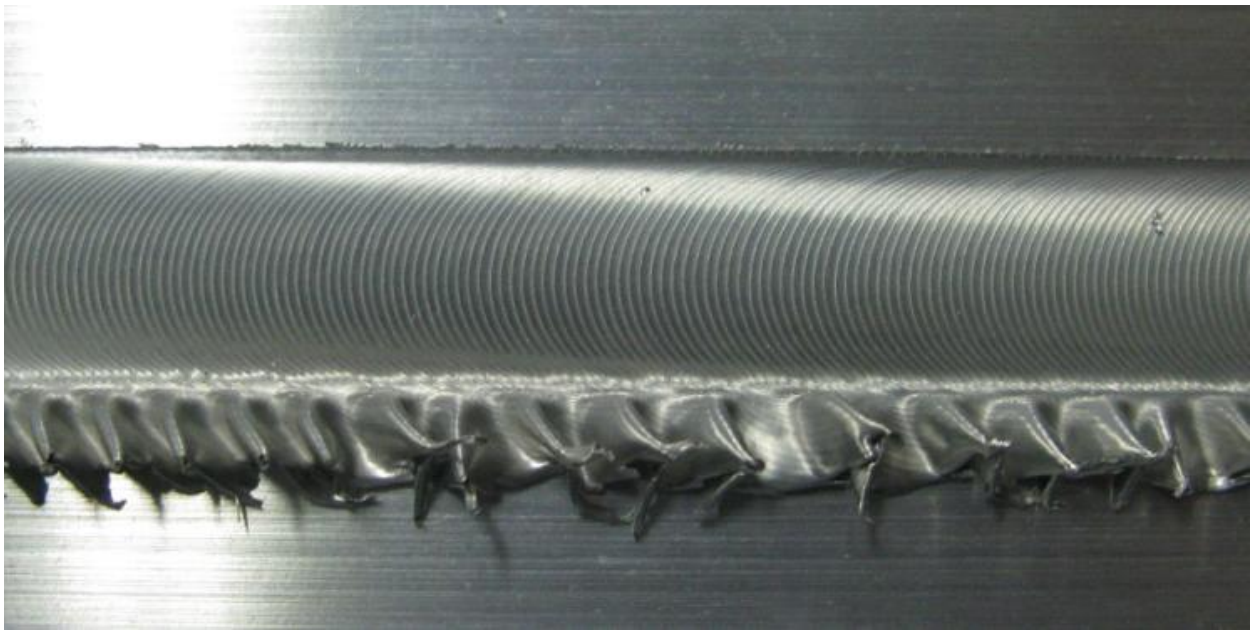

Figure 3.2.7: Excessively hot weld appearance

The bottom of figure 3.2.7 displays excessive flash – material ejected by the shoulder. This volume of material is subtracted from the weld thickness, which weakens the weld. The higher the peak temperature in the weld nugget, the more damage to the parent metal temper, weakening the weld unnecessarily. Aerospace structures require smooth surfaces, and hot welds would require post weld machining to remove excess flash.

The first trial welds with the convex shoulder pin tools required a more than anticipated increase in forge force. At sufficient forge forces to produce a consolidated weld, the probe tip was intermittently striking the anvil. Figures 3.2.8 and 3.2.9 show the damage sustained by the pin tool and anvil respectively.

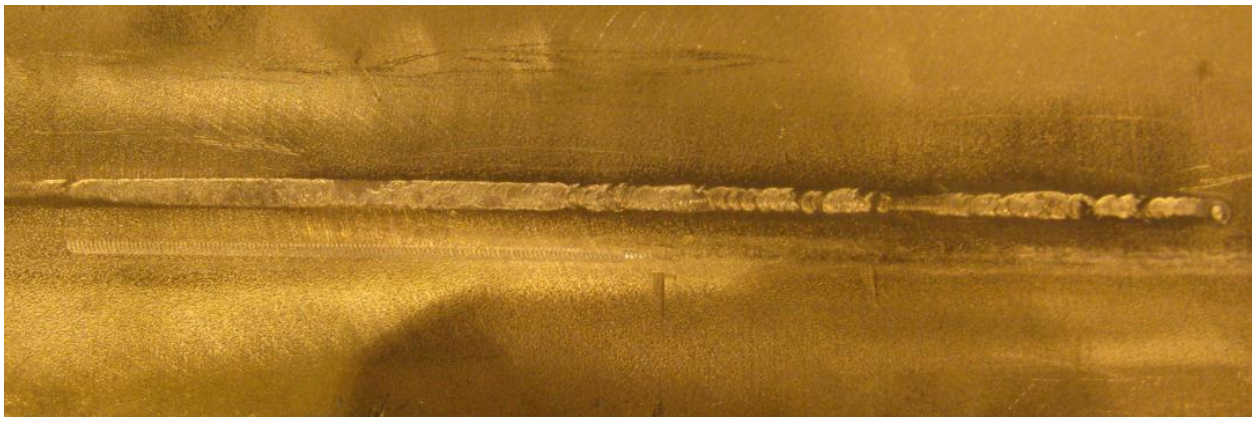

Figure 3.2.8: Damage to anvil from probe tip due to excessive plunge depth

Figure 3.2.9: Stainless steel residue welded to probe tip

The available tool rotation speed window for the convex shoulder tool was not wide enough to deliver meaningful variation for this study. As mentioned previously, outside of a narrow process window of tool rotation speeds, calamitous anvil strikes were a real possibility. A new pin design was needed.

Whereas spherical shoulders provide a mushy response of forge force vs plunge depth, a flat shoulder provides a positive stop. The probe length of a pin tool with a flat shoulder is also straightforward to calculate. A new tool was designed with a flat shoulder, and a slightly shorter probe length. All other pin geometries were unchanged. This pin tool proved to have a suitable process window and posed no danger of anvil strikes.

3.3 Parameter Bounding

Three parameters were varied to ascertain their effect on the weld properties: clamp spacing (pitch), clamp tightening torque, and pin tool rotation speed. Shi showed that rotation was the dominant parameter in FSW distortion and that travel speed had an unclear effect (31). Schenk showed (for fusion welds) that increasing clamping pressure decreased distortion (50). The clamp distance from the weld can affect distortion (51), but in FSW the clamps are generally placed as close to the weld as is practical. Much of the data on welding distortion is either for fusion welds, or based on FEM. There is no experimental data on the combined effects of clamping and FSW parameters on distortion. Rotation speed, clamping force, and clamping pitch are easy to control both in the lab, and in a production environment and all have been individually shown to affect distortion.

The first welds were conducted with a nominal clamping arrangement and a new flat shoulder pin tool. Based on vast industrial experience, an initial weld schedule was selected, scaled down for the pin tool and material used in the study. A reasonable travel speed and forge force were determined, and for those parameters an acceptable tool rotation speed range was 300-400rpm. The criterion for selecting acceptability was the application of years of industrial experience by studying the visual appearance of the weld surface.

The 300-400rpm range was determined with a nominal clamp pitch of 6” and a clamping torque of approximately 50ft-lbs. The lone source of heat for FSW is the spindle power of the machine. There are many heat sinks, but the prime one is conduction into the tooling fixture (50). By altering both the number of clamps, and the amount of per clamp force, the thermal contact between the panel and the machine bed is altered. As seen in figure 3.1.1, many interfaces exist between the welded panel and the large thermal mass of the machine bed (a 6” thick 4’x12’ cast iron slab). Both the stainless steel anvil and the aluminum weld fixture have been used for many welds and suffer from thermal distortion and surface roughness. By increasing the total clamping force, both the area for conductive transport and the intimacy of the contact between the weld and the machine bed were increased. With nominal clamping, the acceptable tool rotation speed range was 300-400rpm. Once this rotation speed was attempted with high and low values of clamp spacing and torque, it was determined that the change in the heat sink that accompanied different clamping would narrow the suitable rotation speed range.

The part labeled “weld fixture” in section 3.1 is a 2” thick 2219-T8 aluminum plate with Helicoil thread inserts at 2” spacing to provide purchase for clamps. It was desired to maintain a consistent clamp pitch throughout the panel, which limited the range of available clamp pitches to whole number factors of 24” – the panel length. In past experience, four clamps (with a pitch of 6”) have been considered nominal. A survey of Lockheed Martin FSW operators showed that 50in-lb of clamping torque was also average. The minimum clamp pitch allowed by the fixture was 2” (12 clamps on each side). The maximum pitch was selected as 8”; it was decided that fewer than three clamps would pose a danger of the panel coming loose during the weld. The most central medium pitch value allowed by the fixture was then 4” (6 clamps on each side). Taking 50ft-lb as the moderate clamp tightening torque value, 25ft-lb and 75ft-lb were chosen as the low and high values with similar reasoning.

The same three rotation speeds would be used on all combinations of clamping pitch and tightening torque, and they needed to produce acceptable welds with each clamping arrangement. If the highest rotation speed (highest heat input) produces acceptable welds with the lowest heat sink clamping configuration (high pitch, low tightening torque) and the lowest rotation speed (lowest heat input) produced acceptable welds with the highest heat sink (low clamp pitch, high torque), then all the combinations should work. Using a consistent travel speed and forge force, the two extreme welds were tested: 300/2/75 and 400/8/25 (rpm/clamp pitch/tightening torque). The 400rpm weld schedule with the loosest clamping (lowest heat sink) produced a weld that was too hot. Acceptable welds were produced by decreasing the rotation speed to 380rpm. Similarly, the 300 rpm weld schedule with the tightest clamping (highest heat sink) required an increase of the rotation speed to 340rpm to produce visually acceptable welds. The nominal clamping rpm window was 300-400, a range of 25%. To have the same parameters for all welds in the study, the rotation speed operation window had to shrink to 340-380rpm – a range of 8%. Tool rotation speeds as low as 8% can lead to appreciable changes in weld distortion, so this was deemed acceptable (31). The shrinking of the rotation speed range was not convenient from an experimental standpoint (it being desired to have the widest possible level range for each factor), but it did prove that the selected clamping parameter ranges had an appreciable effect on the FSW thermal environment. Table 3.3.1 shows the parameter values used in this study.

	Rotation Speed (rpm)	Clamp Pitch (in)	Clamping Torque (ft-lb)
low	340	2	25
medium	360	6	50
high	380	8	75

Table 3.3.1: Factor levels

The high, medium, and low levels for the rotation speed, clamping pitch, and clamping torque were chosen to be as disparate as allowed by the pin design, machine, and tooling. This gave each factor a “fair chance” at affecting the distortion; it was hoped that erroneous conclusions are not made

because one or more factors had insufficient range to affect distortion. As a final check to determine if the factor levels were chosen with enough range, the two new extreme welds were performed – that which was expected to produce the highest weld temperature (and thus least distortion: 340/2/75) and that expected to produce the most distortion (380/8/25). These two welded panels are compared in figure 3.3.1.

Figure 3.3.1: Low and high distortion weld schedules

It can be seen in figure 3.3.1 that the amount of bowing of the rear panel (380/8/25) is more than the panel in the foreground (340/2/75). This followed the expected trend and validated the factor level selection.

3.4 Experimental Design

A commercial software package (DOE Pro XL) was used to generate the test matrices and perform the statistical analysis in this study. A three factor three level central composite design was generated using the values in table 3.4.1.

Rotation Speed (rpm)	Clamp Pitch (in)	Clamp Torque (in-lb)
340	8	25
340	8	75
340	2	25
340	2	75
380	8	25
380	8	75
380	2	25
380	2	75
360	**4**	**50**
360	**4**	**50**
340	4	50
380	4	50
360	8	50
360	2	50
360	4	25
360	4	75

Table 3.4.1: Experimental test matrix

The bolded 360/4/50 test is performed twice as these levels are the middle range for each factor. A full factorial design would require 27 tests, with no replication, as opposed to the 16 tests for this fractional factorial design. This test matrix was performed twice – there were two replications of this experiment for 32 welds total. Here the application of DOE allowed for doubling the fidelity of the data, by performing only 20% more tests.

3.5 Welding and Measurements

The total distortion of each welded panel was characterized by monitoring the change in length of the panel (both transversely and longitudinally with respect to the weld) and the out of plane distortion of the panel. A precision punch was used to mark the panels at 2” intervals, and a separation caliper measured the pre weld punch mark separations. Figure 3.5.1 shows the tools used for the separation measurements, and 3.5.2 shows a panel with the punch mark locations.

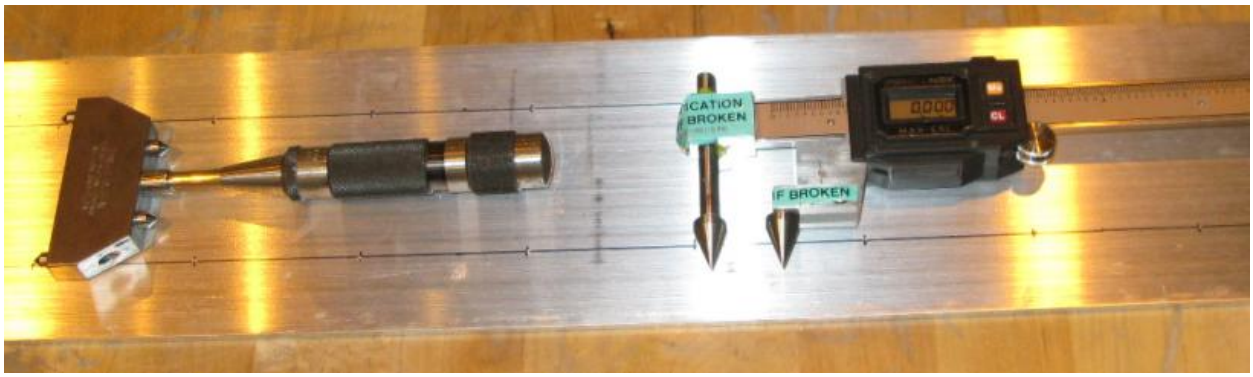

Figure 3.5.1: Separation measurement tools

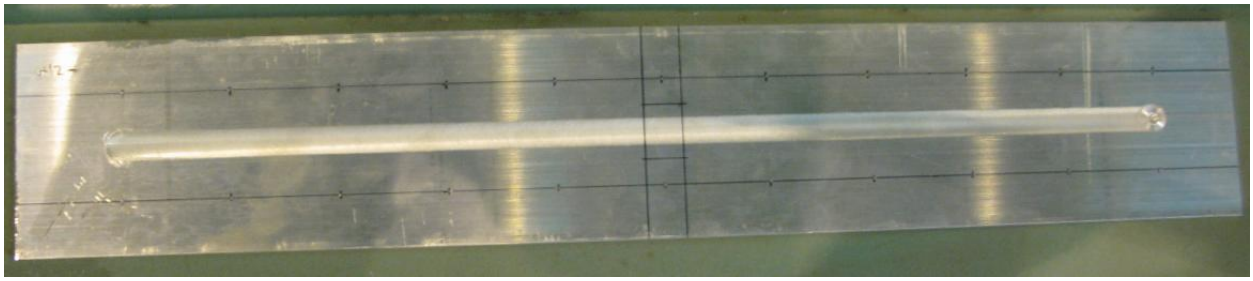

Figure 3.5.2: Separation punch and macro locations

The out of plane distortion measurements were taken beneath each punch mark (on the underside of the panel), as well as between each (the weld centerline). Figure 3.5.2 also shows the location of the excised macro used to measure nugget hardness.

The out of plane distortion measurements were performed using a dial indicator precisely moved over the panel using the PDS as seen in figure 3.5.3. A Starrett dial indicator with 0.0005” accuracy is seen held the PDS machining chuck.

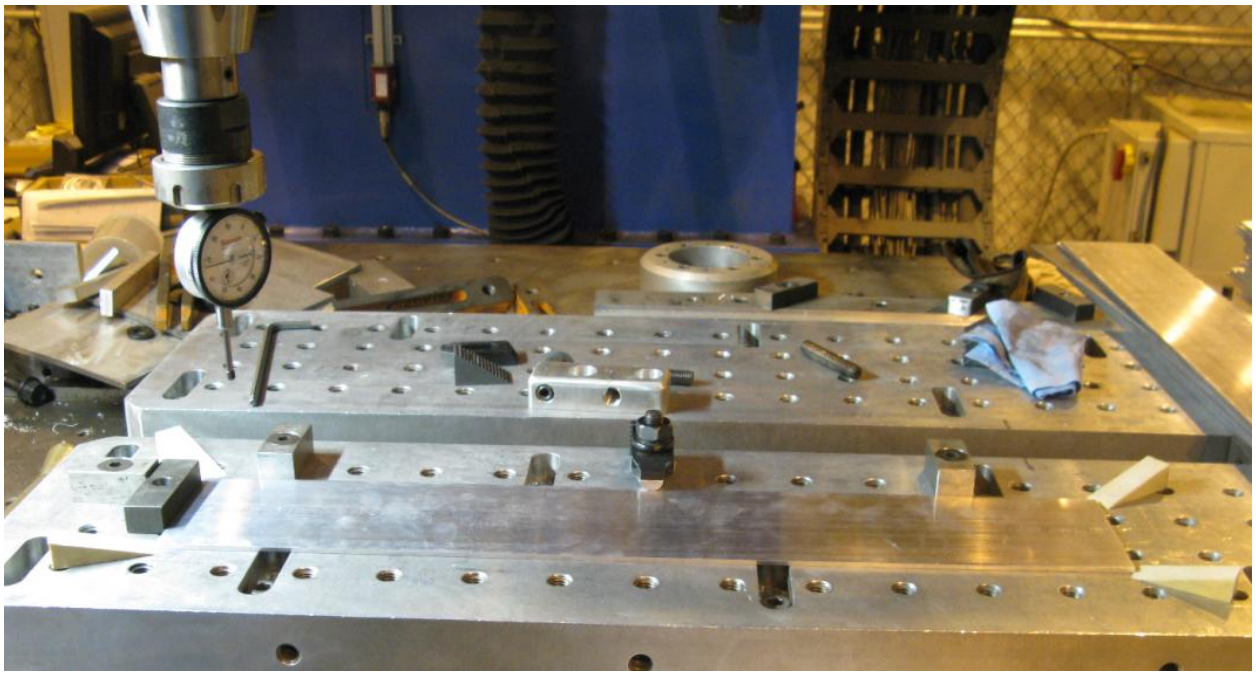

Figure 3.5.3: Distortion measuring fixture

The panels were measured "concave up" (the root side is up). One central edge clamp was delicately applied to prevent the panel from distorting. At the edges, both the weight of the panel itself, and the zero return spring of the dial indicator caused deformation from the natural distortion. Tapered wooden wedges were carefully inserted under the raised corners of the panels to lock in the natural distortion. This arrangement provided good repeatability and was suggested by the literature (60). A CNC program was written to move the dial indicator across the panel, stopping at key locations: each of the separation punch locations, and between each separation punch in the middle of the panel, directly under the weld path. As with separation, distortion was measured before and after each weld. The reported values are the difference between these two measurements.

Each replication was performed on a separate day. It was not feasible to perform all 32 welds on one day. The replications were, however, performed on consecutive days. The machine bed and surrounding air temperature are the biggest factors that change day to day, but both were within 1°F on each day of testing. During the weld execution, the PDS data capture system

measured a host of data streams including all commanded machine parameters, power input, and reaction forces.

At the beginning of each day a warm up panel was welded with the 360/4/50 schedule to ensure that each experimental panel was welded on a warmed-up machine and fixture. The temperature of the weld fixture was monitored for two reasons: to prevent cumulative heating from skewing the later welded panel data and to ensure that each panel was left constrained by the clamps until they had cooled to room temperature. This kept the panels constrained in the clamping fixture for a "cold release" as suggested by Choobi (51). Welded panels were removed when the anvil reached the machine bed temperature.

The DOE software develops an ordered test matrix. To prevent possible bias of the same schedule being welded in the same order between the two replications, the order of the welds seen in table 3.4.1 were randomized for both replications.

After welding, the panels were stored flat at room temperature to await post weld measurements, which were conducted as swiftly as possible to mitigate the effects of natural aging of the welds on distortion response.

Once the post weld deformation was measured, samples were excised from each panel to study the microstructure and to determine the Vickers hardness across the weld nugget. Hardness was determined along the T/2 thickness plane, at room temperature. The load and duration of the indentation was 40Kg and 10s respectively. Measurements were taken every 0.3mm. The excised sample came from the middle of the weld length (as seen in 3.5.2) to mitigate edge effects, and to attempt to study the microstructure once the weld had reached steady state.

4.0 Results

4.1 Out of Plane Distortion

Each of the 33 distortion values for each weld was calculated as the difference between the pre and post weld measurements. This created a surface between x = 1" to 3" (the x axis being

perpendicular to the weld direction) and y = 2 to 22” (the y axis being parallel to the weld direction) as seen in figure 4.1.1, where the z axis is the out of plane measurement.

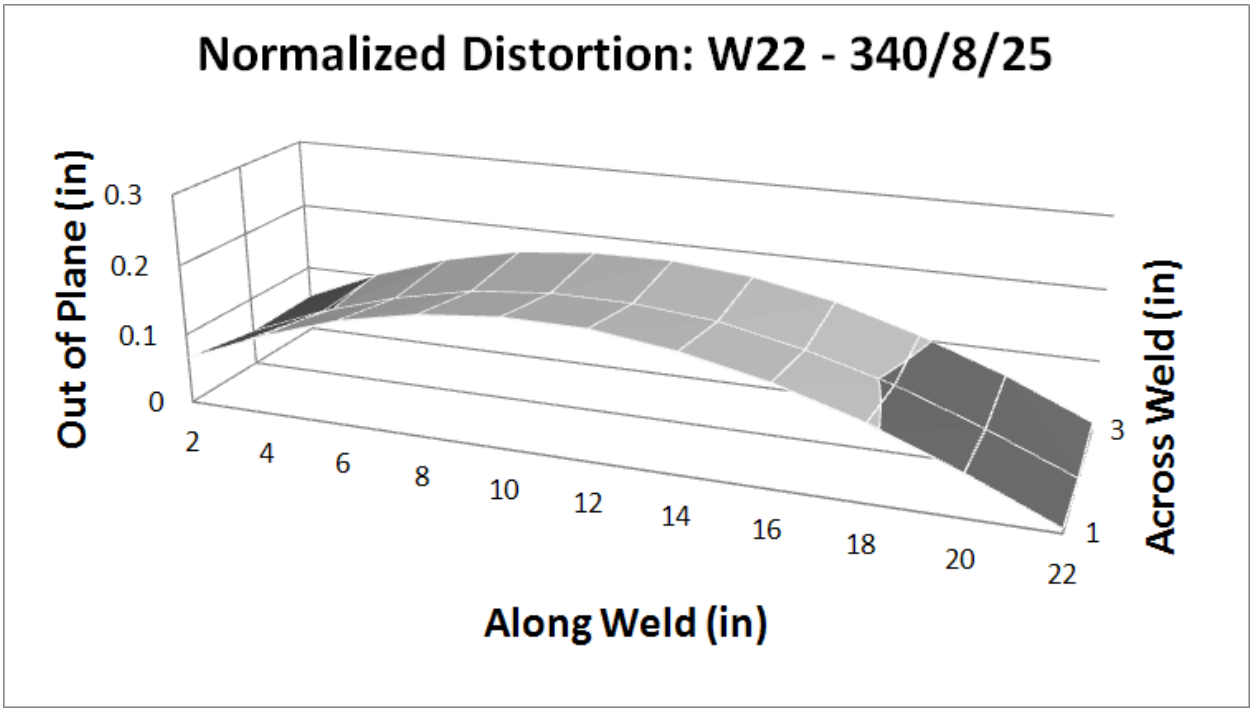

Figure 4.1.1: Graphical representation of FSW induced out of plane distortion for weld #22

The DOE software requires a single number representation of each experimental response. The volume under the surface in figure 4.1.1 was used for the DOE response value for distortion. This volume was calculated with Simpson’s rule using equation 4.1.1.

$$Volume = \frac{2}{3}\left[f(y_0) + 2\sum_{j=1}^{\frac{n}{2}-1} f(y_{2j}) + 4\sum_{j=1}^{n/2} f(y_{2j-1}) + f(y_n)\right]$$

Where:

$$f\ y\ = \frac{1}{3}\ f'\ 3\ + 4f'\ 2\ + f'(1)$$

Equation 4.1.1: Distortion volume

Here f(y) is the area under the parabola in the transverse direction at each value of y along the weld (61).

To better illustrate the transverse out of plane distortion, figure 4.1.2 shows the change in panel height from welding in the transverse direction. At each y position, the three out of plane measurements form a "v" shape, due to the concave transverse bowing. The central point of each "v" shaped curve corresponds to the location along the weld that each measurement was taken (read from the X axis in the figure). Again, this is the difference between pre and post weld measurements. Note from figure 4.1.1 this is in contrast to the convex longitudinal bowing. This distortion, concave perpendicular to the weld and convex parallel to the weld (when viewed from the crown side) is consistent with the observations by Shi (31) and was displayed by all welds in this study.

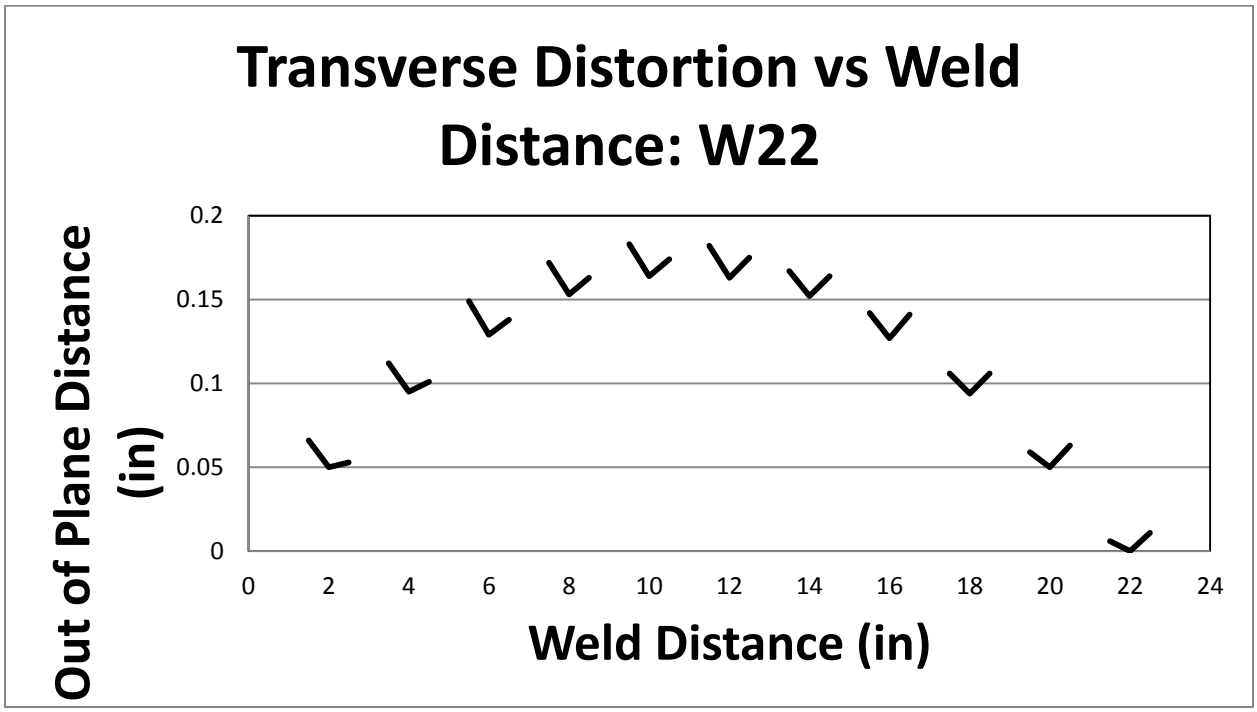

Figure 4.1.2: Transverse out of plane distortion

Figures 4.1.1 and 4.1.2 are shown for each weld in the appendix.

Table 4.1.1 shows the distortion data for each weld. The distortion volume in table 4.1.1 is the difference between the pre and post weld distortion and is thus not a physical

representation of the welded extrusion. The difference between pre and post welded out of plane distortion measurements was used to construct a surface (many of the extrusions had out of plane distortion prior to welding). The volume constrained by a plane (intersecting the lowest point of this surface) and the surface is the value reported in table 4.1.1.

The transverse out of plane distortion is the perpendicular distance between the central measurement point of each "v" shaped curve and a constructed line through the two outer measurement points. The left side of figure 4.1.3 shows a typical case (and looks in the direction of the weld). Here, the central measurement point is lower than the two edge points, and the line between the two edge points is not necessarily parallel to the measurement coordinate system (or with other transverse curves further along the weld). The maximum value for each weld is reported in the table. The maximum longitudinal out of plane distortion is the distance in the z direction from the datum plane to the highest point (typically an edge point, near the middle of the panel, as in figure 4.1.1). Figure 4.1.3 shows how these points were determined. Again, these values do not necessarily represent physical reality, but are the difference between pre and post weld measurements.

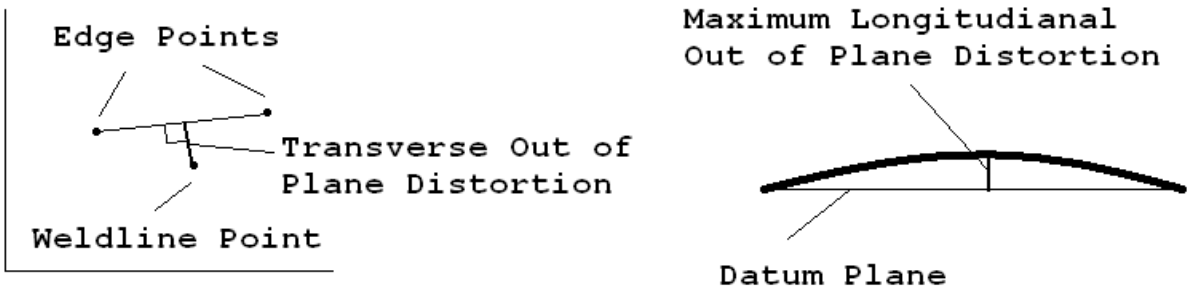

Figure 4.1.3: Maximum out of plane distortion depiction

Weld Schedule (rpm/in/ft-lbs)	Weld ID	Distortion Volume (in^3)	Maximum Transverse Distortion (in)	Maximum Longitudinal Distortion (in)
340/8/25	w10	5.061	0.025	0.195
	w22	4.816	0.025	0.183
340/8/75	w16	3.805	0.022	0.143
	w28	3.571	0.019	0.134
340/2/25	w15	3.577	0.018	0.131
	w23	3.034	0.008	0.117
340/2/75	w5	1.571	0.028	0.076
	w17	1.328	0.017	0.053
380/8/25	w9	5.408	0.026	0.207
	w30	6.198	0.032	0.236
380/8/75	w2	4.822	0.008	0.178
	w27	4.706	0.047	0.194
380/2/25	w13	2.806	0.017	0.105
	w31	6.467	0.035	0.242
380/2/75	w11	1.542	0.012	0.062
	w29	1.826	0.021	0.077
360/4/50	w12	2.693	0.016	0.102
	w25	3.17	0.024	0.122
360/4/50	w6	2.228	0.025	0.090
	w24	2.853	0.011	0.112
340/4/50	w3	3.817	0.022	0.145
	w19	2.913	0.026	0.104
380/4/50	w14	2.617	0.016	0.105
	w26	2.672	0.007	0.103
360/8/50	w4	3.868	0.031	0.153
	w32	7.31	0.059	0.292
360/2/50	w1	2.639	0.014	0.103
	w20	2.018	0.022	0.079
360/4/25	w8	3.819	0.020	0.149
	w18	1.344	0.021	0.051
360/4/75	w7	1.778	0.015	0.069
	w21	2.873	0.016	0.104

Table 4.1.1: Distortion data

As expected, the lowest distortion volume (the average between the two replications) is for the 340/2/75 weld schedule and the

largest distortion volume is the 380/8/25 schedule. This trend does not hold with maximum transverse out of plane distortion.

All welded panels exhibited out of plane distortion of the form seen in figure 4.1.1. This agreed with the findings in reference (31) – when viewed from the crown side, the panels displayed convex longitudinal distortion, and concave transverse distortion. Reference (31) found that the size of the panel played a role in distortion, and the pin tool design and weld schedules used differed from this study, so comparisons must be made carefully. Reference (31) reported transverse distortion of 0.04-0.08” and longitudinal distortion of 0.08-0.16” which at least overlaps this data.

Further statistical analysis will be discussed in the DOE section.

4.2 In Plane Linear Distortion

Again, a representative single numerical value for linear distortion was sought for input to the DOE software. Two distortion responses were measured: transverse (perpendicular to the weld) and longitudinal (parallel to the weld). These were determined by comparing the pre and post weld distances between punch marks.

Figure 4.2.1 shows the representative form of linear distortion displayed by all welds. The in-plane transverse linear distortion is negative – in this case the panel was ~0.01” narrower after the weld. All welds in the study displayed transverse shrinkage in this manner. The transverse shrinkage vs longitudinal distance curve is typically “u” shaped. Since the first and last 2” of the extrusions were not welded, linear distortion is constrained by un-welded material at the beginning and end of the weld. In-plane linear distortion was also measured in the longitudinal direction. This measurement was taken on both the advancing and retreating side of the weld. As displayed in figure 4.2.1, the average longitudinal linear distortion was more positive than the transverse distortion. The clamp locations and spacing had no obvious effect on the longitudinal linear distortion.

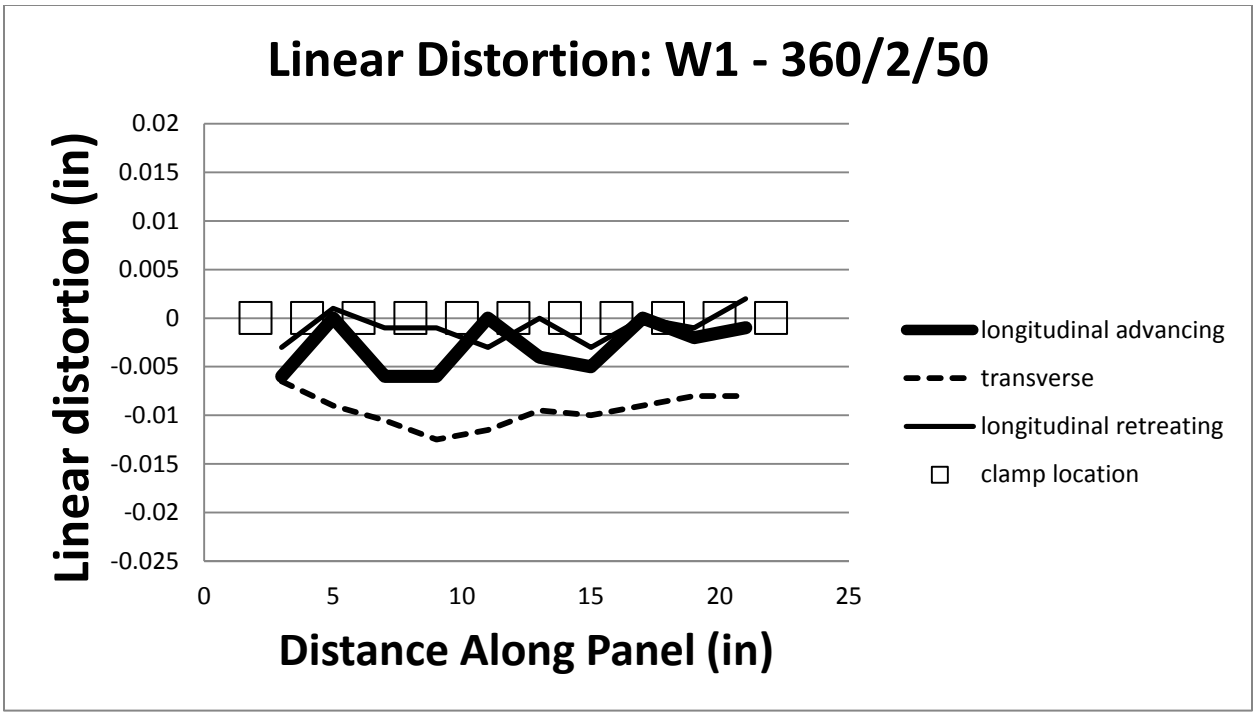

Figure 4.2.1: Linear distortion for weld 1

Table 4.2.1 shows the average transverse distortion and the total longitudinal distortion for both the advancing and retreating sides, for each weld. Negative numbers imply shrinkage, and positive numbers imply expansion. Figure 4.2.1 is shown for each weld in the appendix.

Weld ID	Weld Schedule	Total Linear Distortion, Retreating Side (in)	Total Linear Distortion, Advancing Side (in)	Average Transverse Distortion (in)
w1	360/2/50	-0.009	-0.030	-0.009
w2	380/8/75	-0.026	0.012	-0.012
w3	340/4/50	-0.017	-0.007	-0.007
w4	360/8/50	-0.031	-0.026	-0.012
w5	340/2/75	-0.016	-0.015	-0.008
w6	360/4/50	-0.060	-0.020	-0.008
w7	360/4/75	-0.003	-0.018	-0.008
w8	360/4/25	-0.020	-0.021	-0.011
w9	380/8/25	-0.023	-0.010	-0.013
w10	340/8/25	-0.029	-0.026	-0.010
w11	380/2/75	-0.024	-0.027	-0.008
w12	360/4/50	-0.016	0.007	-0.008
w13	380/2/25	-0.022	-0.016	-0.010
w14	380/4/50	-0.007	0.015	-0.008
w15	340/2/25	0.017	-0.006	-0.006
w16	340/8/75	0.015	0.000	-0.008
w17	340/2/75	-0.022	-0.019	-0.006
w18	360/4/25	-0.007	-0.017	-0.011
w19	340/4/50	-0.010	-0.004	-0.009
w20	360/2/50	-0.017	-0.013	-0.009
w21	360/4/75	-0.024	-0.019	-0.008
w22	340/8/25	-0.018	-0.033	-0.010
w23	340/2/25	-0.036	-0.033	-0.010
w24	360/4/50	-0.028	-0.033	-0.010
w25	360/4/50	-0.026	-0.032	-0.007
w26	380/4/50	-0.035	-0.029	-0.011
w27	380/8/75	-0.015	-0.015	-0.012
w28	340/8/75	-0.005	-0.011	-0.009
w29	380/2/75	-0.007	-0.013	-0.006
w30	380/2/25	-0.007	-0.002	-0.011
w31	380/8/25	-0.010	-0.042	-0.010
w32	360/8/50	0.016	-0.012	-0.012

Table 4.2.1: In plane linear distortion

The largest distortion volume welds (380/8/25) have large transverse linear distortion (in the case of W9, the largest). The lowest distortion volume welds (340/2/75) have low transverse linear distortion (in the case of W17, the lowest).

The longitudinal distortion measurements show no compelling correlation with volumetric distortion data. The erraticism of the data for the longitudinal distortion further calls into question the validity of these measurements. All welds in the study increased in crown side convexity (as well as actually being convex after welding), so a crown side transverse expansion was expected. Root side shrinkage is not expected to be the mechanism, since most of the heat is generated at the crown side by the pin tool shoulder. Figure 4.2.2 shows a possible explanation for this discrepancy.

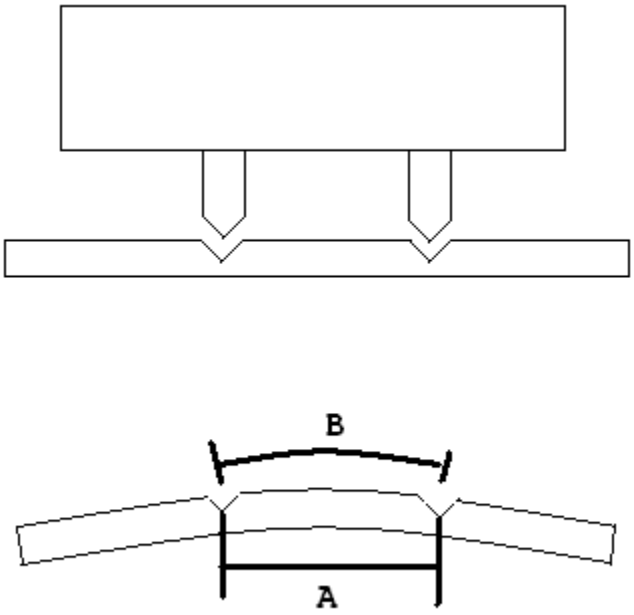

Figure 4.2.2: Punch measurement clarification

The punch distance measurement calipers measure the distance A in the curved post weld representation. Distance B is parameter that should dictate longitudinal bowing of the welds. The difference between A and B gets larger with larger radii of curvature. This may have contributed to both the erratic nature of the longitudinal shrinkage measurements, as well as them

being mostly negative (when a positive result was expected). Whatever the case, the longitudinal linear distortion measurements show little regularity and are of ambiguous physical significance; they will not be analyzed in the DOE section.

4.3 Weld Power

The required spindle torque to maintain a given rotation speed in an FSW arises from two mechanisms: friction between the pin tool at the weld material and the work required to deform the weld nugget. Since the material properties that dictate those mechanisms are temperature dependant, a complex inherent feedback loop exists. Therefore, when an FSW machine's spindle is operating in speed control mode (the usual case), the torque experienced by the spindle is a response parameter based on – in this study – the rotation speed and clamping environment. The spindle torque on the PDS is calculated from the pressure drop across the hydraulic motor that drives the spindle. The weld power is the product of the spindle torque and the spindle speed, both of which are logged at a frequency of 1Hz.

Equation 3.5.1 gives the frictional contribution to torque and suggests that the torque for the pin tool used in this study should be ~140in-lb. The measured torques for all welds in this study were in the narrow band of 26-28in-lb. Since this is much lower than predicted with frictional reasoning, other factors must be at play. The friction model may benefit by substituting the friction coefficient (with the suggested value of 0.5) with a much lower effective friction coefficient – in the study ~0.1.

The measured power for each weld is shown in table 4.3.1 (which has been sorted for increasing weld power).

Weld ID	Weld Schedule	Power (watts)
w3	340/4/50	109.6
w16	340/8/75	109.7
w5	340/2/75	109.7
w15	340/2/25	109.7
w10	340/8/25	109.7
w28	340/8/75	110.2
w19	340/4/50	110.3
w23	340/2/25	110.5
w22	340/8/25	111.0
w17	340/2/75	111.3
w8	360/4/25	114.1
w1	360/2/50	114.2
w12	360/4/50	114.2
w7	360/4/75	114.2
w4	360/8/50	114.3
w25	360/4/50	114.4
w24	360/4/50	114.5
w21	360/4/75	114.5
w32	360/8/50	114.5
w18	360/4/25	114.5
w20	360/2/50	114.6
w6	360/4/50	115.7
w9	380/8/25	118.2
w2	380/8/75	118.3
w14	380/4/50	118.3
w11	380/2/75	118.3
w13	380/2/25	118.3
w29	380/2/75	118.4
w27	380/8/75	118.4
w30	380/2/25	118.4
w31	380/8/25	118.4
w26	380/4/50	118.5

Table 4.3.1: Weld power

A strong correlation between tool rotation speed and power is obvious. The relationship between power and clamp pitch or tightening torque is not clear.

The variation of weld power for a given tool rotation speed is low, but following the trend for rpm, the lowest average distortion volume welds (340/2/75) were in the lowest power range, and the highest average distortion welds (380/8/25) were in the high power range. This could indicate that distortion is affected by peak temperature, amount of plastic deformation, or both.

Further statistical analysis will be discussed in the DOE section.

4.4 Nugget Hardness

A sample was excised from each weld (along with one parent metal sample) for microstructural analysis. The samples were polished, etched, and photographed for a qualitative examination of the weld nugget. Each sample was tested for Vicker's hardness at room temperature. The samples were tested at T/2 thickness. The indentation load and time was 40kg and 10s respectively. Measurements were taken every 0.3mm. The samples were removed from the middle of the weld length. Additionally, 2 welds, taken at random from each replication, had a second hardness sample taken 1" further down the weld from the middle sample.

Table 4.4.1 shows the Vicker's Hardness for each weld. A single representative value was sought for input to the DOE software. The stir zone of all welds in this study was the location of minimum hardness. This "U" shape contrasts with the more typical "W" shape as seen in figure 2.2.2. The lowest 16 hardness values were averaged for each weld. This roughly corresponds to the swept diameter of the pin tool probe.

Weld Schedule	Weld ID	Vicker's Hardness
340/8/25	w10	61.7
	w22	58.8
340/8/75	w16	60.7
	w28	60.4
340/2/25	w15	65.3
	w23	64.9
340/2/75	w5	62.6
	w17	62.8
380/8/25	w9	60.7
	w30	59.3
380/8/75	w2	56.3
	w27	56.6
380/2/25	w13	59.9
	w31	56.5
380/2/75	w11	60.4
	w29	56.9
360/4/50	w12	62.2
	w25	59.9
360/4/50	w6	60.8
	w24	58.5
340/4/50	w3	61.4
	w19	60.4
380/4/50	w14	59.0
	w26	58.1
360/8/50	w4	60.0
	w32	56.5
360/2/50	w1	57.6
	w20	59.4
360/4/25	w8	63.6
	w18	58.5
360/4/75	w7	59.6
	w21	61.3

Table 4.4.1: Hardness data

Reynolds showed that, for 7075 aluminum FSW, nugget hardness can be correlated with maximum nugget temperature (26). Low hardness then, indicates that a higher peak temperature was

experienced in the nugget and high hardness indicates that a lower temperature was experienced. The hardness data continues to follow the previously observed trend – the 340/2/25 has the highest average hardness and the 380/2/75 has the second lowest hardness (the lowest being 380/8/75).

All the hardness profiles in this study were U shaped as seen in figure 4.4.1. This plot shows the Vicker's Hardness Number (VHN) vs distance from the edge of the macro.

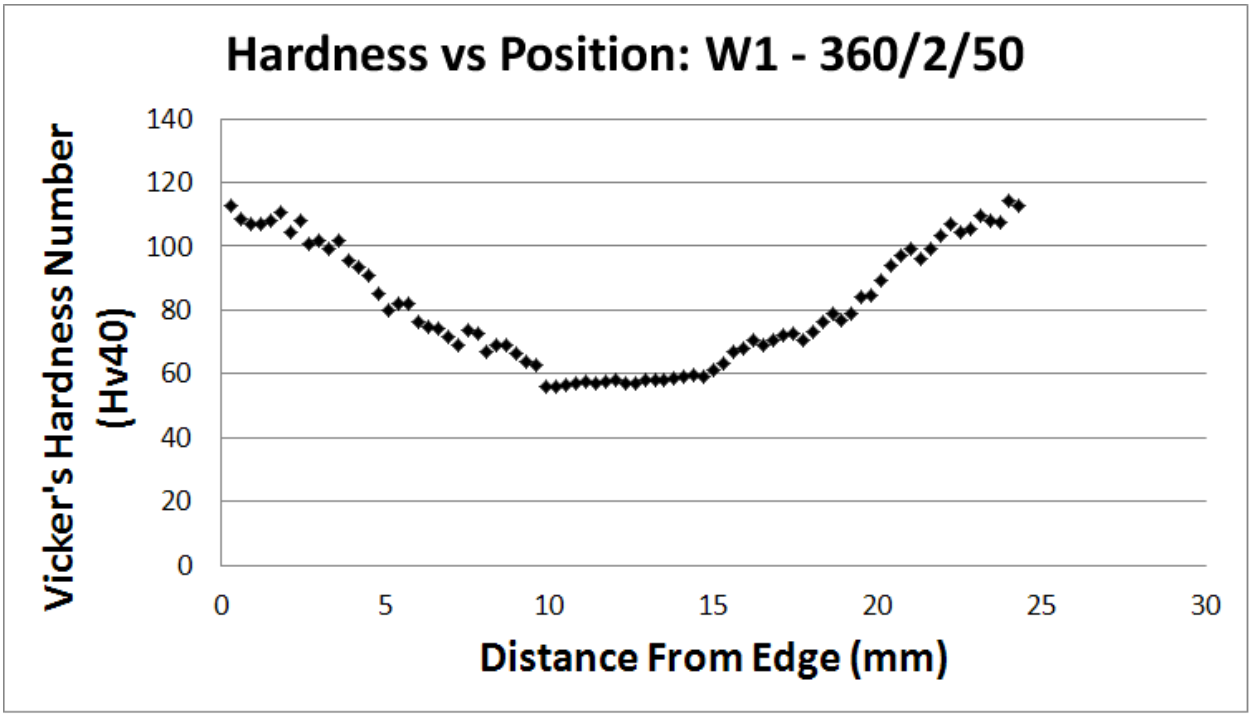

Figure 4.4.1: Typical hardness profile

The average hardness of the parent extrusion was VHN 111.8, so the chosen width of the macro was sufficient to encompass metal with virgin properties, and show the entire structure of the stir zone and HAZ.

A macro from each weld was excised from the middle of the weld length. To confirm that this was an appropriate location, some welds (two taken at random from each of the two replications) had a second macro removed a further 1" down the weld length. Figure 4.4.2 shows the two hardness profiles of weld 5 (one of the welds randomly selected to have two macros removed). The close agreement of the two profiles indicates that at least a

pseudo steady state had been reached in nugget hardness; the same being inferred for temperature. Thus, the macro location for each weld (the middle of the weld length) is assumed to be a good indicator of steady state properties for that weld.

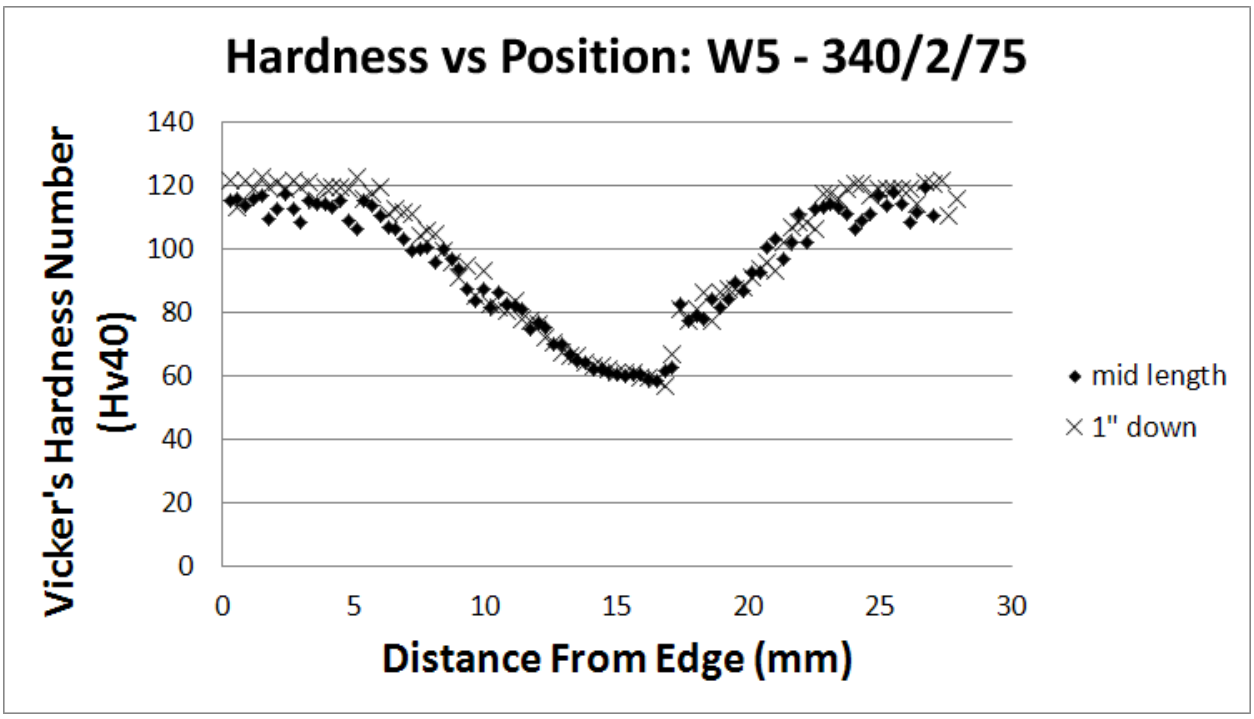

Figure 4.4.2: Comparison of two hardness profiles from same weld

A hardness profile for each weld (two where appropriate) is shown in the appendix, along with a photograph of the macro.

Further statistical analysis will be discussed in the DOE section.

4.5 DOE Analysis

The DOE analysis was performed using the same software that generated the test matrix – DOE Pro XL. The input factors were tool rotation speed, clamp pitch, and clamp tightening torque. The same DOE analysis tools will be applied to each of the four responses: out of plane distortion volume, in plane transverse linear distortion, weld power, and nugget hardness.

Iterative linear regression will determine which factors and factor interactions are significant in affecting the response

variable. The software calculates the P(2tail) for each factor, which is the probability that a factor does not belong in the regression model. DOE PRO suggests elimination of factors with P(2tail)>=0.1.

The DOE model coefficients (β values from equation 2.7.1) are displayed in table 4.5.2 for all factors combinations, and the reduced model (where the insignificant factors are disregarded). This table also shows the R^2 value for both the full and reduced models.

The reduced model is shown graphically in figure 4.5.1. For clarity, the modeled response values were sorted by size, and plotted with their corresponding measured data. The X-axis of figure 4.5.1 is thus "weld ID number", but because of sorting, they are not in order. For each value of X, if the point and the curve are close, the model is accurate for that combination of parameters. The closer the R^2 is to 1, the better the model is at predicting the response behavior over the entire parameter space. The regression model, which is in the form of equation 2.7.1, is shown in tabular form where the coefficients are shown for both the full and reduced models.

An ANOVA (ANalysis Of VAriance) will determine the percent contribution of each factor on the response variable. DOE Pro is incapable of generating ANOVA tables for three level designs, so the ANOVA tables are based on only the low and high levels for each factor. It is understood that this is not a perfect representation of the experimental data, but should provide an indication of the factor contributions to the response variables.

Marginal means plots show the effect of each factor on the response variable. Marginal means plots show the averaged values of the response for each value of an input variable. Four marginal means plots are shown. This first shows all input variables on one plot (the X axis for each variable is different, but is read low to high, left to right). The next three plots show each input variable separately, with the total range of the response variable indicated.

Volumetric Distortion

The following tables and figures describe the volumetric distortion response. The volumetric distortion of FSW panels is most strongly affected by clamp pitch and clamp tightening torque. It is somewhat surprising that tool rotation speed is not a significant factor. The inconsistent effect of rotation speed (the "V shape of the curve) seen in the marginal means plot may be contributing to this. The marginal means plot shows that clamping pitch may have reached a saturation value at 4", since a decrease to 2" only slightly decreased distortion volume. The saturation value of clamping torque was not reached by 75ft-lb, and volumetric distortion could likely be decreased further with increasing clamping torque. The explanation for the shape of the rotation speed curve is not obvious. The R^2 value of the reduced model (0.57) indicates a rather poor fit of the data.

		All factors	Reduced Model
Factor	**Name**	**P(2 Tail)**	**P(2 Tail)**
A	rpm	0.242	
B	clamp pitch	0.000	0.000
C	torque	0.006	0.004
AB		0.712	
AC		0.679	
BC		0.334	
ABC		0.542	
AA		0.665	
BB		0.111	
CC		0.456	

Table 4.5.1: Significant factors for distortion volume

Factor	Name	All Factors	Reduced Model
Const		5.39E+01	3.00E+00
A	rotation speed	-3.19E-01	
B	clamp pitch	6.10E-01	4.08E-01
C	clamp torque	2.86E-01	-2.94E-02
AB		-3.82E-03	
AC		-7.66E-04	
BC		-3.58E-02	
ABC		1.09E-04	
AA		5.05E-04	
BB		9.71E-02	
CC		-5.59E-04	
	R^2	**0.68**	**0.57**

Table 4.5.2: DOE model coefficients

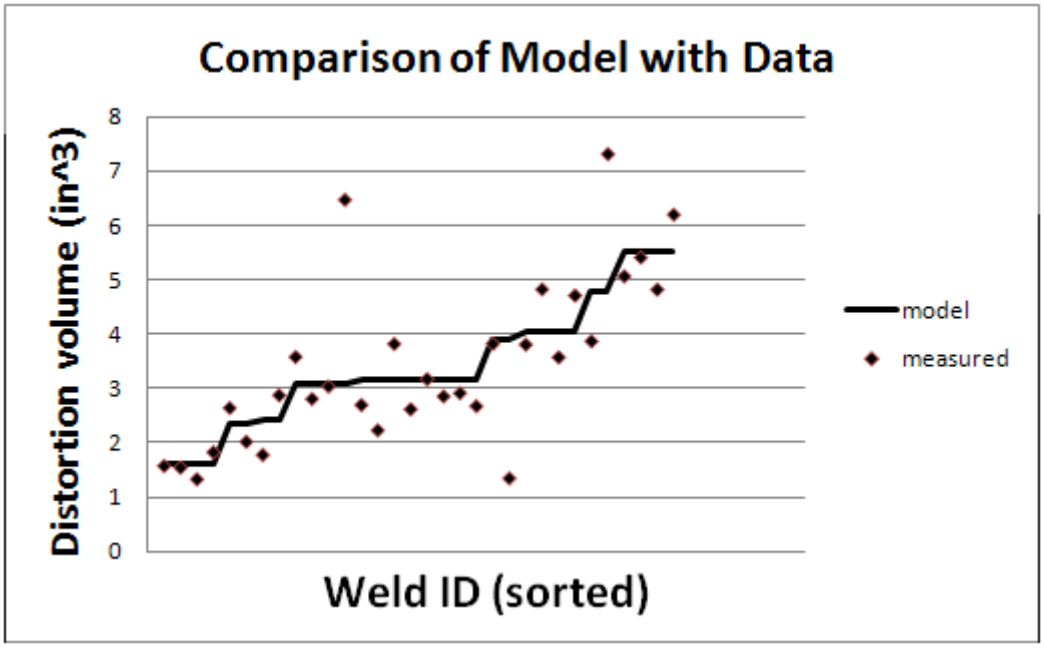

Figure 4.5.1: Reduced regression model for distortion volume

	Factor	Contribution
A	rpm	7.4%
B	pitch	39.5%
C	torque	30.2%
AB		0.1%
AC		0.5%
BC		3.8%
ABC		1.0%
error		17.5%

Table 4.5.3: ANOVA factor contribution for distortion volume

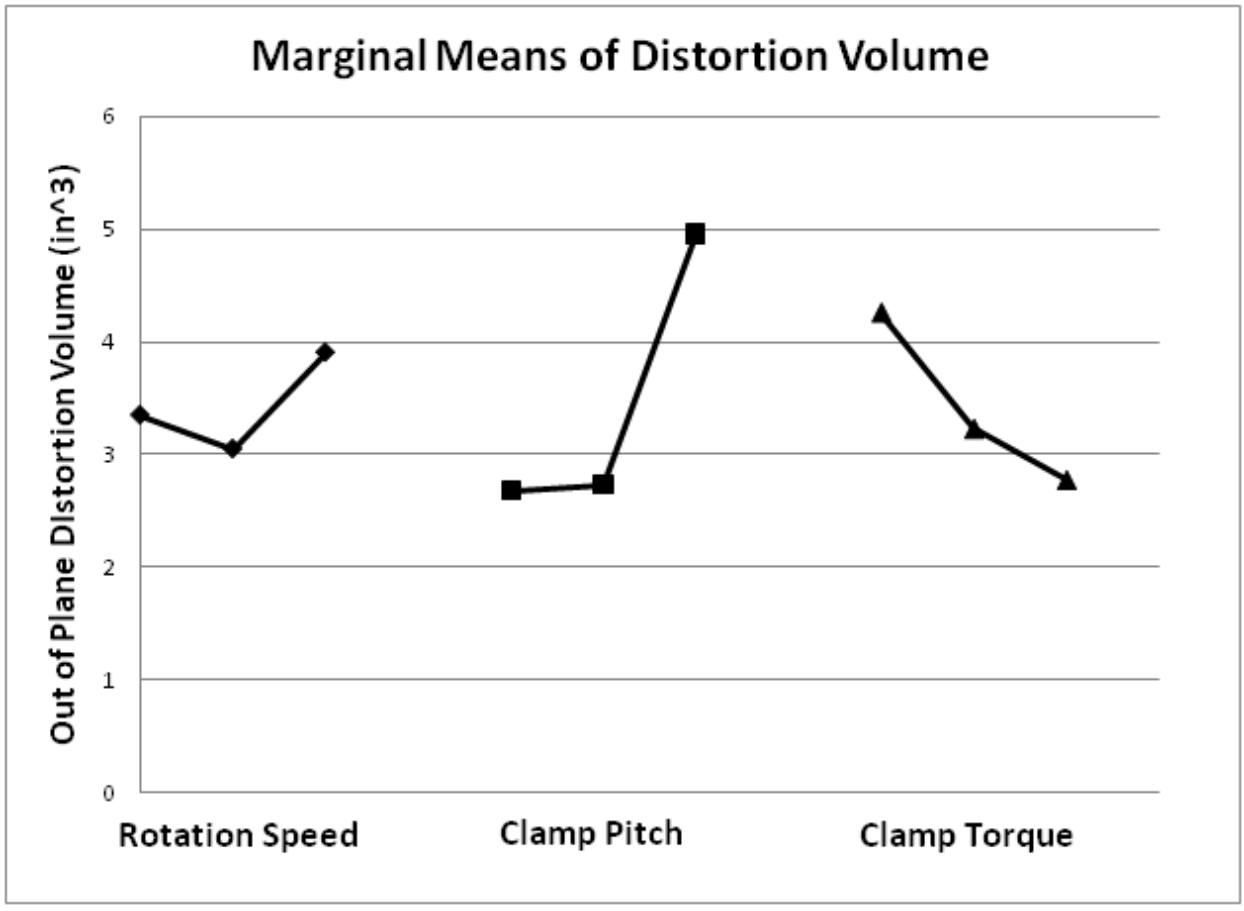

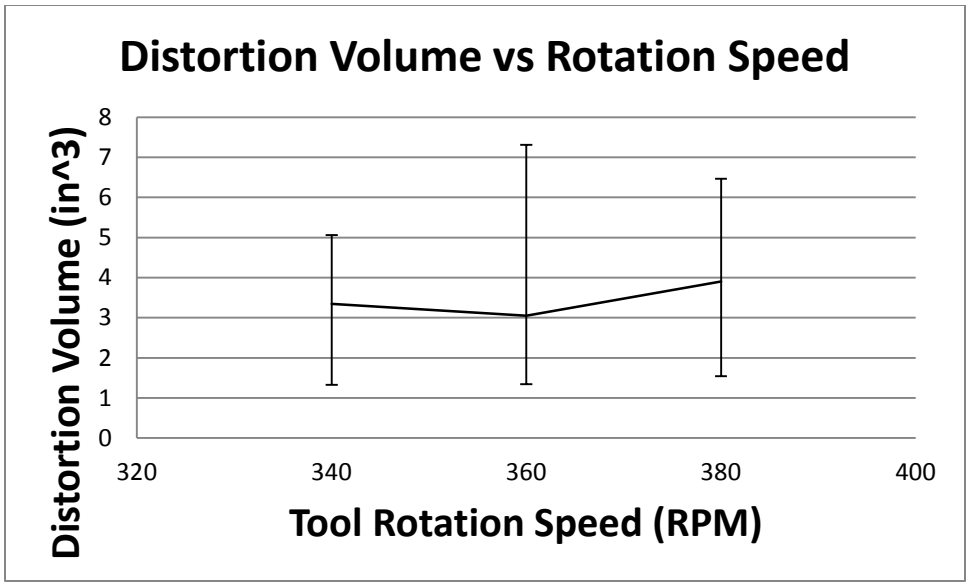
Distortion Volume vs Rotation Speed
Distortion Volume (in^3)
0
1
2
3
4
5
6
7
8
320
340
360
380
400
Tool Rotation Speed (RPM)

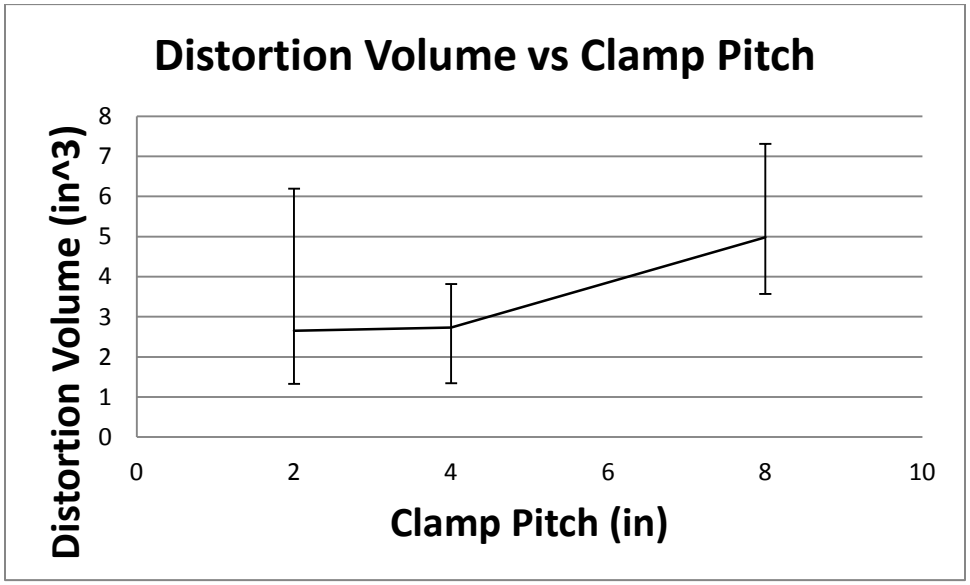
Distortion Volume vs Clamp Pitch
Distortion Volume (in^3)
0
1
2
3
4
5
6
7
8
0
2
4
6
8
10
Clamp Pitch (in)

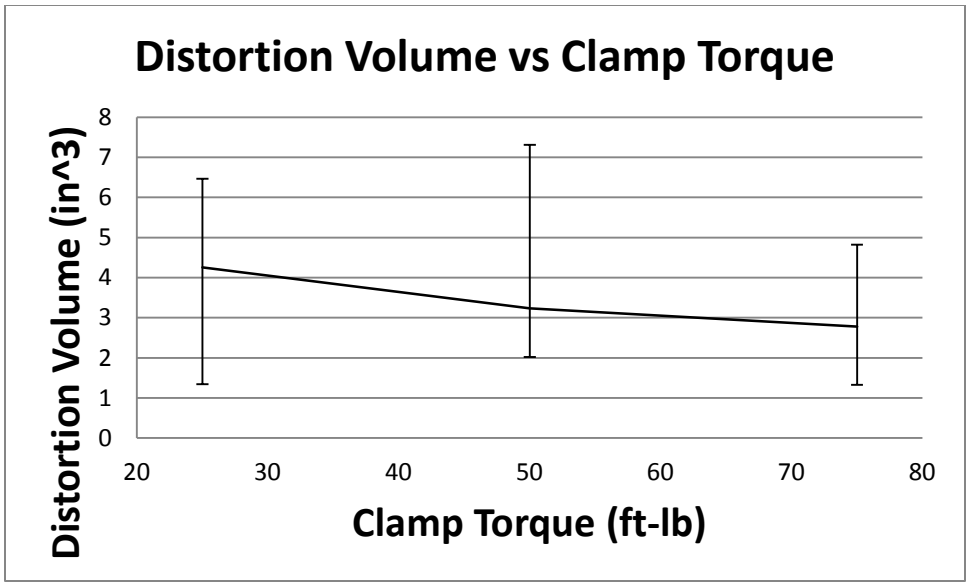

Figure 4.5.2: Marginal means plots for distortion volume

Linear Distortion

The following tables and figures describe the average transverse shrinkage response. Unlike for distortion volume, tool rotation speed has both a consistent and significant effect on transverse shrinkage. The clamp pitch saturation effect seen in distortion volume is also displayed by transverse shrinkage, but is less pronounced. As with distortion volume, clamp pitch is the most significant factor controlling linear distortion. The accuracy of the linear distortion reduced model is not much better than the one for distortion volume, with a R^2 value of 0.62.

		All Factors	Reduced Model
Factor	**Name**	**P(2 Tail)**	**P(2 Tail)**
A	rpm	0.003	0.005
B	clamp pitch	0.000	0.000
C	torque	0.005	0.005
AB		0.132	
AC		0.834	
BC		0.232	
ABC		0.153	
AA		0.108	
BB		0.201	
CC		0.791	

Table 4.5.4: Significant factors for average transverse shrinkage

Factor	Name	All Factors	Reduced Model
Const		-2.97E-01	-6.50E-03
A	rotation speed	1.64E-03	4.25E-05
B	clamp pitch	1.86E-03	4.64E-04
C	clamp torque	4.91E-04	-3.40E-05
AB		-6.97E-06	
AC		-1.58E-06	
BC		-1.00E-04	
ABC		2.92E-07	
AA		-2.16E-06	
BB		8.60E-05	
CC		2.21E-07	
	R^2	**0.74**	**0.62**

Table 4.3.5: DOE model coefficients

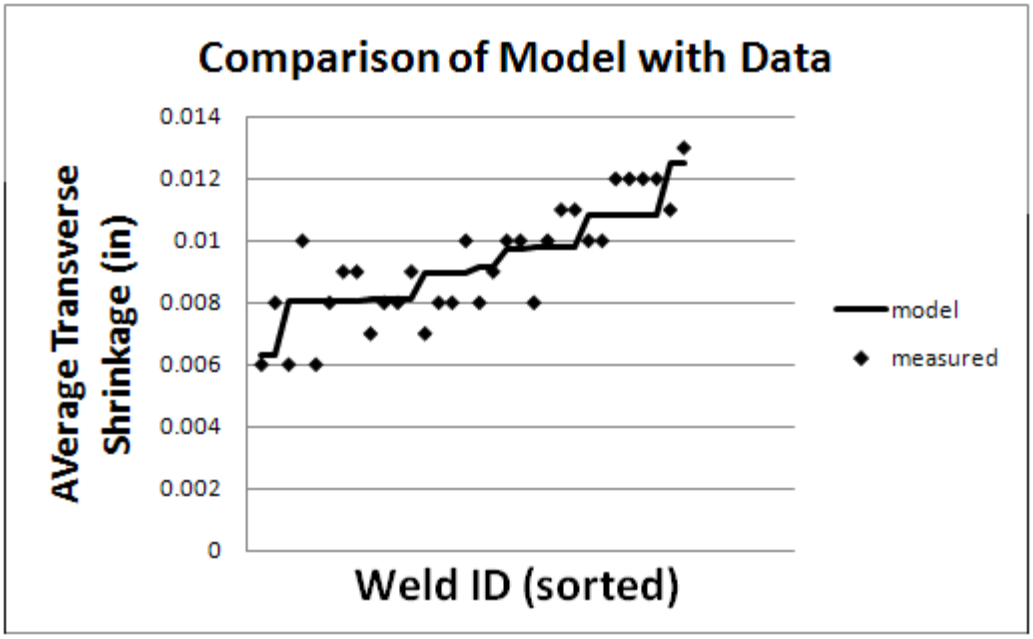

Figure 4.5.3: Reduced regression model for average transverse shrinkage

	Factor	Contribution
A	rpm	19.7%
B	pitch	38.6%
C	torque	10.6%
AB		4.3%
AC		0.1%
BC		2.2%
ABC		4.3%
error		20.2%

Table 4.5.6: ANOVA factor contribution for average transverse shrinkage

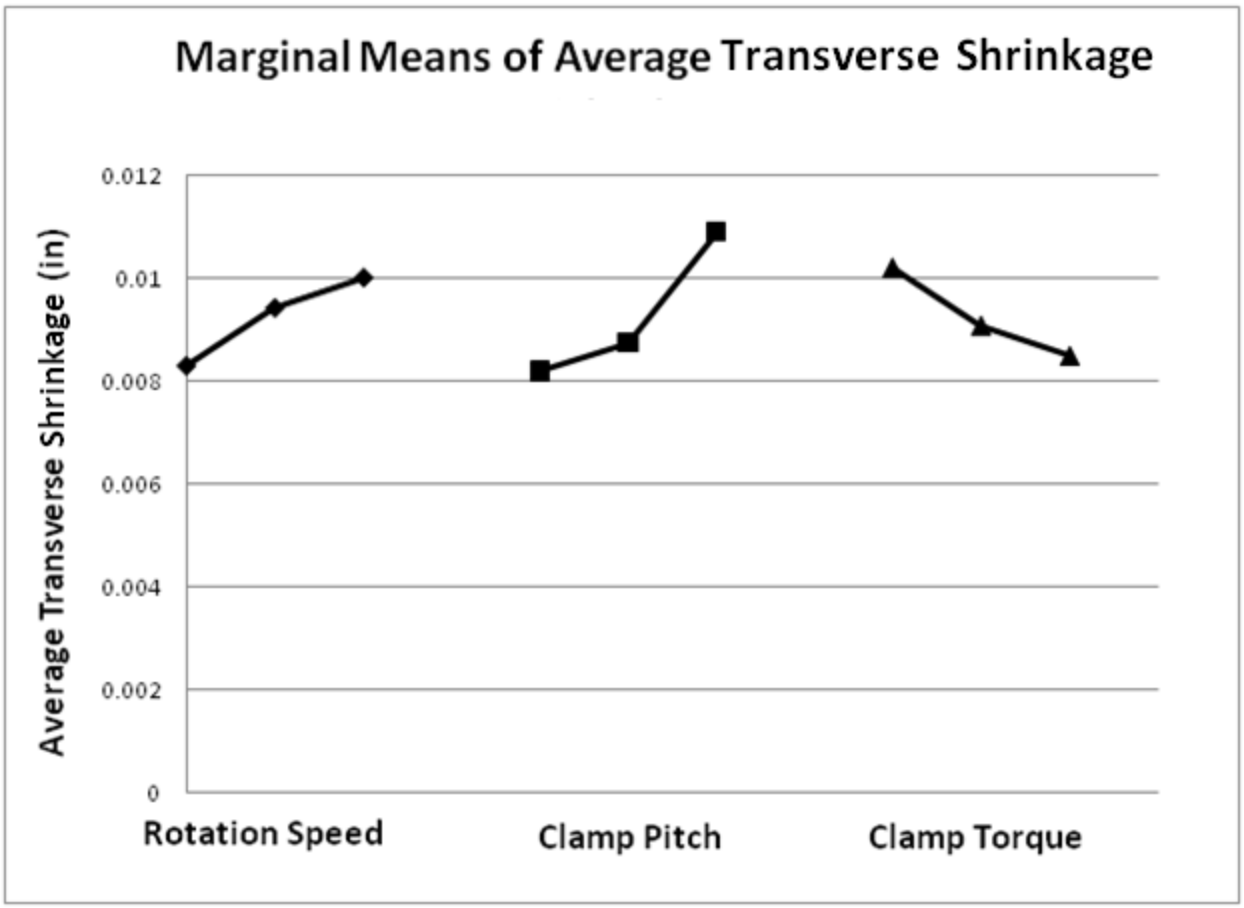
Marginal Means of Average Transverse Shrinkage
Average Transverse Shrinkage (in)
0.012
0.01
0.008
0.006
0.004
0.002
0
Rotation Speed
Clamp Pitch
Clamp Torque

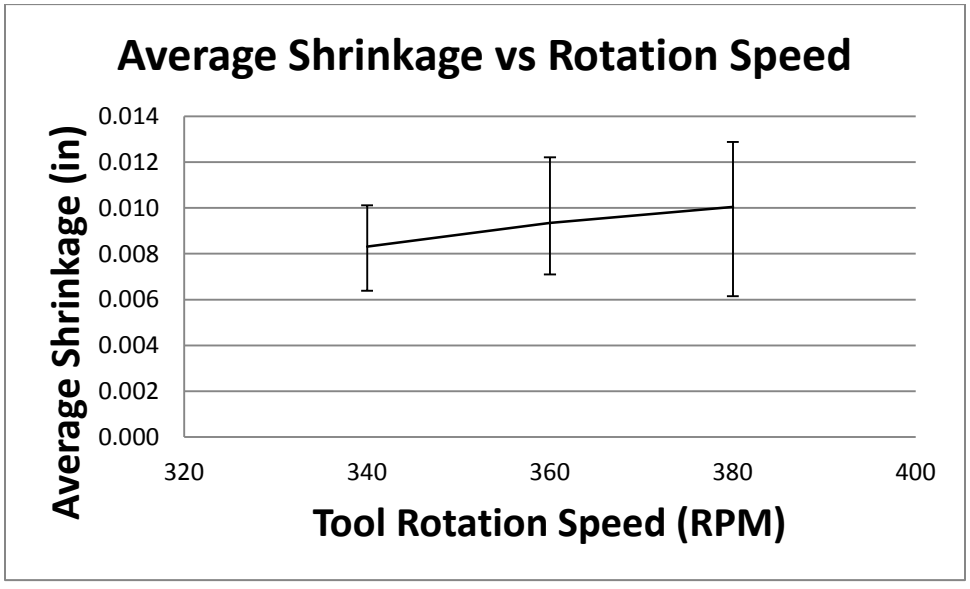
Average Shrinkage vs Rotation Speed
Average Shrinkage (in)
0.014
0.012
0.010
0.008
0.006
0.004
0.002
0.000
320
340
360
380
400
Tool Rotation Speed (RPM)

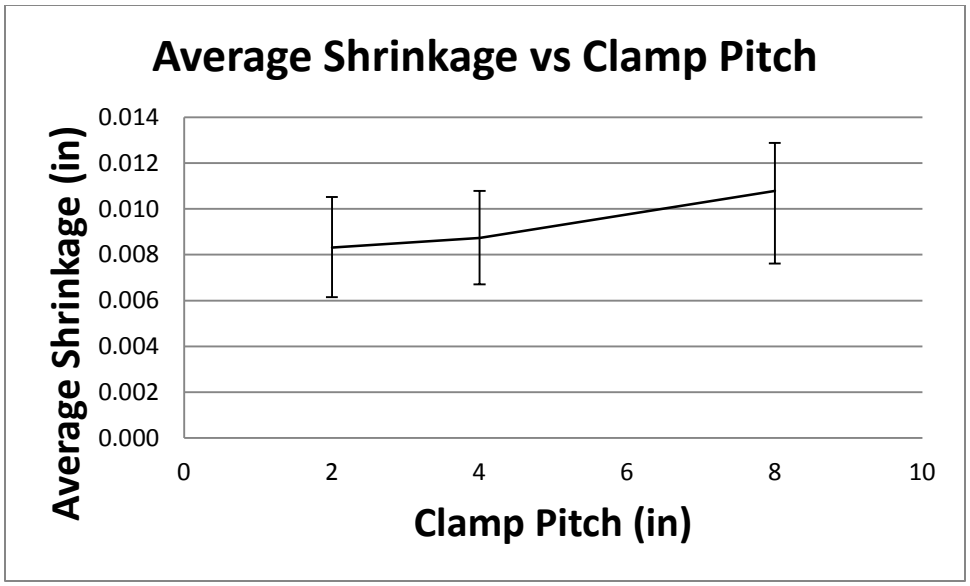

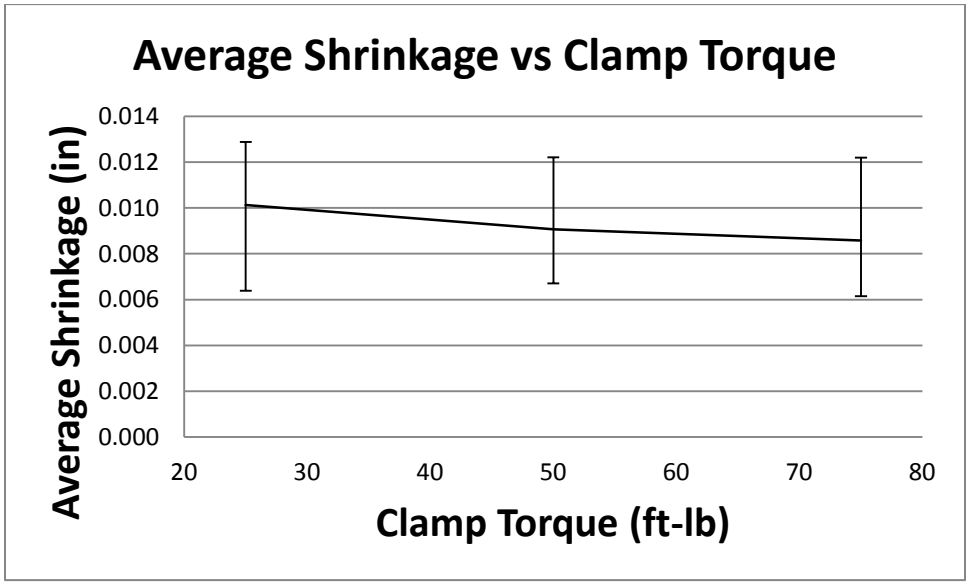

Figure 4.5.4: Marginal means plots for average transverse shrinkage

Weld Power

The following tables and figures describe the weld power response. Weld power is overwhelmingly dominated by tool rotation speed. The regression generated model fits the observed data with an R^2 value of 0.98. The altered heat sink that required the narrowing of the tool rotation speed range during the bounding welds apparently had no effect on weld

power, since neither of the clamping factors is significant on weld power.

		All Factors	Reduced Model
Factor	**Name**	**P(2 Tail)**	**P(2 Tail)**
A	rpm	0.000	0.000
B	clamp pitch	0.761	
C	torque	0.974	
AB		0.792	
AC		0.980	
BC		0.457	
ABC		0.416	
AA		0.364	
BB		0.952	
CC		0.804	

Table 4.5.7: Significant factors for weld power

Factor	Name	All Factors	Reduced Model
Const		-3.04E+01	4.06E+01
A	rotation speed	5.83E-01	2.05E-01
B	clamp pitch	1.08E+00	
C	clamp torque	1.42E-01	
AB		-2.90E-03	
AC		-3.52E-04	
BC		-2.61E-02	
ABC		6.91E-05	
AA		-5.05E-04	
BB		1.47E-03	
CC		-8.76E-05	
	R^2	**0.98**	**0.98**

Table 4.5.8: DOE model coefficients

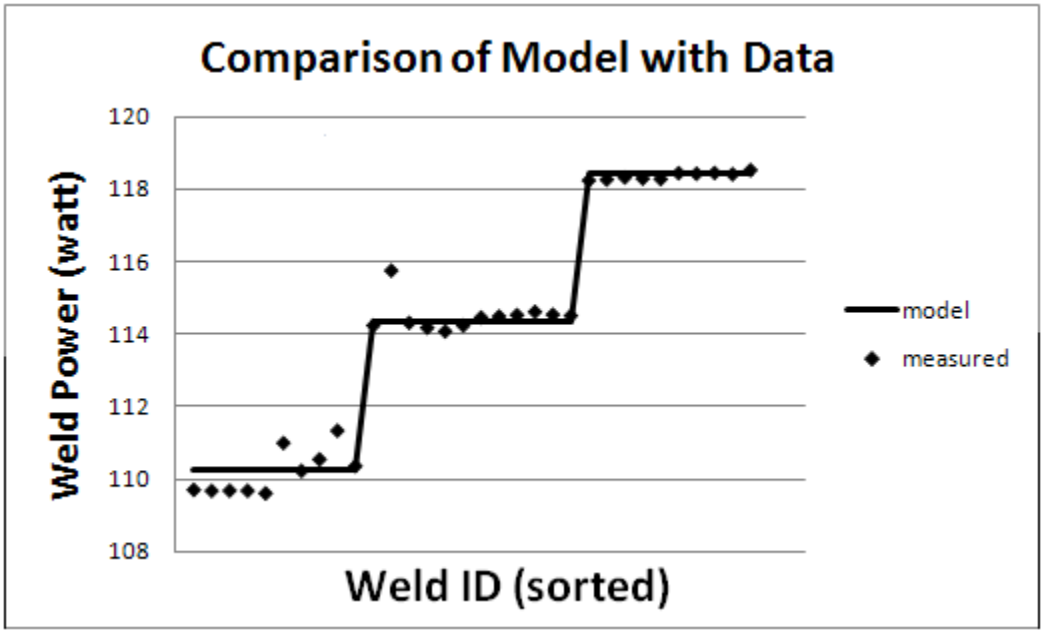

Figure 4.5.5: Reduced regression model for weld power

	Factor	Contribution
A	rpm	98.8%
B	pitch	0.0%
C	torque	0.0%
AB		0.0%
AC		0.0%
BC		0.1%
ABC		0.1%
Error		1%

Table 4.5.9: ANOVA factor contribution for weld power

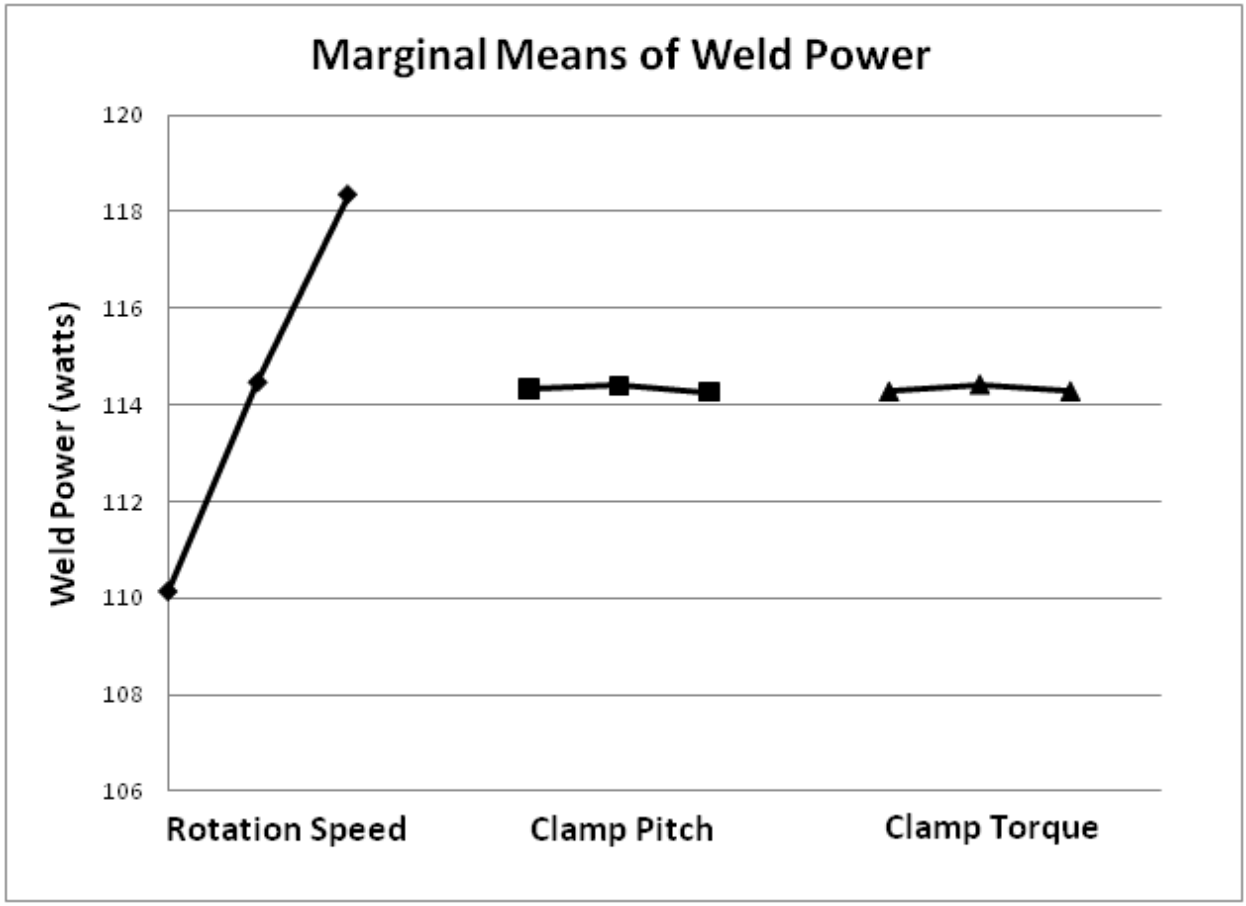
Marginal Means of Weld Power
Weld Power (watts)
120
118
116
114
112
110
108
106
Rotation Speed
Clamp Pitch
Clamp Torque

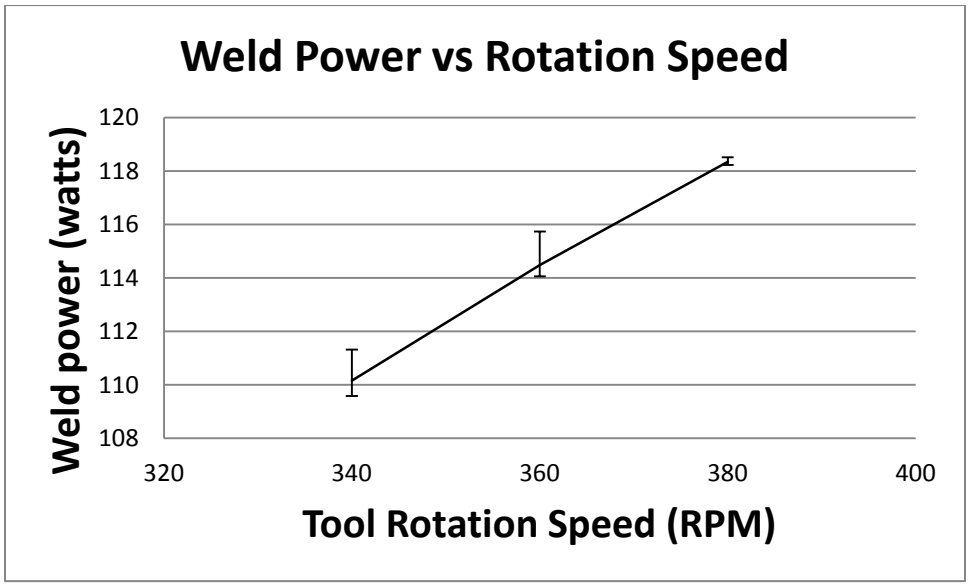
Weld Power vs Rotation Speed
Weld power (watts)
120
118
116
114
112
110
108
320
340
360
380
400
Tool Rotation Speed (RPM)

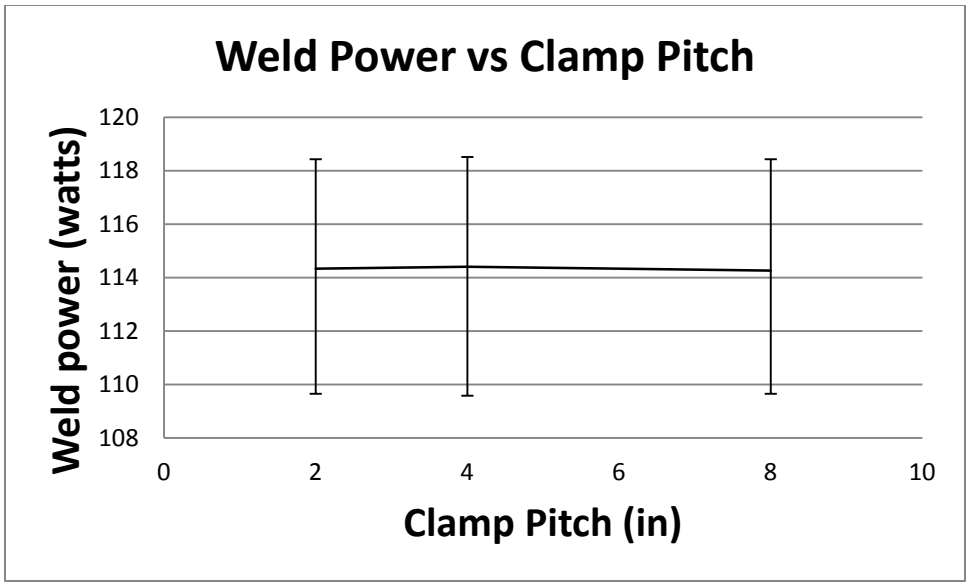

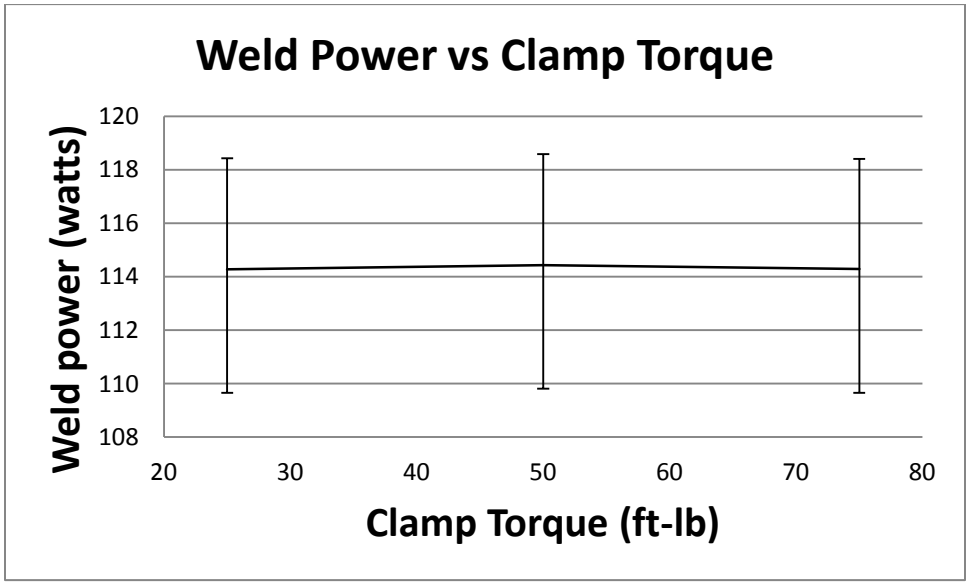

Figure 4.5.6: Marginal means plots for weld power

Hardness

The following tables and figures describe the nugget hardness response. The hardness response is the only one that is a function of combinations of input variables. The sole heat source for FSW is the spindle power, so it is not surprising that stir zone average hardness (a temperature dependent response) is affected mainly by rotation speed. The marginal means plot shows that a threshold in reached for a clamp torque of 50ft-lb; further clamp tightness did not affect hardness.

The R^2 of the regression model was 0.58, low, but consistent with the other models.

		All Factors	Reduced Model
Factor	**Name**	**P(2 Tail)**	**P(2 Tail)**
A	rpm	0.000	0.000
B	clamp pitch	0.096	0.089
C	torque	0.116	
AB		0.049	0.043
AC		0.755	
BC		0.685	
ABC		0.046	0.041
AA		0.918	
BB		0.340	
CC		0.180	

Table 4.5.10: Significant factors for weld hardness

Factor	Name	All Factors	Reduced Model
Const		1.43E+02	1.18E+02
A	rotation speed	-1.55E-01	-1.57E-01
B	clamp pitch	-1.44E+01	-5.15E+00
C	clamp torque	-1.08E+00	
AB		4.17E-02	1.43E-02
AC		2.54E-03	
BC		1.99E-01	
ABC		-5.58E-04	-1.18E-05
AA		-1.79E-04	
BB		-7.46E-02	
CC		1.53E-03	
	R^2	**0.67**	**0.56**

Table 4.5.11: DOE model coefficients

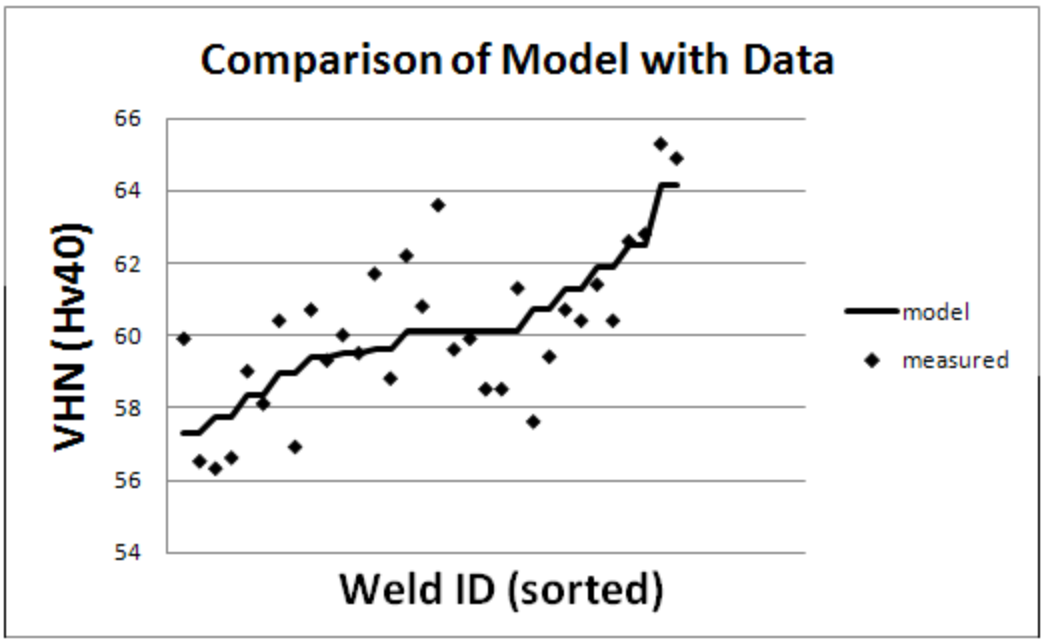

Figure 4.5.7: Regression model for weld hardness

	Source	Contribution
A	rpm	49.16%
B	pitch	11.50%
C	torque	5.68%
AB		9.15%
AC		0.21%
BC		0.35%
ABC		9.43%
error		14.52%

Table 4.5.12: ANOVA factor contribution for weld hardness

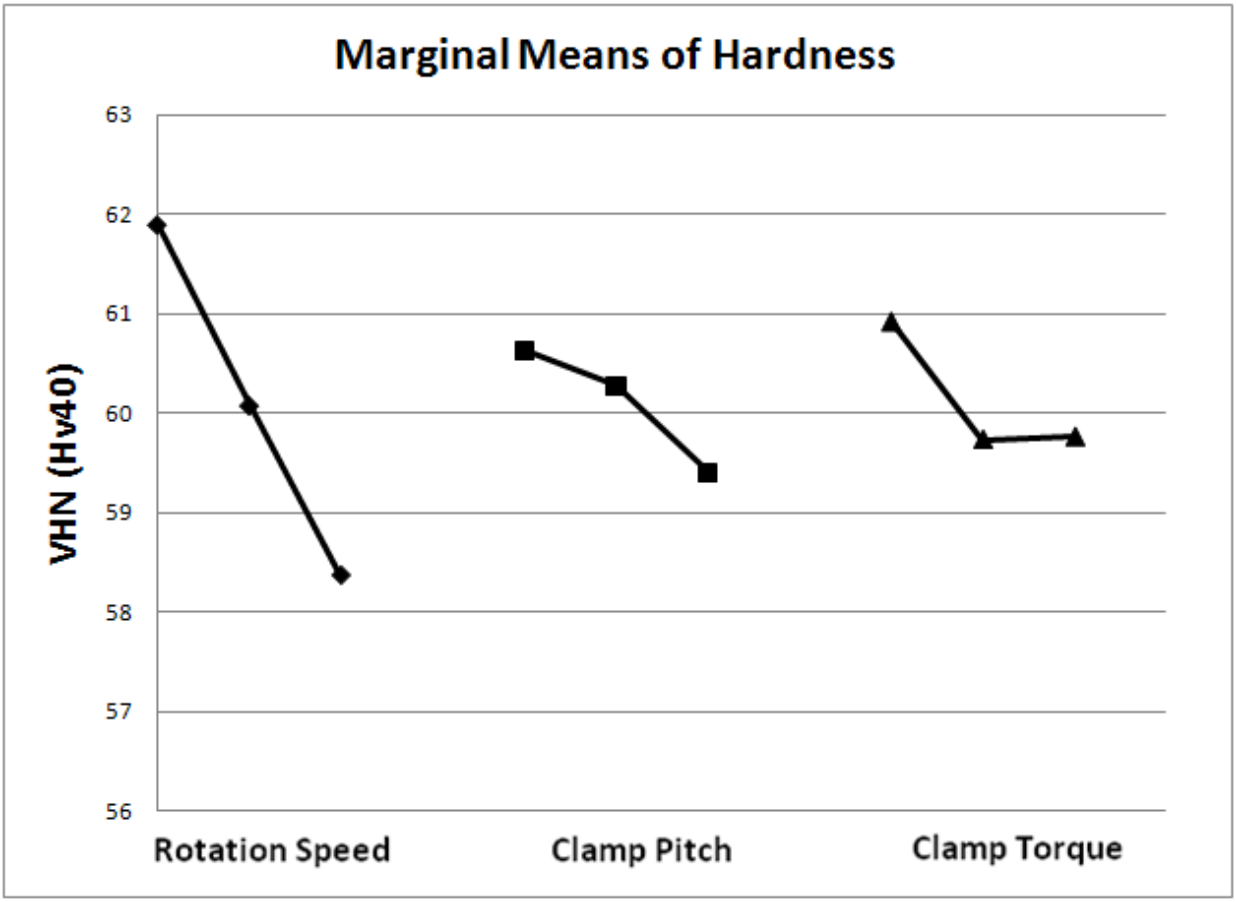
Marginal Means of Hardness
VHN (Hv40)
63
62
61
60
59
58
57
56
Rotation Speed
Clamp Pitch
Clamp Torque

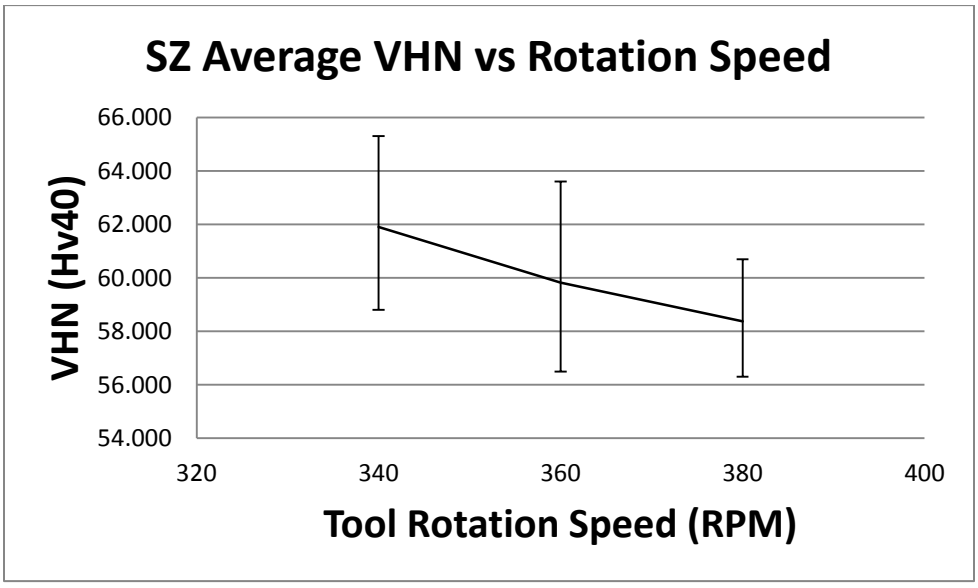
SZ Average VHN vs Rotation Speed
VHN (Hv40)
66.000
64.000
62.000
60.000
58.000
56.000
54.000
320
340
360
380
400
Tool Rotation Speed (RPM)

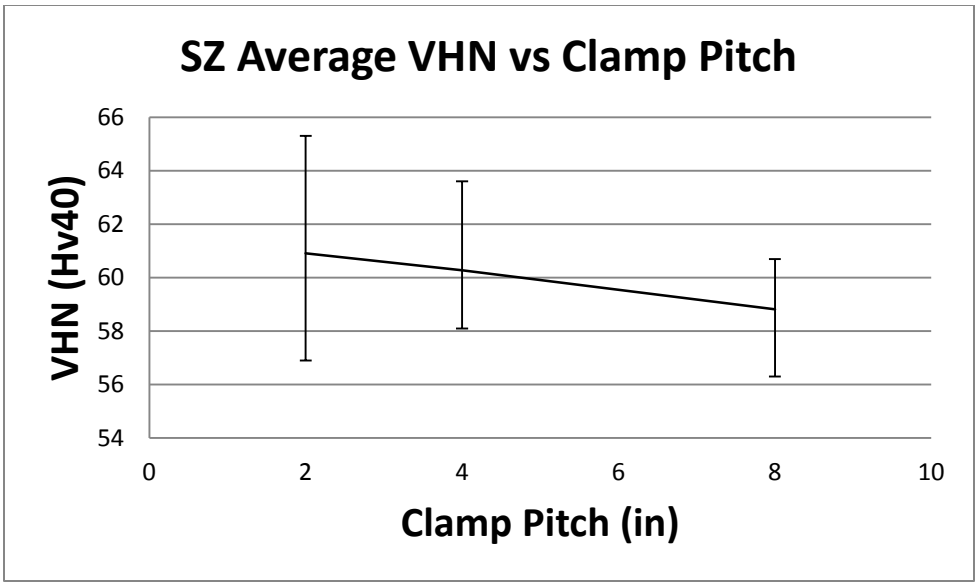

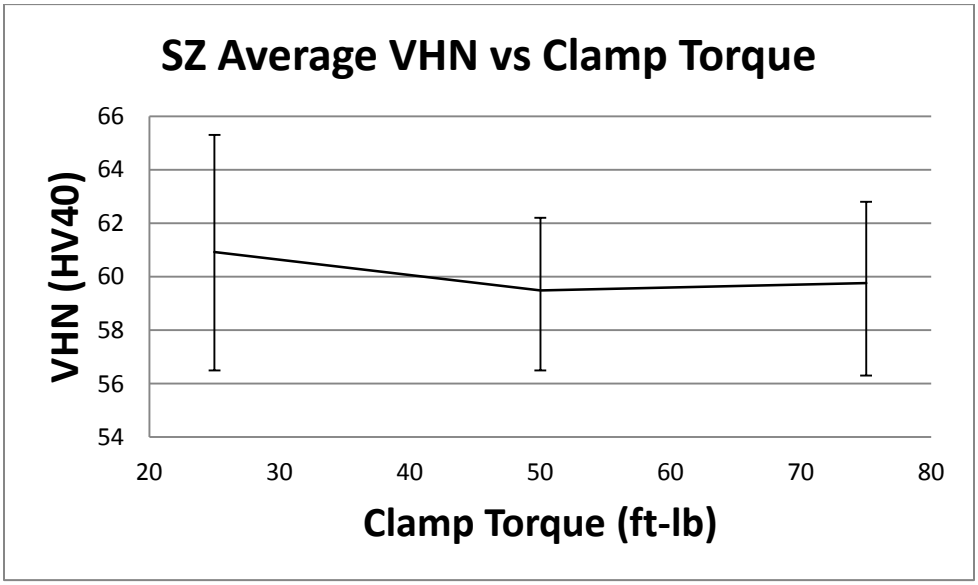

Figure 4.5.8: Marginal means plots for weld hardness

DOE Reduced Model Surfaces

The following surfaces were generated with the reduced model. They show the functional dependence of plane distortion volume, average transverse shrinkage, and average hardness on rotation speed, clamp pitch, and clamp torque. Since weld power is only dependent on rotation speed, weld power charts are omitted. Each chart shows the response variable on the vertical axis (whose scale is constant for each response). Since only two

input factors can be shown at once, the surface was generated with the third factor at its mid-range value.

Recall that the significant factors for distortion volume are clamp pitch and clamp torque – rotation speed was not a significant factor for distortion volume. The minimum value of distortion volume in the torque/pitch plot is therefore a point. This represents the singular weld schedule the produces the minimum distortion. The other plots (which include rotation speed) show a line of minimum distortion, not a point. The non-dependence of distortion volume on rotation speed allows an FSW operator to select an optimal rotation speed based on another factor, without affecting distortion volume.

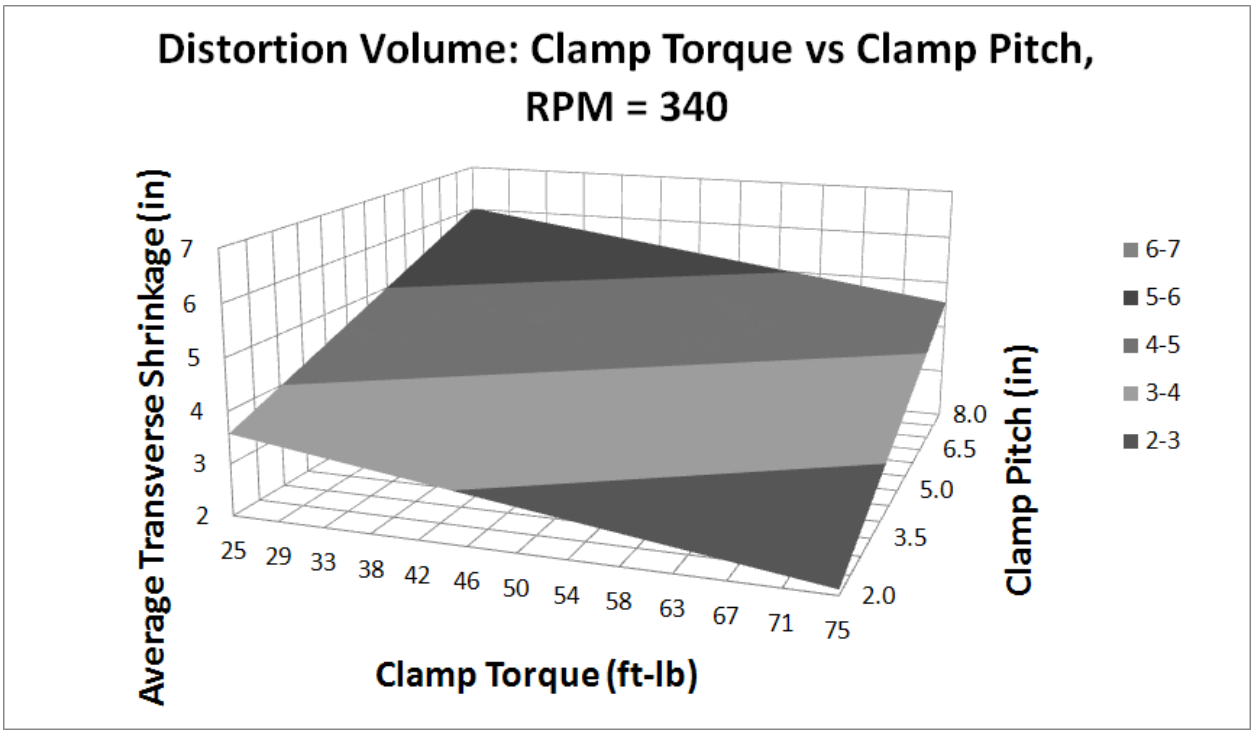

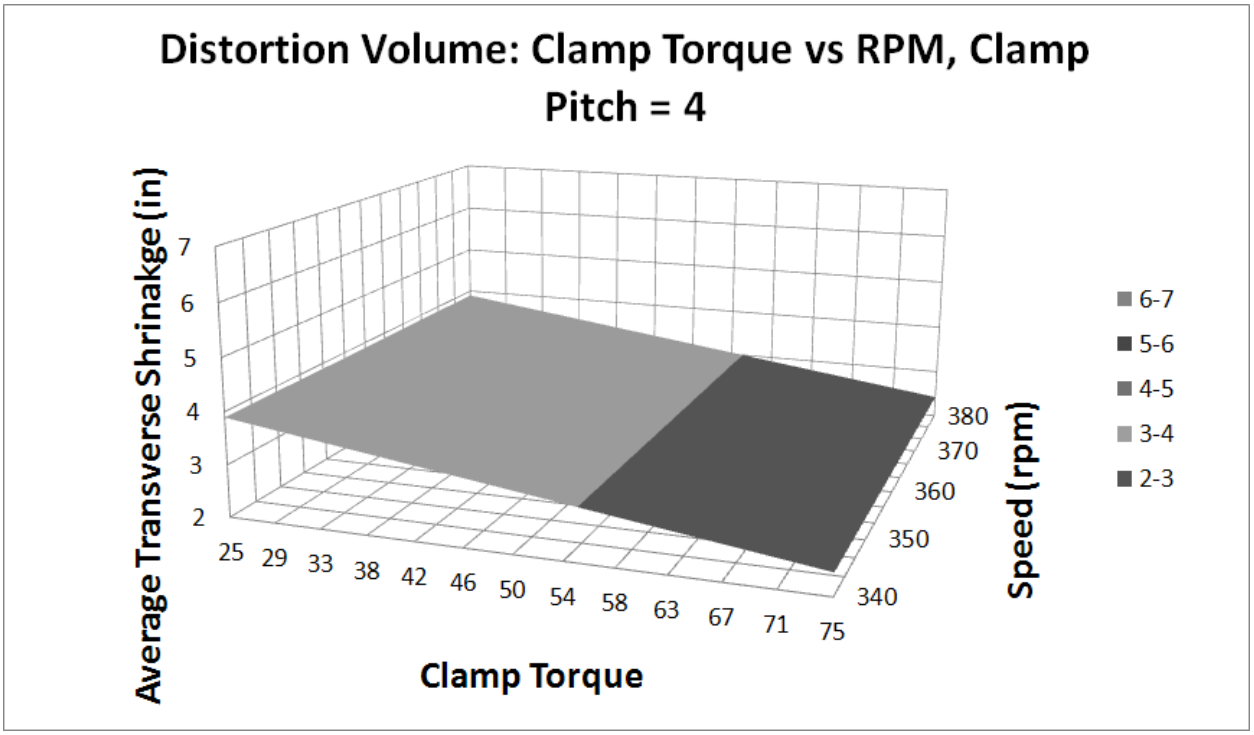

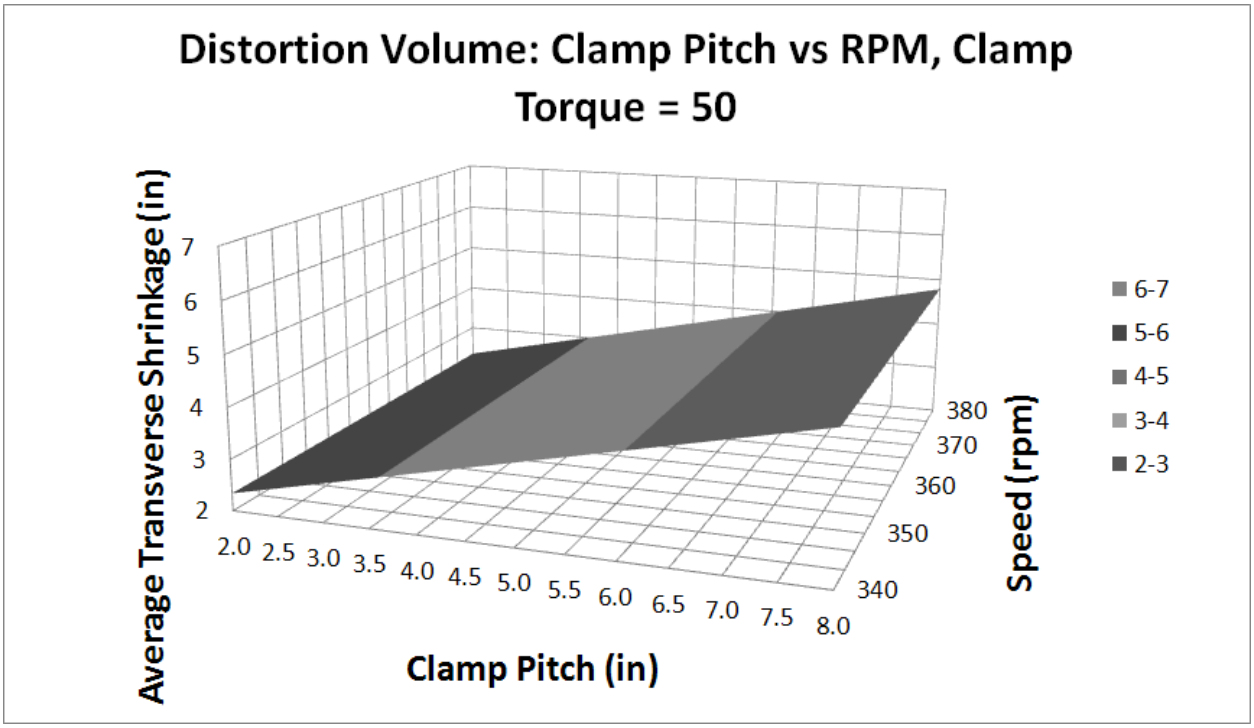

Figure 4.5.9: Out of plane distortion volume

Recall that all input factors were significant on average transverse shrinkage. The flexibility to alter rotation speed

while maintaining optimal distortion volume is not present for average transverse shrinkage.

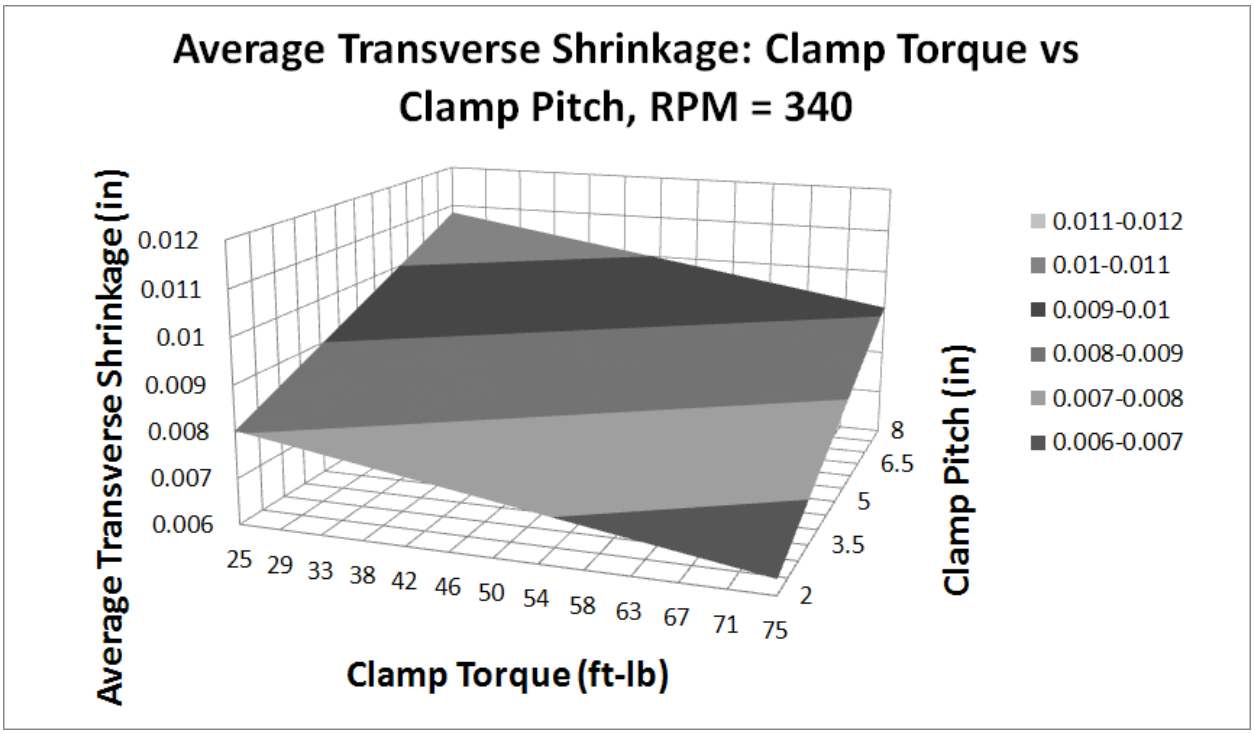

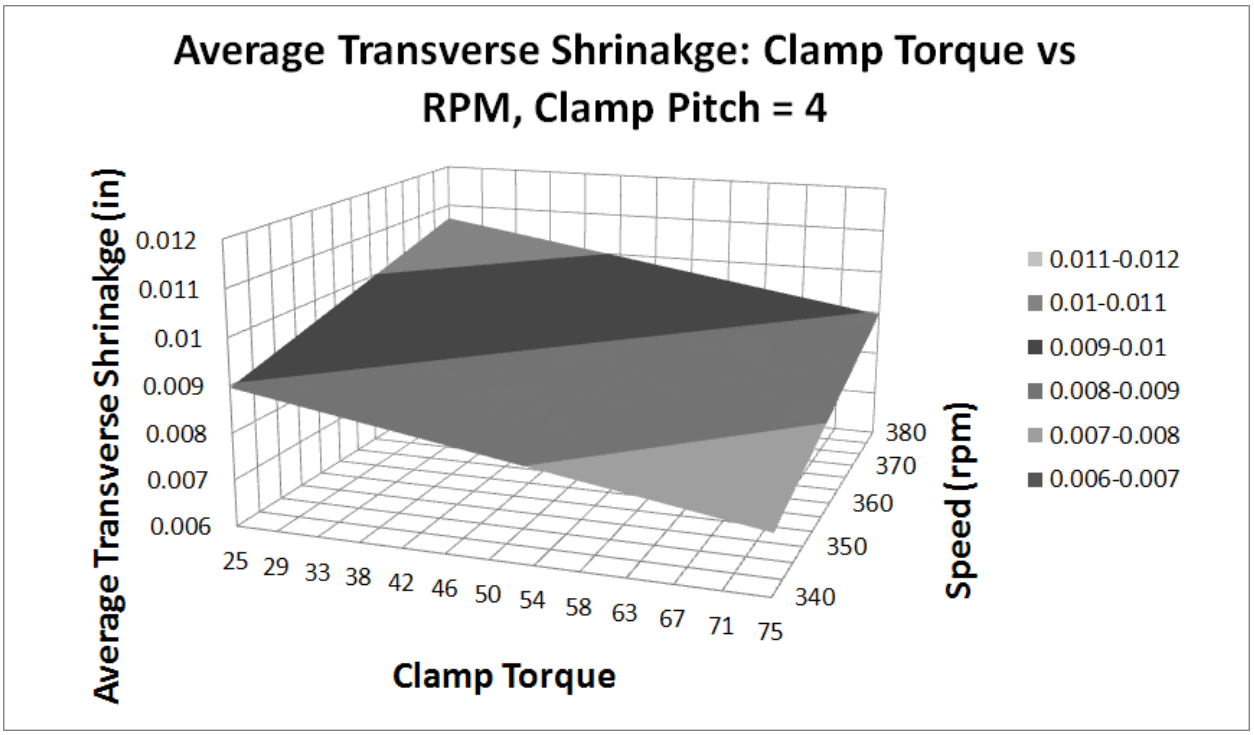

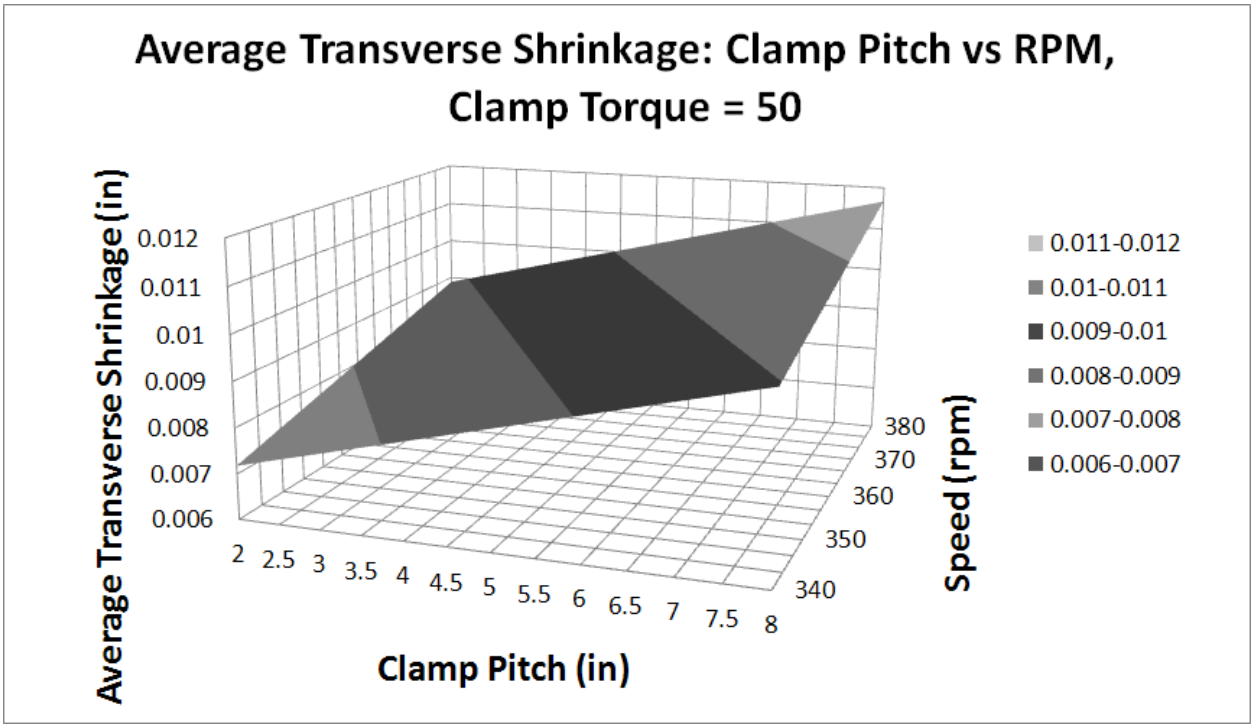

Figure 4.5.10: Average transverse shrinkage

Recall that average nugget hardness was the only response that was a function of the higher order factor combinations (rpm, pitch, rpm*pitch, and rpm*pitch*torque). This higher order dependence gives the surfaces in the hardness plots curvature not seen in the first order dependent distortion responses.

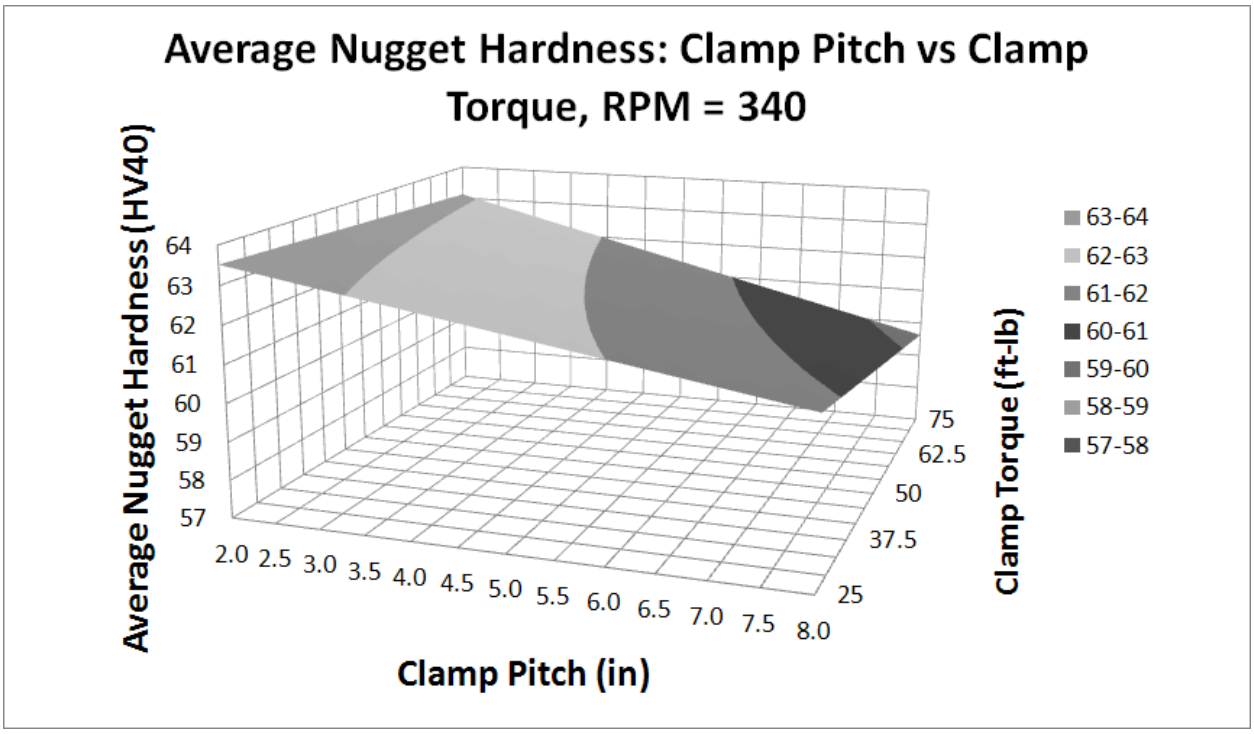
Average Nugget Hardness: Clamp Pitch vs Clamp Torque, RPM = 340
Average Nugget Hardness (HV40)
64
63
62
61
60
59
58
57
2.0 2.5 3.0 3.5 4.0 4.5 5.0 5.5 6.0 6.5 7.0 7.5 8.0
Clamp Pitch (in)
75
62.5
50
37.5
25
Clamp Torque (ft-lb)
63-64
62-63
61-62
60-61
59-60
58-59
57-58

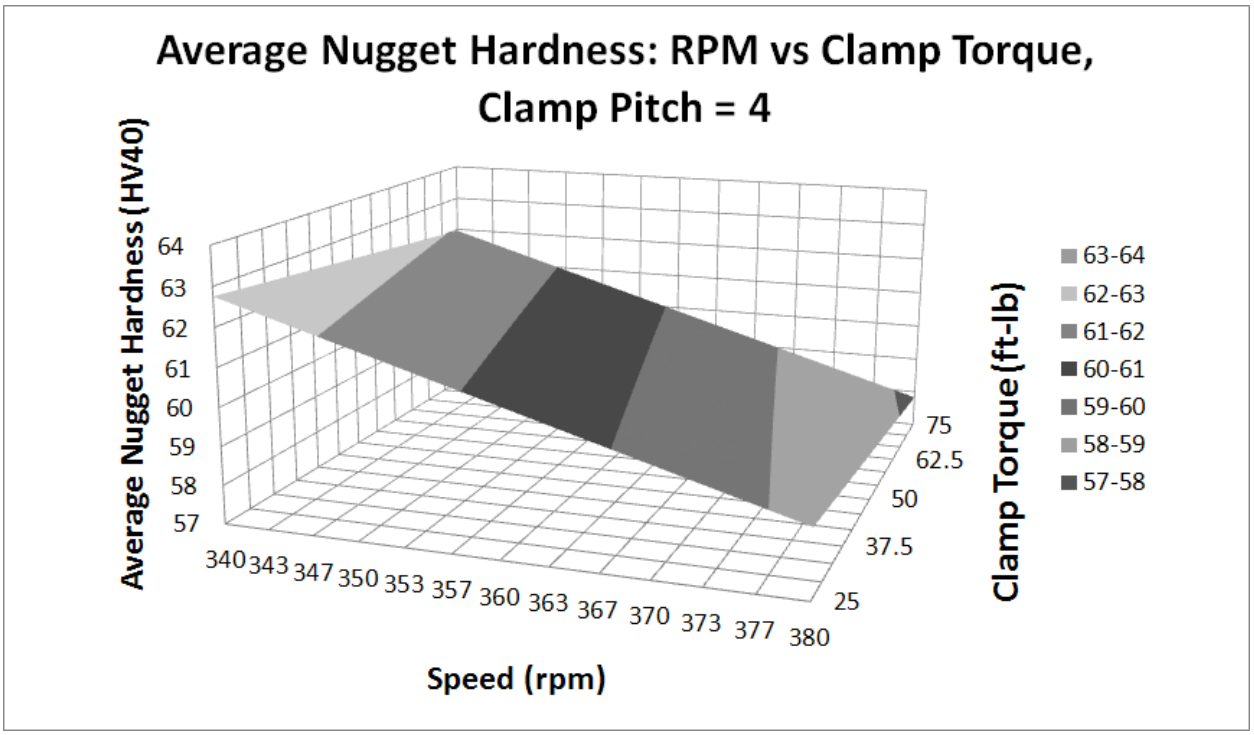
Average Nugget Hardness: RPM vs Clamp Torque, Clamp Pitch = 4
Average Nugget Hardness (HV40)
64
63
62
61
60
59
58
57
340 343 347 350 353 357 360 363 367 370 373 377 380
Speed (rpm)
75
62.5
50
37.5
25
Clamp Torque (ft-lb)
63-64
62-63
61-62
60-61
59-60
58-59
57-58

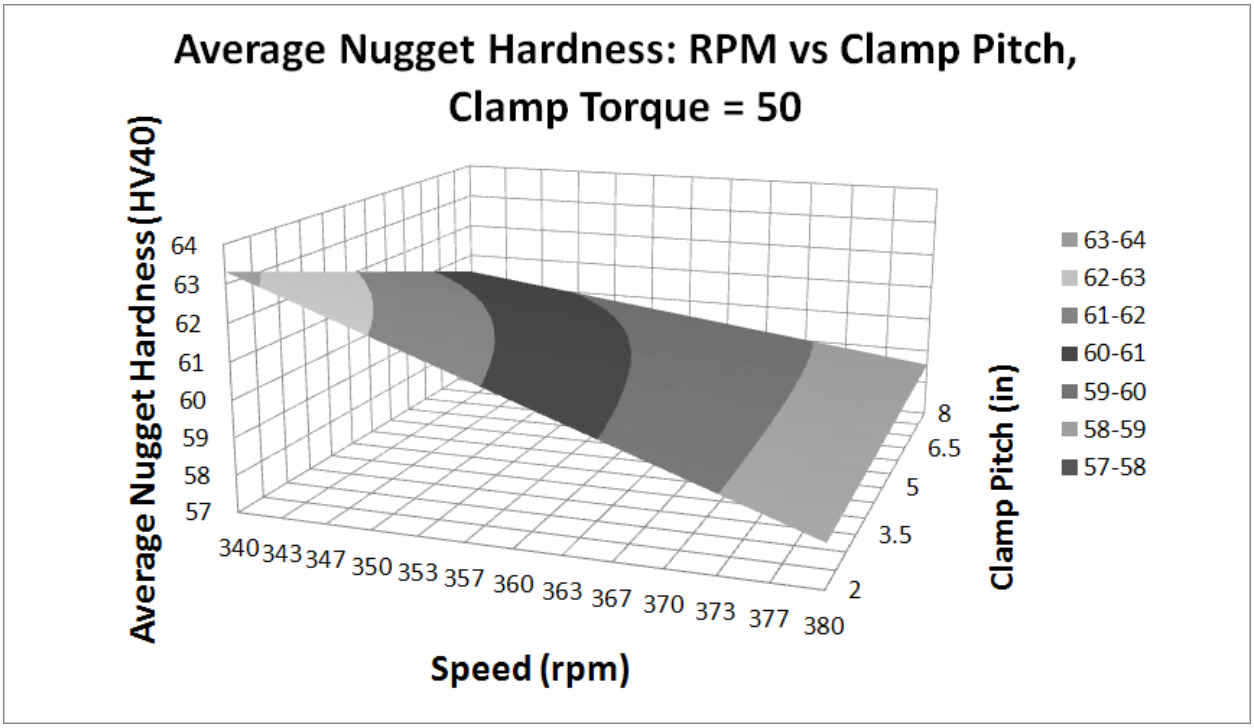

Figure 4.5.11: Average nugget hardness

DOE Validation

As a final check of the linear and volumetric distortion models, two more extrusions were welded. To validate the model outside of the previously tested parameters, a wholly new weld schedule was tested: 370 rpm, 4" clamp spacing, and 63 ft-lb clamping torque. The results are listed in table 4.5.13.

	Distortion Volume (in^3)	Model Error	Average Transverse Shrinkage (in)	Model Error
model	2.774	N/A	0.009	N/A
V1	2.598	6%	0.008	11%
V2	2.448	12%	0.009	0%
average	2.523	9%	0.009	6%

Table 4.5.13: DOE validation results

Even with the large spread seen in the response values, and the low R^2 values for the distortion regression models, the models predicted the distortion behavior of a previously untested combination of weld parameters to below 10% error, on average.

4.6 Recommended Further Testing

In an industrial development program, the typical responses that are optimized are weld strength or toughness. Detectable volumetric defects are typically not tolerated. Producing optimally strong welds was outside the scope of this testing. From an application standpoint, it would be most useful to determine if distortion could be controlled while maintaining the optimal design properties required by welded structures.

Pin tool design has perhaps the most dramatic effect on FSW responses. Since the weld schedule process window of each pin is different, and there are limitless possibilities for pin design, studying pin tool geometry effects would be incredibly involved, but is expected to have some effect on distortion response.

A full understanding of the heat flow in FSW would add to the understanding of distortion. Calorimetry during the welding would have built a clearer picture as to the effect of heat on distortion, and its relative importance compared to physical impetuses to distortion. Thermal modeling of the clamping fixture could lead to a better understanding of heat flux and how this might affect distortion.

Many techniques exist for measuring the residual stresses induced by FSW. This could lead to a better understanding of the interaction of heat and deformation.

The separation punch technique was not successful in determining longitudinal deformation. If a more accurate technique were developed, and applied to both the crown and root side of the weld panel, further key distortion data could be ascertained.

The tightening torque might not have had a linear effect on the desired property of clamp force. A more direct method for controlling clamp force might decrease some of the noise seen in the data.

5.0 Conclusions

The surest way to decrease distortion in friction stir welded aluminum extrusions is to decrease the spacing between clamps. This will limit both out of plane bending, and transverse shrinkage. Tool rotation speed had negligible effect on out of plane distortion, but decreasing rotation speed does decrease transverse shrinkage (where it has double the effect of clamp torque). Table 5.0.1 shows the ANOVA percent contribution of each significant parameter on distortion.

Parameter	Transverse Shrinkage	Out of Plane Distortion
Rotation Speed	19.70%	N/A
Clamp Spacing	38.60%	39.50%
Clamp Torque	10.60%	30.20%

Table 5.0.1: Significant factors distortion response

The values in table 5.0.1 indicate the relative abilities of each factor to alter distortion. The distortion response correlates with higher temperatures. For confirmation of this observation, the weld power and hardness data is analyzed.

The only source of heat in FSW is the spindle power. Higher spindle powers indicate that more heat is being driven into the weld. For constant a heat sink, this means the peak temperature in the weld will increase with increasing weld power. The primary heat sink is conduction into the anvil and clamping fixture. By decreasing the spacing of clamps, the area for heat conduction into the fixture increases; by increasing the clamp torque, the heat transfer coefficient of the clamping interfaces should be increased. The hottest welds should thus have the highest tool rotation speed, and least amount of clamping (high pitch, low clamp torque). The effects of clamping on heat sink were proven during the bounding testing, leading to the contraction of the tool rotation speed window. Because 6061 is a heat treatable alloy, the nugget hardness correlates with the maximum temperature experienced by the weld. Here, time at temperature is ignored, since a single weld speed was used.

The spindle power and hardness ANOVA results are listed in table 5.0.2.

	Parameter	Weld Power	Nugget Hardness
A	Rotation Speed	98.80%	49.16%
B	Clamp Spacing	N/A	11.50%
C	Clamp Torque	N/A	N/A
AB		N/A	9.15%
ABC		N/A	9.43%

Table 5.0.2: Significant factors for temperature response

Since weld strength correlates with average nugget hardness, the combination of table 5.0.1 and 5.0.2 suggests an optimal weld schedule: 340/2/75. This is a somewhat trivial result (which was expected prior to testing), since all measured responses improve with the same trends on the input factors.

Table 5.0.3 summarizes the output variable responses to an increase in each input parameter. The table only has the significant factors (P(2 tail)>=0.1) for each response. The weld temperature column is bordered in bold to highlight that this is assumed behavior (since temperature was not directly measured). If the four output responses behave consistently with this thermal reasoning, these temperature assumptions should be correct. Furthermore, the mechanism by which the input variables affect the responses is most likely thermal in nature.

Parameter	Weld Temperature	Weld Power	Nugget Hardness	Transverse Shrinkage	Out of Plane Distortion
Rotation Speed	↑	↑	↓	↑	
Clamp Spacing	↑		↓	↑	↑
Clamp Torque	↓			↓	↓

Table 5.0.3: Output responses to increasing each variable

Increasing rotation speed increases weld power and heat flux into the weld. This leads to lower hardness and higher transverse shrinkage - consistent with higher weld temperatures.

Increasing clamp spacing (decreasing the number of clamps) decreases the heat flux out of the weld, by decreasing the cross sectional area for conduction. This leads to lower hardness, and higher values for both transverse shrinkage and out of plane distortion - consistent with higher weld temperatures. Increasing clamp torque increases the heat flux out of the weld, by increasing the heat transfer coefficient between the extrusion and the fixture. This leads to lower transverse shrinkage and out of plane distortion - consistent with lower weld temperatures. Since the presumed effect of the input variables on the weld temperature is consistent with all output responses, weld temperature is almost certainly part of the mechanism at play.

Although all significant factors in table 5.0.3 were consistent with presumed weld temperatures, some holes are present in the table: clamp torque is not significant on hardness, and rotation speed is not significant on out of plane distortion.

The hardness anomaly may indicate that thermal effects are not the lone mechanism at play. The increased physical constraint of increased clamping may be responsible for some of the distortion behavior. Heating the metal leads to both expansion and a decrease in strength. If the mechanism by which increased clamping prevents distortion is purely physical (preventing movement from thermal expansion, until the metal cools back down, and regains full strength), distortion would still be mitigated by increased clamp torque, even if it had no heat effect. If clamp torque was solely a mechanical effect, this would also lead to an insignificant effect on nugget hardness, since changing clamp torque would not change the weld temperature. Based on this inconsistency, it can be assumed that both mechanical and thermal mechanisms affect the response variables.

The cause of the out of plane distortion anomaly may be seen in the marginal means plot in figure 4.5.2. The rotation speed curve shows an inconsistent effect of rpm on out of plane distortion - it decreases from 340-360rpm and increases from 360-380 rpm. This inconsistency is likely the cause of the high P(2 tail) value for rotation speed on out of plane distortion

(0.242 vs <0.1 for significance). The data range for the rpm=360 out of plane distortion is not comparatively large enough to fully discount this behavior. The ANOVA table (4.5.2) shows that, based on the low and high rpm data, that tool rotation speed has a 7% contribution to out of plane distortion. The general trend is that out of plane distortion increases with increasing rotation speed and this is consistent with the behavior of transverse shrinkage.

Even without a total understanding of the mechanism for distortion, and with the low R^2 values of the DOE models, predictions made for both modes of distortion were 90% accurate for the two verification welds tested. Based on the DOE models, an optimum weld is 340rpm, 2" clamp pitch, and 75ft-lb clamp torque. This weld schedule leads to the lowest out of plane distortion, the lowest transverse shrinkage, and the hardest nugget (from which can be inferred, highest strength). This is a somewhat trivial – and expected - result, since all measured responses improve with decreasing weld temperature. A more interesting problem might be to obtain the lowest distortion weld with the highest toughness (correlating with the lowest hardness). Figures 4.5.9, 4.5.10, and 4.5.11 reveal the answer. Rotation speed has no effect on out of plane distortion volume, and increasing rotation speed decreases hardness (increases toughness). Comparing the 340rpm and 380rpm values in the 4.5.10 figures shows that this increase in rotation speed increases average transverse shrinkage by only 0.002". If this slightly higher shrinkage is acceptable, then the distortion and toughness optimized rotation speed is 380 rpm. Since clamp spacing and torque have much larger effects on distortion than they do for hardness, the clamping parameters should be chosen based on distortion concerns (if the relatively smaller percent change in hardness is acceptable). The distortion and toughness optimized weld schedule would then be 380/2/75.

6.0 References

1. http://www.naval-technology.com/projects/littoral/. [Online]

2. **Naval Metal Working Center.** Friction Stir Welding - Strong Ductile and Environmentally Friendly. *NMC information Services.* Concurrent Technologies Services, 2006.

3. *The Joining of Aluminum Extrusions.* **Dolby, R. E.** s.l. : La Metallurgia Italliana, 2003, Alumino E Leghe, pp. 25-30.

4. **Thomas, W.** *Friction Welding. US patent #5,460,317* october 24, 1995.

5. **Mishra, R.** *Friction Stir Welding.* Materials Park : AMS international, 2007.

6. *Friction Stir Welding of Aluminum 7136-t76511 Extrusions.* **Hamilton, C.** 8, s.l. : Institute of Materials, 2008, Science and Technology of Welding, Vol. 13, pp. 714-720.

7. *Thermo-mechanical Analyses of Welding Aluminum Alloy with TIG and Friction Stir Welding.* **Shi, Q.** s.l. : ASM International, 2003. 6th International Trends in Welding. pp. 247-252.

8. *Corrosion Resistance in FSW and in MIG Welding Techniques of AA6XXX.* **Maggliolino, Stefano.** 1-3, Trieste : s.n., June 2007, Journal of Materials Processing Technology, Vol. 197.

9. *Comaprison of Buckling Distortion Propensity for SAW, GMAW, and FSW.* **Bhide, S. R.** s.l. : American Welding Society, 2006, Supplement to teh Welding Journal, pp. 189-195.

10. *Experimental Comparison of MIG and Friction Stir Welding Processes for EN A-6061-T6 (Al Mg Si Cu) Aluminum Alloy.* **Kulekei, Mustafa.** 1B, 2009, The Arabian Journal for Science and Engineering, Vol. 35, pp. 321-330.

11. *Influences of Tool Pin Profile and Axial Forces on the Formation of Friction Stir Processing Zone in AA6061 Aluminum Alloy .* **K., Elangovan.** 3-4, August 2008, International journal of Advanced Manufacturing Technology, Vol. 38, pp. 285-295.

12. *Alloy, Tool Geometry, and Process Parameter effect on Weld Energies and Resultant FSW Joint Properties.* **Reynolds, A. P.** [ed.] K.V. Jata. s.l. : TMS, 2001, Friction Stir Welding and Processing, pp. 15-23.

13. *A Multi-objective optimization application in Friction Stir Welding: Considering thermo-mechanical aspects.* **Tutum, C. C.** barcelona: IEEE, 2010. 2010 IEEE Congress on Evolutionary Computation. pp. 1-8.

14. **Thurlby, Nicholas.** Advances in High Rotational Speed - Friction Stir Welding for Naval Applications . [MS Thesis]. Witchita: Witchita State University, 2009.

15. *Friction Stir Welding of Sc-Modified Al-Zn-Mg-Cu Alloy extrusions.* **Hamilton, Carter.** Boston : ASME, 2008. 2008 ASME International Mechnical Engineering Congress and Exposition. pp. 257-264.

16. *Relationship Between Process Variables REalted to HEat Generation in Friction Stir Welding of Aluminum.* **Colligan, Kevin.** [ed.] Rajiv Mishra. s.l. : TMS, 2007. Friction Stir Welding and Processing IV. pp. 39-54.

17. *Microstructural Aspects of the Friction-Stir Welding of 6061-T6.* **Liu, G.** 3, s.l. : Acta Metallurgica, 1997, Scripta Materialia, Vol. 37, pp. 355-361.

18. *Microstructural Analysis and Modeling of the Heat Affected Zone in Al 2519 Friction Stir Welds.* **Fonda, R. W.** Pine Mountain : ASM International, 2003. 6th International Trends in Welding Research Conference Proceedings. pp. 241-246.

19. *Mechanical Properties Related to Microstructural Variation of 6061 Al Alloy Joints by Friction Stir Welding.* **Lee, Won-Bae.** 5, s.l. : The Japan Institute of Materials, 2004, Materials Transactions, Vol. 45, pp. 1700-1705.

20. *Measurement and Simulation of Temperature and Residual Stress Distributions from Friction Stir Welding AA2024 Al Alloy.* **Wang, L.** 3, s.l. : Science Reviews, 2010, Materials at High Temperatures, Vol. 27, pp. 167-178.

21. *Effects of Heat Treatments on the Microstructure and Mechanical Properties of a 6061 Aluminum Alloy.* **Maisonnette, D.** s.l. : Elsevier, 2011, Materials Science and Engineering A, Vol. 528, pp. 2718-2724.

22. **Ditzel, Peter.** Microstructure/Property Relationships in Aluminum Friction Stir Welds. *Mater's Thesis .* s.l. : Ohio State University, 1997.

23. *TEM study of the FSW nugget in AA2195-T81.* **Schneider, J. A.** s.l. : Springer Science + Business Media, 2005, Journal of Materials SCience, Vol. 40, pp. 4341-4345.

24. *Recent Advances in Friction Stir Welding - Process, Weldment Structure and Properties.* **Nandan, R.** 2008, Progress in Material Science, Vol. 53, pp. 980-1023.

25. *Tensile Properties and Fracture Locations of Friction-Stir Welded Joints of 6061-T6 Aluminum Alloy .* **Liu, Huijie.** s.l. : Kluwer Academic Publishers, 2003, Journal of Materials Science Letters, Vol. 22, pp. 1061-1063.

26. *Relationships between Weld Parameters, Hardness Distribution and Temperature history in Alloy 7050 Friction Stir Welds.* **Reynolds, A. P.** 2, s.l. : Institute of Materials, Minerals and Mining, 2005, Science and Technology of Welding and Joining, Vol. 10, pp. 190-199.

27. *Mechanical Behaviour of Joints in FSW: Residual Stresses, Inherent Strain and Heat Input by Friction Stir Welding.* **Terisaki, T.** 11/12, 2003, Welding in the World, Vol. 47, pp. 24-31.

28. *Controll of Rotational Distortion in Friction Stir Welding.* **Nishikawa, Hiroyasu.** 2004, Journal of the Kansai Society of Naval Architects, Vol. 242, pp. 79-85.

29. *Residula Stresses and Distortions in Welded Structures: What We Know Today.* **Dong, Prngsha.** Pine Mountain : ASM International, 2002. 6th International Trends in Welding Research Conference Proceedings. pp. 815-825.

30. *Buckling analysis for an Integrally Stiffened Panel Structure with Friction Stir Weld.* **Yoon, J. W.** s.l. : Elsevier, 2009, Thin Walled Structures, Vol. 47, pp. 1608-1622.

31. *Experimental Study on the Distortion of Al-6013 Plate After Friction Stir Welding.* **Shi, Q.** 5, s.l. : Institute of Materials, minerals and Mining, 2008, Science and Technology of Welding and Joining , Vol. 13, pp. 472-478.

32. *The Characterisation of Friction Stire Welding Process Effects on Stiffened Panel Buckling Performance.* **Murphy, A.** s.l. : Elsevier, 2007, Thin Walled Sturctures, Vol. 45, pp. 339-351.

33. *Finite Element Analysis of Thermal Tensioning Techniques Mitigating Weld Buckling Distortion.* **Michaleris, Pantagiotis.** 11, s.l. : American Welding Society, 1997, Welding Journal, Vol. 76, pp. 451-457.

34. *Distortion Control in Welding by Mechanical Tensioning.* **Price, D. A.** 7, s.l. : Institute of Materials, Minerals and Mining, 2007, Science and Technology of Welding, Vol. 12, pp. 620-633.

35. *Residual Stresses in AA7108 Aluminum Alloy Sheets Joined by Friction Stir Welding.* **Gachi, Salicha.** 3, s.l. : Taylor and Francis, 2009, Nondestructive Testing and Evaluation, Vol. 24, pp. 301-309.

36. *Predicting Residual Thermal Stresses in Friction Stir Welded Metals.* **Khandkar, Mir Zahedul H.** s.l. : Elsevier, 2006, Journal of Materials Processing Technology, Vol. 174, pp. 195-203.

37. *On the Residual Stress Filed in the Aluminum Alloy FSW Joints.* **Dattoman, V.** s.l. : The Authors Journal, 2009, Strain, Vol. 45, pp. 380-386.

38. *A Study of Residual Stresses and microstucture in 2024-T3 Aluminum Friction Stir Butt Welds.* **Sutton, M. A.** s.l. : ASME, April 2002, Journal of Engineering Materials and Technology, Vol. 124, pp. 215-221.

39. *Model for Predicting Heat Generation and Temperature in Friction Stir Welding from the Material Properties.* **Colgrove, P.**

A. 4, s.l. : Institute of Materials, Minerals and Mining , 2007, Science and Technology of Welding and Joinging, Vol. 12, pp. 284-297.

40. *Modelling Temperature Histories in Friction Stir Welding Including Materials Convection Effects.* **Simar, A.** Pine Mountain : AMS, 2005. Proceeedings of the 7th international Conference on Trends in Welding Research. Vol. 7th, pp. 273-278.

41. *Input Torque Masked Thermal Model of Friction Stir Welding of Al-6061.* **Zahedul, Mir.** Pine Mountain : AMS International, 2002. 6th International Trends in Welding Research Conference Proceedings. Vol. 6th, pp. 218-221.

42. *Development of a Torque-Based Weld Power Model for Friction Stir Welding.* **Pew, Jefferson.** [ed.] Rajiv Mishra. s.l. : TMS, 2007. Friction Sitr Welding and Processing. Vol. IV, pp. 73-81.

43. *A Thermal Model of Friction Stir Welding Applied to Sc-Modified Al-Zn-Mg-Cu Alloy Extrusion.* **Hamilton, C.** s.l. : Elsevier, 2009, International Journal of Machine Tools and Manufacture, Vol. 49, pp. 230-238.

44. *Development of a Heat Input Model for Friction Stir Welding.* **Pew, J.W.** Pine Mountain : AMS International, 2006. 7th International Conference on Trends in Welding Research. Vol. 7th, pp. 247-251.

45. *Energy Unilization and Generation During Friction Stir Spot Welding.* **Su, P.** 2, s.l. : Institute of Materials, Minerals, and Mining, 2006, Science and Tehcnology of Welding and Joining, Vol. 11, pp. 163-169.

46. *Numerical Simulation of Transient Temperatures and REsidual Stresses in Friction Stir Welding of 304L Stainless Steel.* **Zhu, X. K.** s.l. : Elsevier, 2004, Journal of Materials Processing Technology, Vol. 146, pp. 263-272.

47. *Process Forces During Friction Stir Welding of Aluminumm alloys.* **Balasubramanian, N.** 2, s.l. : The Institute of Materials, Minerals, and Mining, 2009, Science and Technology of Welding and Joining, Vol. 14, pp. 141-145.

48. *Analysis of Circumfrentially Welded Thin-walled Cylinders to Investigate the Effects of Varying Clamping Conditions.* **Malik, A. M.** Part B: J. Engineering Manufacture, march 2008, Proceedings of the Institution of Mechincal Engineers, Vol. 222, pp. 901-914.

49. *A Study on the Influence of Clamping on Welding Distortion.* **shenk, T.** 2009, Computational Material Sciences, Vol. 45, pp. 999-1005.

50. *Influence of clamping on distortion of Welded s355 T-joints.* **Schenk, T.** 4, s.l. : Institute of Materials, Minerals and Mining, 2009, Sciemce and Technology of Welding and Joining, Vol. 14, pp. 669-675.

51. *Investigation of the Effects of Clamping on Residual Stresses and Distortions in Butt-Welded Plates.* **Choobi, M. Seyyedian.** 5, s.l. : Sharif University of Technology, October 2010, Transactions B: Mechanical Engineering, Vol. 17, pp. 387-394.

52. **Fisher, R.A.** *The Design of Experiments.* Edinburough : Oliver and Boyd, 1935.

53. **Anderson, Mark.** Design of Experiments. *The Industrial Physicist.* September 1997, pp. 24-26.

54. *A Brief Introduction to Design of Experiments.* **Telford, Jacqueline.** 3, Baltimore : Johns Hopkins University, 2007, Johns Hopkins APL Technical Digest, Vol. 27, pp. 224-232.

55. **Williams, Phillip.** Designing Experiments for the Modern Micro Industries. *CEP Magazine.* February 2006, pp. 58-63.

56. *Shrinkage in a Thin Plate with a Central Weld.* **Kamtekar, A. G.** 2, s.l. : IMechE, 1977, Journal of Strain Analysis, Vol. 12, pp. 140-147.

57. *Exploring the Geometry Effects for Convex Scrolled Shoulder, Step Spiral Probe FSW Tools.* **Sorensen, Carl.** [ed.] Rajiv Mishra. s.l. : TMS, 2009. Friction Stir Welding and Processing V. pp. 85-92.

58. *Heat Treatment of a Hot-work Die Steel.* **Qamar, S. Z.** 8, s.l. : OCSCO World Press, 2007, Archives of Materials Science and Engineering, Vol. 28, pp. 503-508.

59. *Control of Structure in Conventional Friction Stir Welds Through a Kinematic Theory of Metal Flow.* **Rubisoff, H. A.** [ed.] Rajiv Mishra. s.l. : TMS, 2009. Friction Stir Welding and Processing. Vol. V, pp. 149-158.

60. *Evaluation of Friction Stir Welded HSLA-65.* **Posada, Maria.** London : Royal Institute of Naval Architects, 2003, Advanced Marine Materials: Technology and Applications.

61. **Craggs, A.** *On the Stability of Sailboats.* Bloomington : Trafford, 2006. pp. 228-232.

7.0 Appendices

W1 – 360/2/50

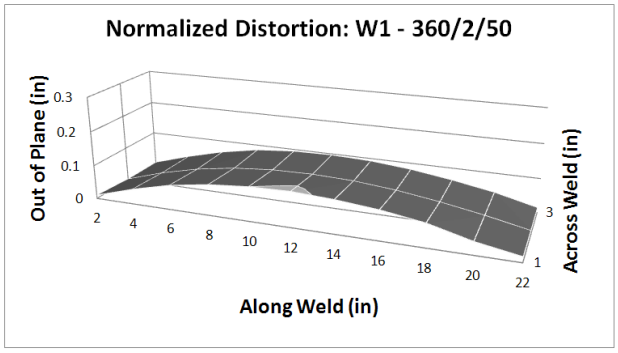

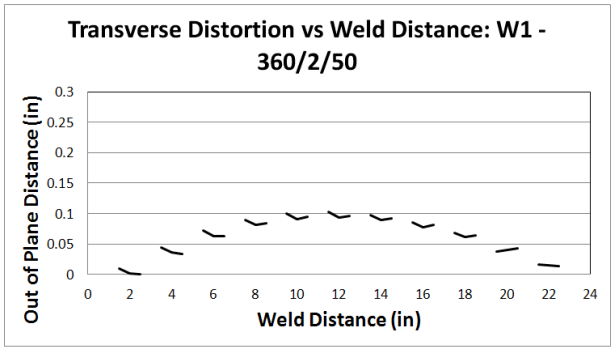

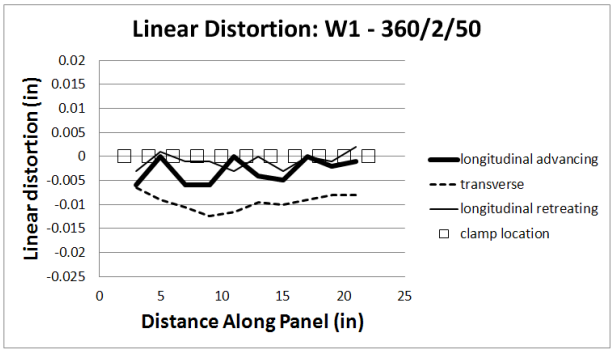

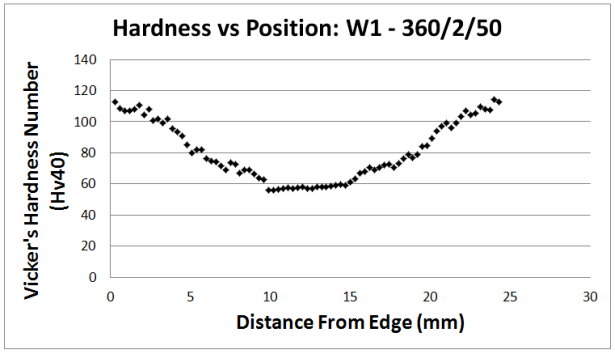

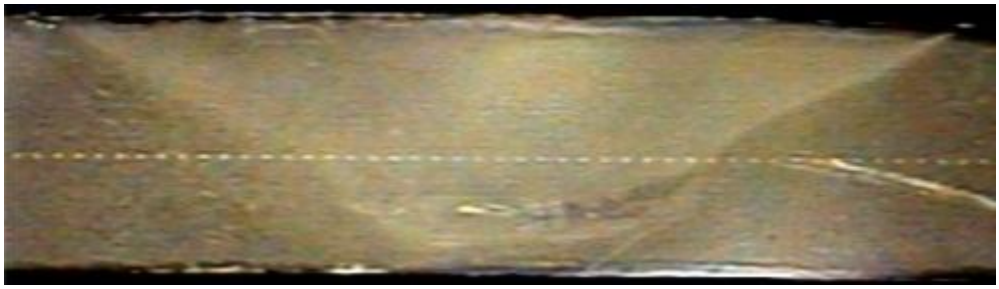

W2 – 380/8/75

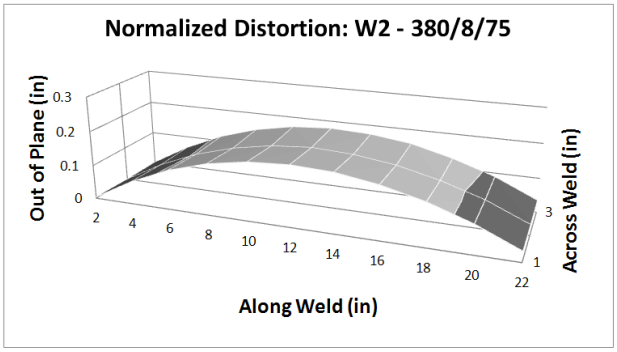
Normalized Distortion: W2 - 380/8/75
Out of Plane (in)
0.3
0.2
0.1
0
2
4
6
8
10
12
14
16
18
20
22
Along Weld (in)
1
3
Across Weld (in)

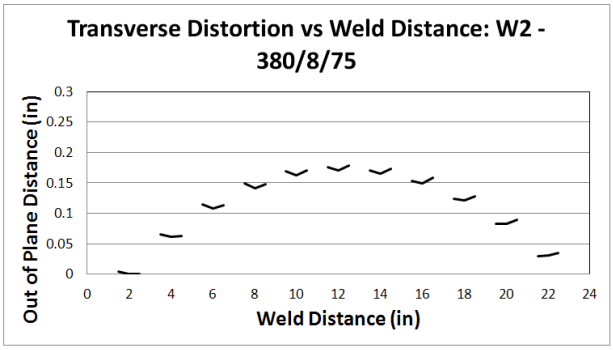
Transverse Distortion vs Weld Distance: W2 - 380/8/75
Out of Plane Distance (in)
0.3
0.25
0.2
0.15
0.1
0.05
0
0
2
4
6
8
10
12
14
16
18
20
22
24
Weld Distance (in)

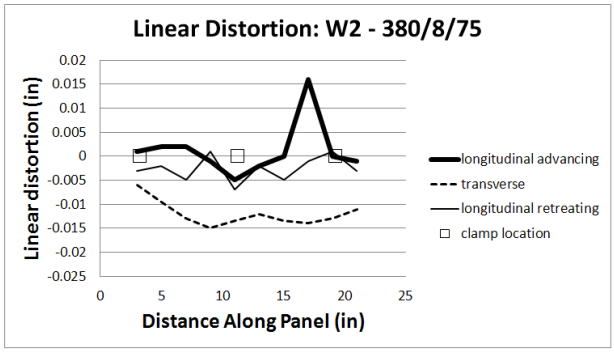
Linear Distortion: W2 - 380/8/75
Linear distortion (in)
0.02
0.015
0.01
0.005
0
-0.005
-0.01
-0.015
-0.02
-0.025
0
5
10
15
20
25
Distance Along Panel (in)
longitudinal advancing
transverse
longitudinal retreating
clamp location

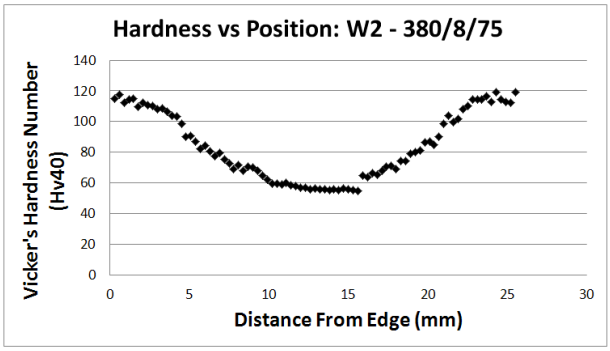
Hardness vs Position: W2 - 380/8/75
Vicker's Hardness Number (Hv40)
140
120
100
80
60
40
20
0
0
5
10
15
20
25
30
Distance From Edge (mm)

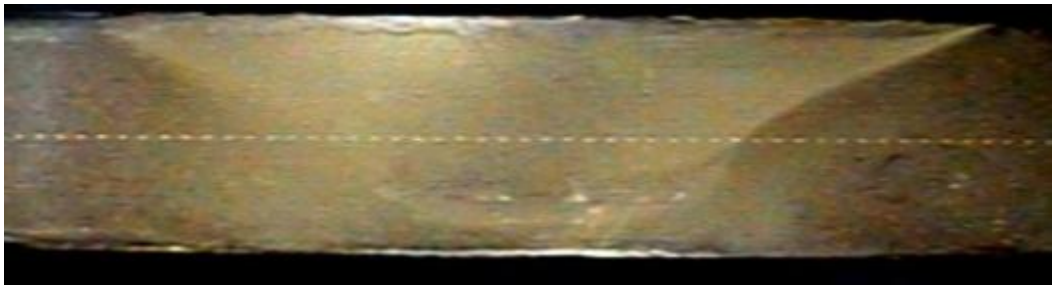

W3 – 340/4/50

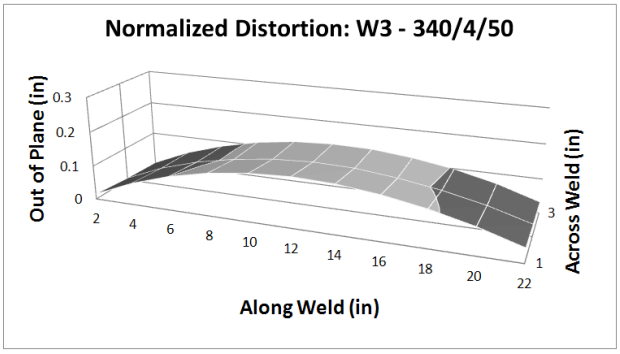
Normalized Distortion: W3 - 340/4/50
Out of Plane (in)
0.3
0.2
0.1
0
2
4
6
8
10
12
14
16
18
20
22
Along Weld (in)
1
3
Across Weld (in)

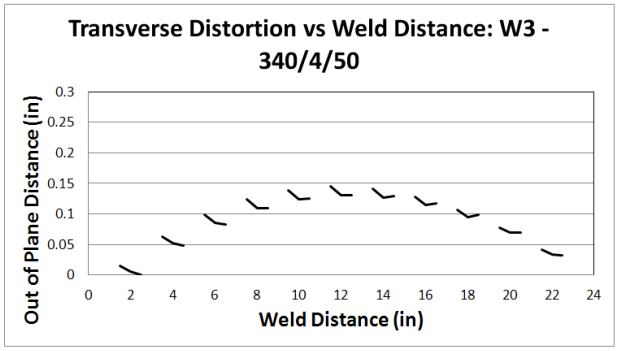
Transverse Distortion vs Weld Distance: W3 - 340/4/50
Out of Plane Distance (in)
0.3
0.25
0.2
0.15
0.1
0.05
0
0
2
4
6
8
10
12
14
16
18
20
22
24
Weld Distance (in)

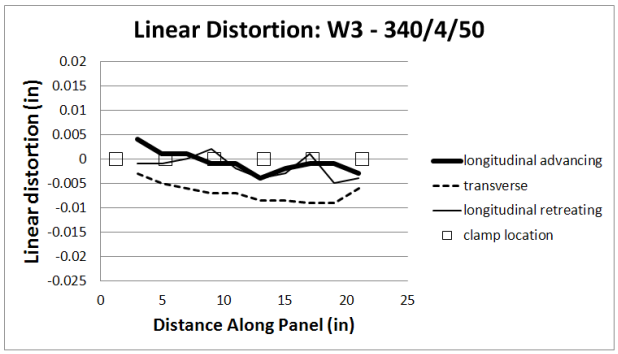
Linear Distortion: W3 - 340/4/50
Linear distortion (in)
0.02
0.015
0.01
0.005
0
-0.005
-0.01
-0.015
-0.02
-0.025
0
5
10
15
20
25
Distance Along Panel (in)
longitudinal advancing
transverse
longitudinal retreating
clamp location

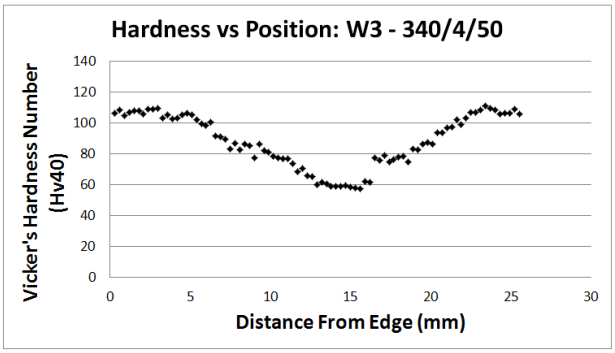
Hardness vs Position: W3 - 340/4/50
Vicker's Hardness Number (Hv40)
140
120
100
80
60
40
20
0
0
5
10
15
20
25
30
Distance From Edge (mm)

W4 – 360/8/50

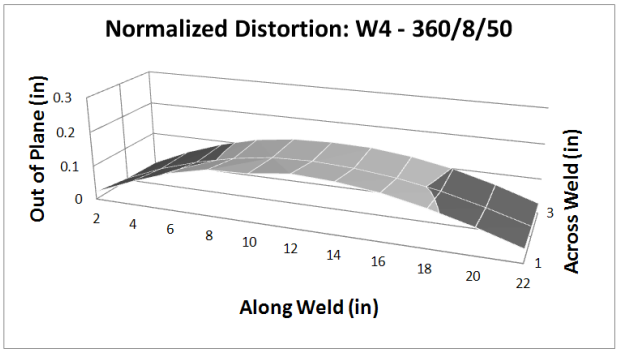
Normalized Distortion: W4 - 360/8/50
Out of Plane (in)
0.3
0.2
0.1
0
2
4
6
8
10
12
14
16
18
20
22
Along Weld (in)
1
3
Across Weld (in)

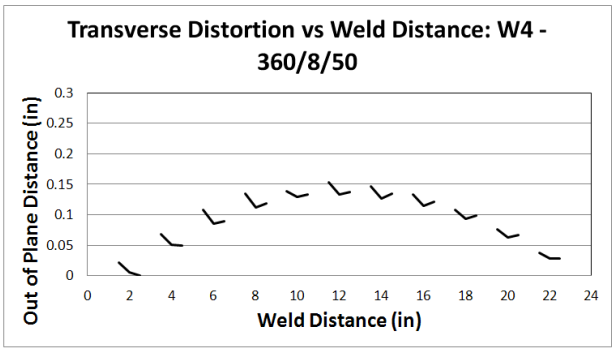
Transverse Distortion vs Weld Distance: W4 - 360/8/50
Out of Plane Distance (in)
0.3
0.25
0.2
0.15
0.1
0.05
0
0
2
4
6
8
10
12
14
16
18
20
22
24
Weld Distance (in)

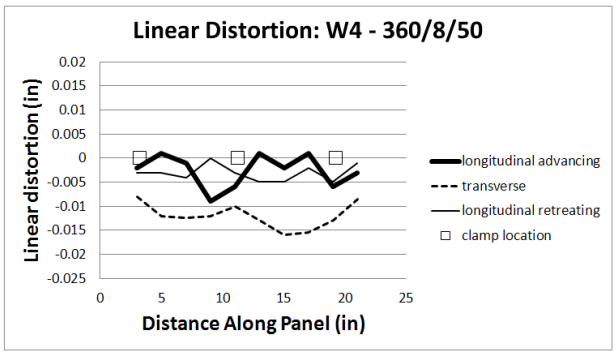
Linear Distortion: W4 - 360/8/50
Linear distortion (in)
0.02
0.015
0.01
0.005
0
-0.005
-0.01
-0.015
-0.02
-0.025
0
5
10
15
20
25
Distance Along Panel (in)
longitudinal advancing
transverse
longitudinal retreating
clamp location

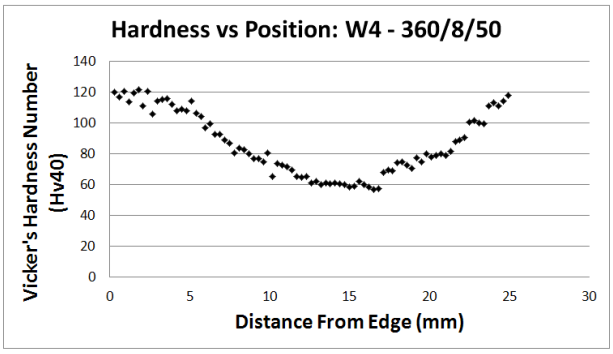
Hardness vs Position: W4 - 360/8/50
Vicker's Hardness Number (Hv40)
140
120
100
80
60
40
20
0
0
5
10
15
20
25
30
Distance From Edge (mm)

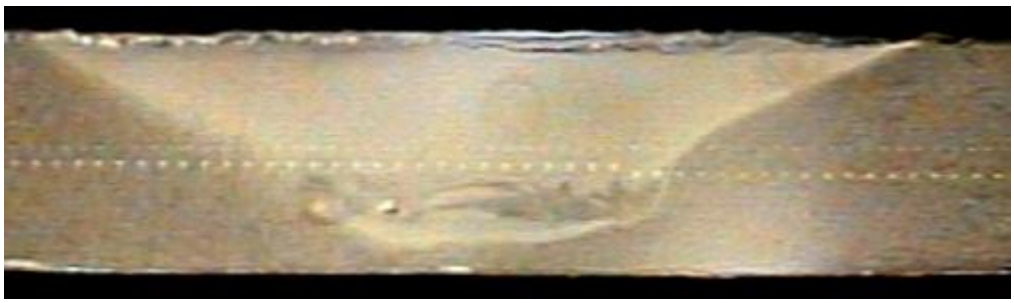

W5 – 340/2/75

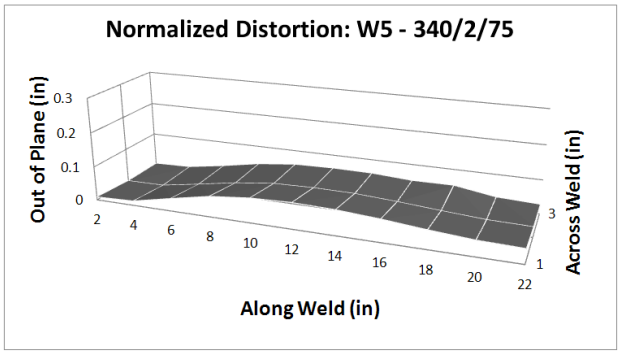

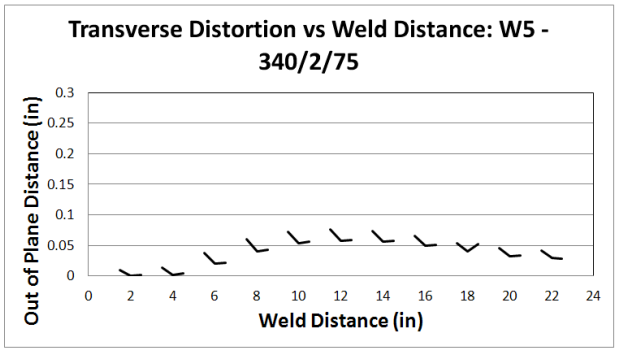

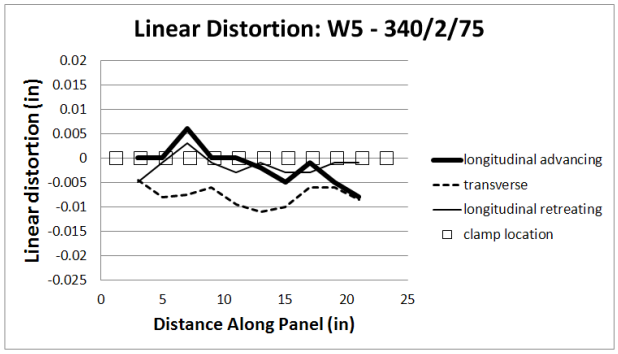

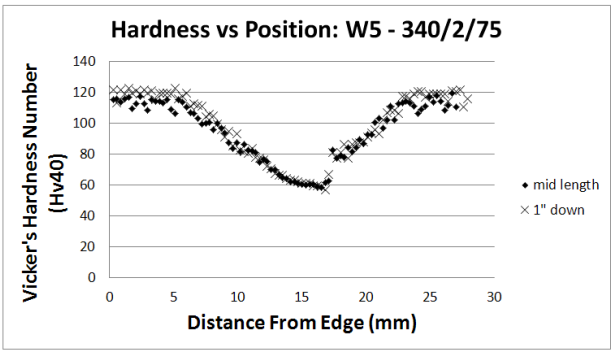

Mid Length:

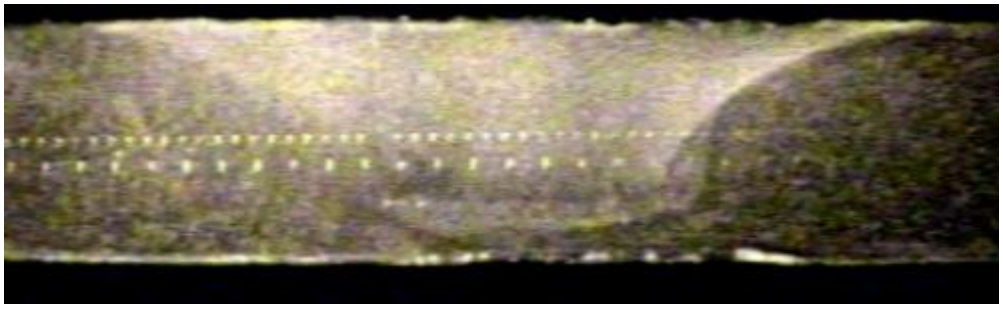

1" Down Weld:

W6 – 360/4/50

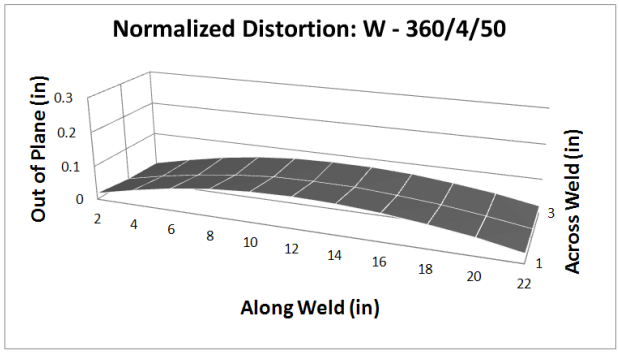
Normalized Distortion: W - 360/4/50
Out of Plane (in)
0.3
0.2
0.1
0
2
4
6
8
10
12
14
16
18
20
22
Along Weld (in)
1
3
Across Weld (in)

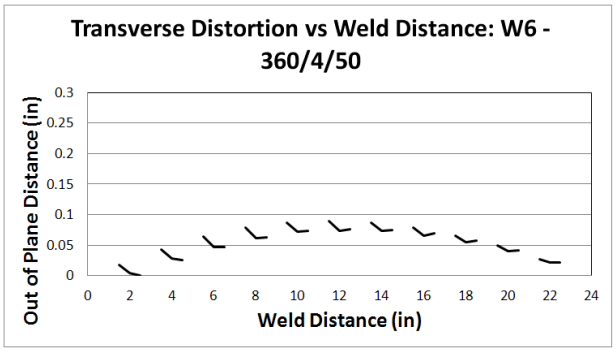
Transverse Distortion vs Weld Distance: W6 - 360/4/50
Out of Plane Distance (in)
0.3
0.25
0.2
0.15
0.1
0.05
0
0
2
4
6
8
10
12
14
16
18
20
22
24
Weld Distance (in)

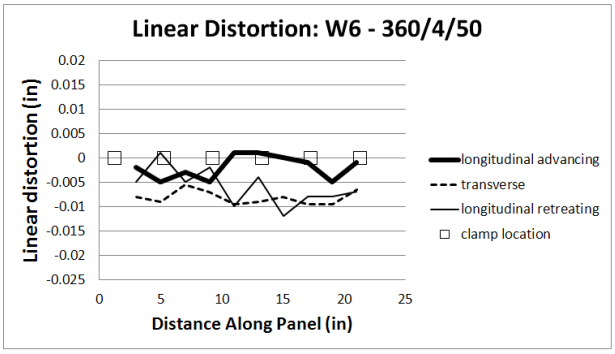
Linear Distortion: W6 - 360/4/50
Linear distortion (in)
0.02
0.015
0.01
0.005
0
-0.005
-0.01
-0.015
-0.02
-0.025
0
5
10
15
20
25
Distance Along Panel (in)
longitudinal advancing
transverse
longitudinal retreating
clamp location

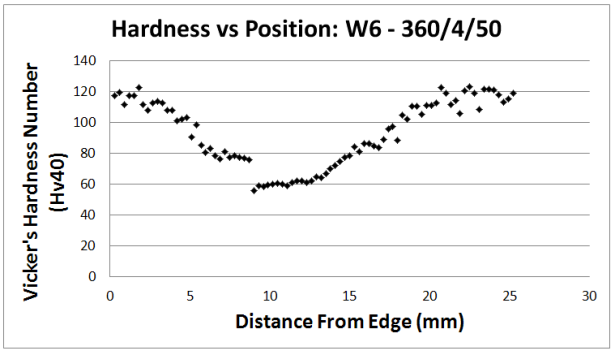
Hardness vs Position: W6 - 360/4/50
Vicker's Hardness Number (Hv40)
140
120
100
80
60
40
20
0
0
5
10
15
20
25
30
Distance From Edge (mm)

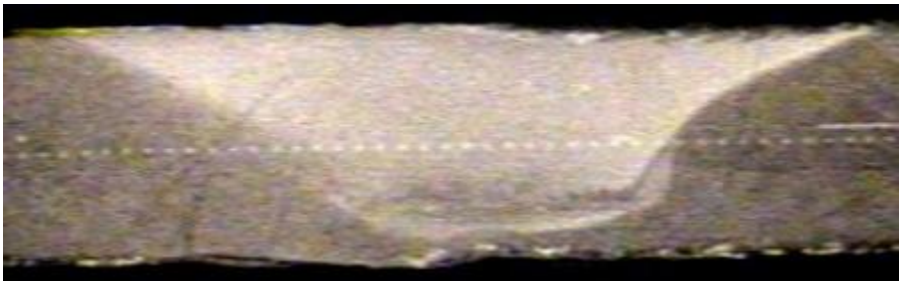

W7 – 360/4/75

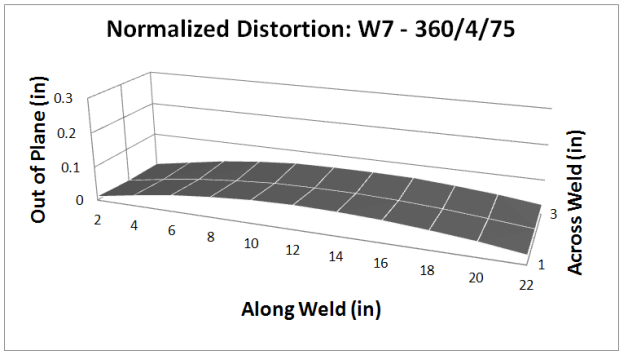
Normalized Distortion: W7 - 360/4/75
Out of Plane (in)
0.3
0.2
0.1
0
2
4
6
8
10
12
14
16
18
20
22
Along Weld (in)
1
3
Across Weld (in)

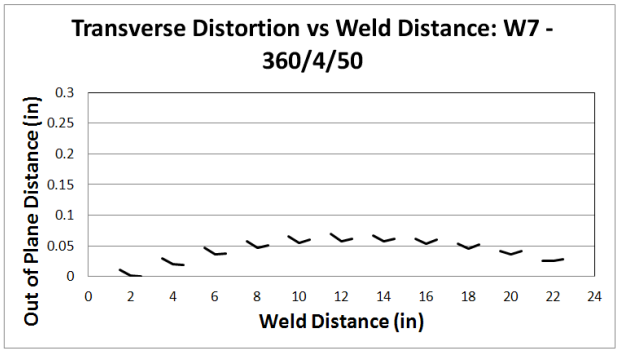
Transverse Distortion vs Weld Distance: W7 - 360/4/50
Out of Plane Distance (in)
0.3
0.25
0.2
0.15
0.1
0.05
0
0
2
4
6
8
10
12
14
16
18
20
22
24
Weld Distance (in)

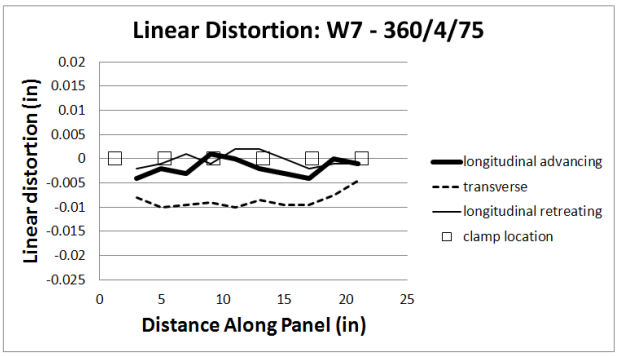
Linear Distortion: W7 - 360/4/75
Linear distortion (in)
0.02
0.015
0.01
0.005
0
-0.005
-0.01
-0.015
-0.02
-0.025
0
5
10
15
20
25
Distance Along Panel (in)
longitudinal advancing
transverse
longitudinal retreating
clamp location

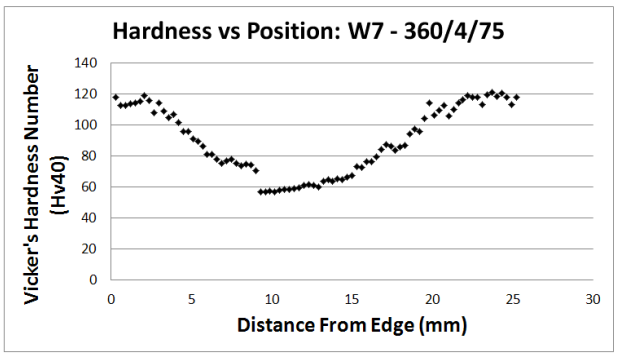
Hardness vs Position: W7 - 360/4/75
Vicker's Hardness Number (Hv40)
140
120
100
80
60
40
20
0
0
5
10
15
20
25
30
Distance From Edge (mm)

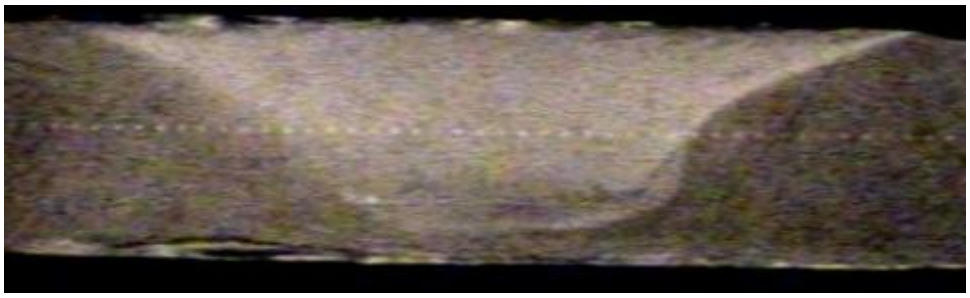

W8 – 360/4/25

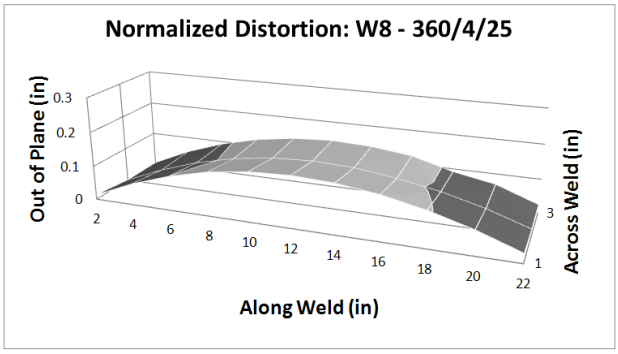
Normalized Distortion: W8 - 360/4/25
Out of Plane (in)
0.3
0.2
0.1
0
2
4
6
8
10
12
14
16
18
20
22
Along Weld (in)
3
1
Across Weld (in)

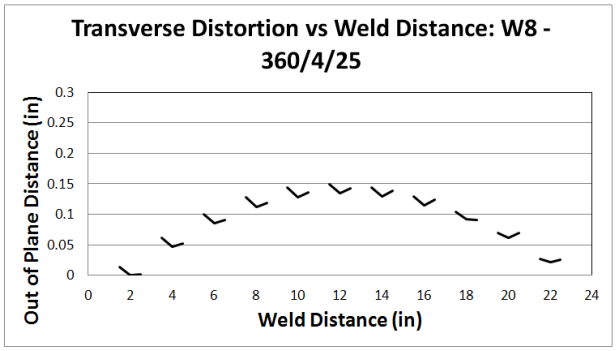
Transverse Distortion vs Weld Distance: W8 - 360/4/25
Out of Plane Distance (in)
0.3
0.25
0.2
0.15
0.1
0.05
0
0
2
4
6
8
10
12
14
16
18
20
22
24
Weld Distance (in)

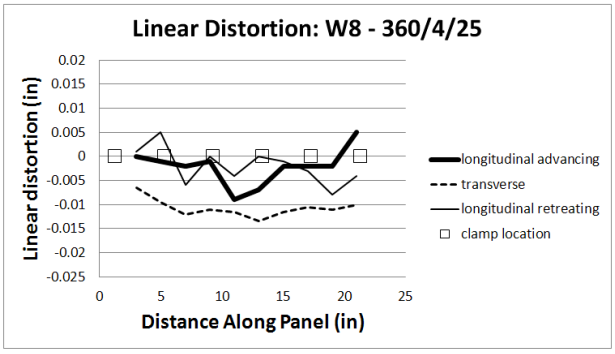
Linear Distortion: W8 - 360/4/25
Linear distortion (in)
0.02
0.015
0.01
0.005
0
-0.005
-0.01
-0.015
-0.02
-0.025
0
5
10
15
20
25
Distance Along Panel (in)
longitudinal advancing
transverse
longitudinal retreating
clamp location

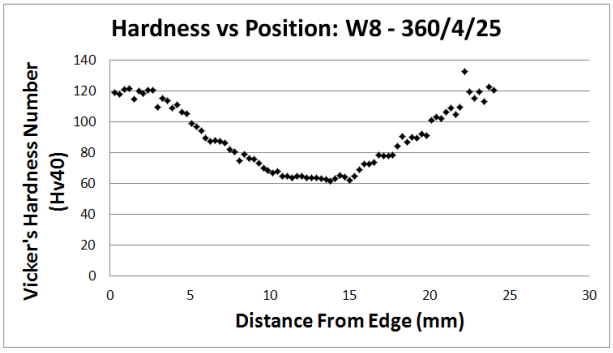
Hardness vs Position: W8 - 360/4/25
Vicker's Hardness Number (Hv40)
140
120
100
80
60
40
20
0
0
5
10
15
20
25
30
Distance From Edge (mm)

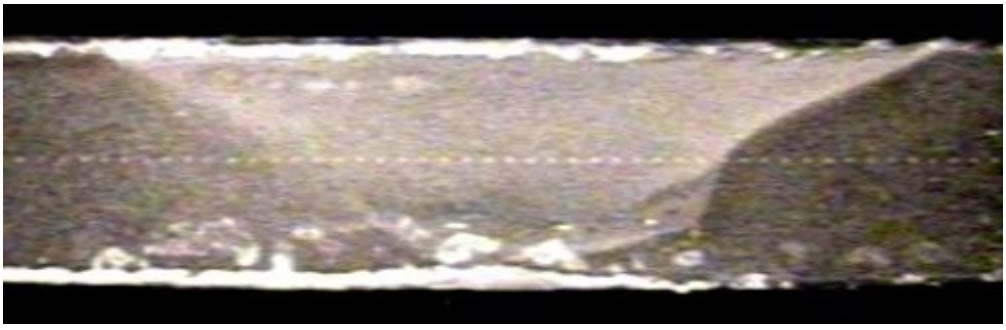

W9 – 380/8/25

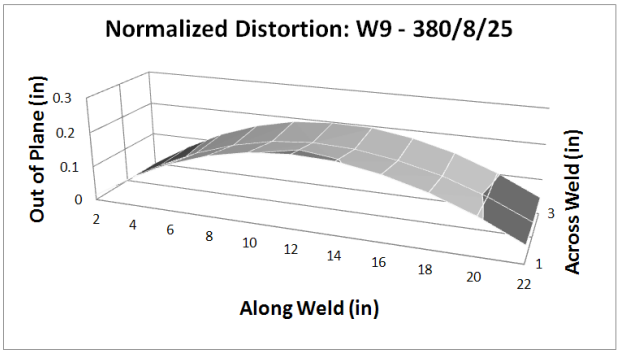

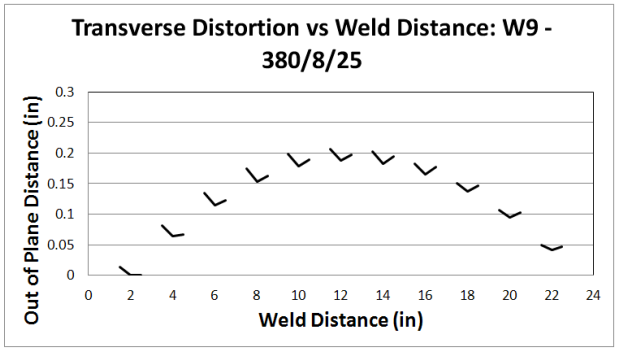

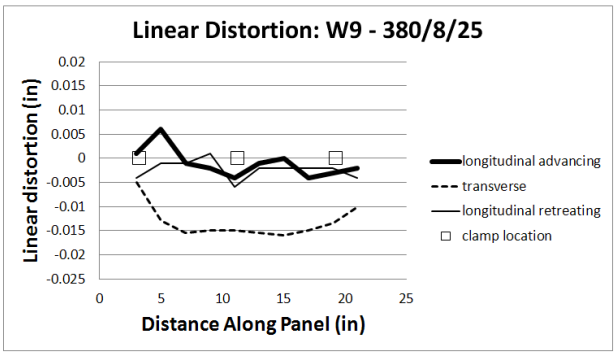

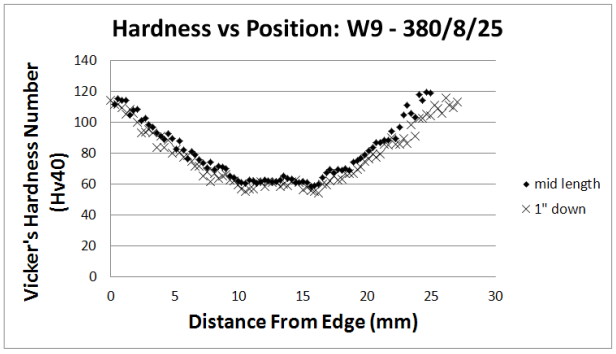

Mid Length:

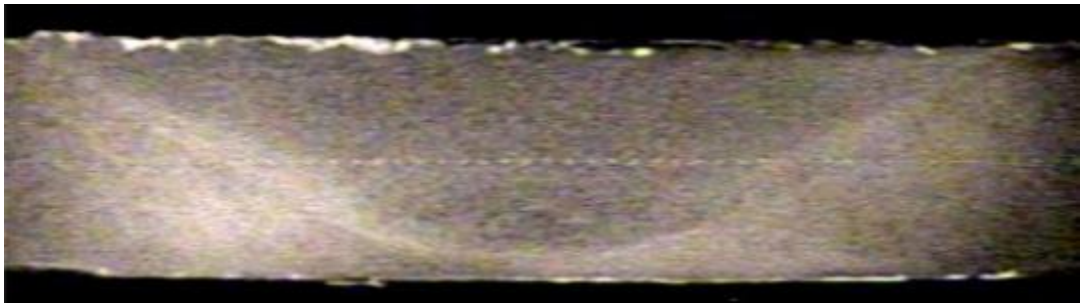

1" Down Weld:

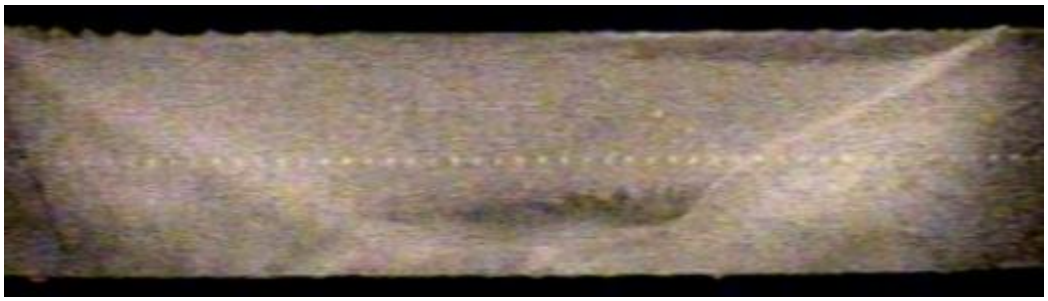

W10 – 340/8/25

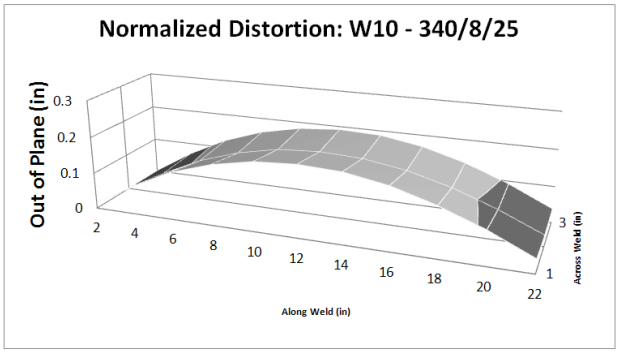
Normalized Distortion: W10 - 340/8/25
Out of Plane (in)
0.3
0.2
0.1
0
2
4
6
8
10
12
14
16
18
20
22
Along Weld (in)
3
1
Across Weld (in)

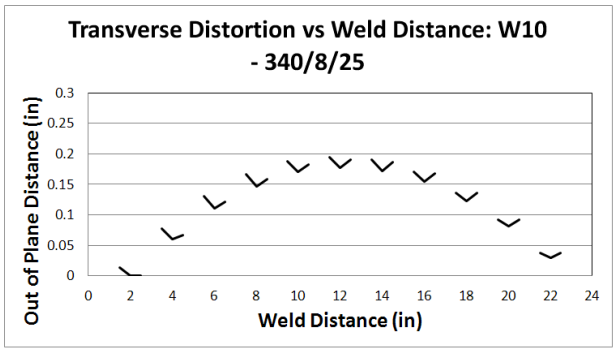
Transverse Distortion vs Weld Distance: W10 - 340/8/25
Out of Plane Distance (in)
0.3
0.25
0.2
0.15
0.1
0.05
0
0
2
4
6
8
10
12
14
16
18
20
22
24
Weld Distance (in)

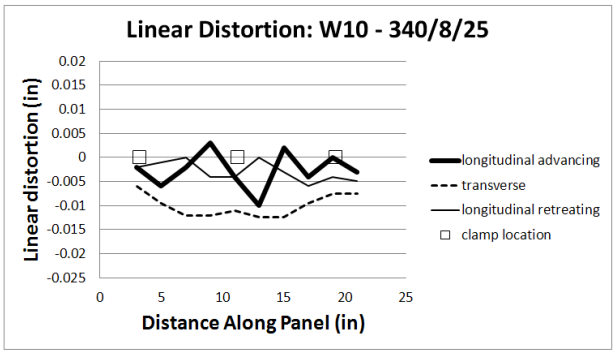
Linear Distortion: W10 - 340/8/25
Linear distortion (in)
0.02
0.015
0.01
0.005
0
-0.005
-0.01
-0.015
-0.02
-0.025
0
5
10
15
20
25
Distance Along Panel (in)
longitudinal advancing
transverse
longitudinal retreating
clamp location

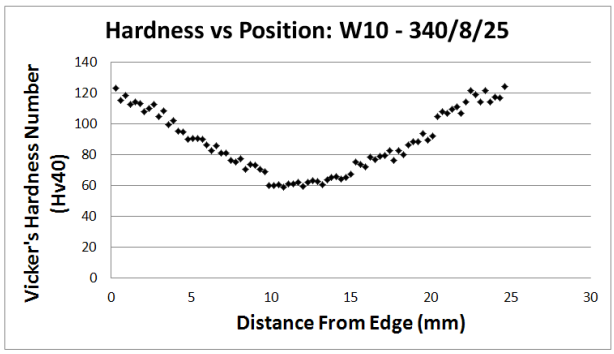
Hardness vs Position: W10 - 340/8/25
Vicker's Hardness Number (Hv40)
140
120
100
80
60
40
20
0
0
5
10
15
20
25
30
Distance From Edge (mm)

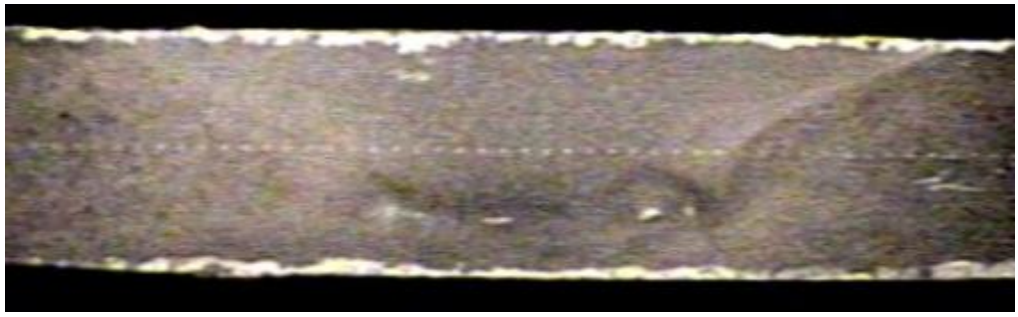

W11 – 380/2/75

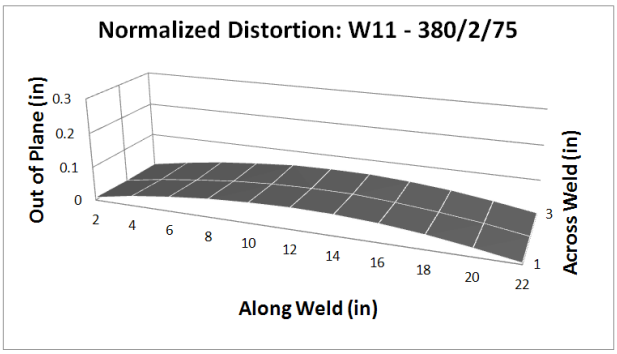
Normalized Distortion: W11 - 380/2/75
Out of Plane (in)
0.3
0.2
0.1
0
2
4
6
8
10
12
14
16
18
20
22
Along Weld (in)
1
3
Across Weld (in)

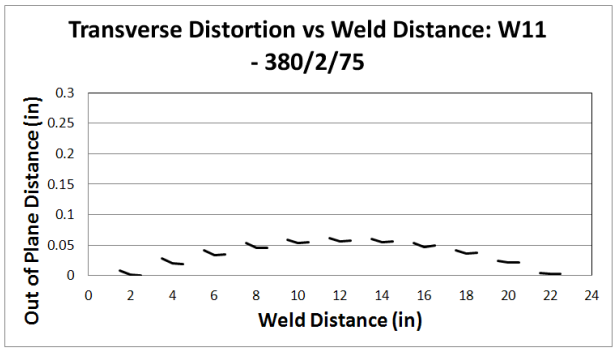
Transverse Distortion vs Weld Distance: W11 - 380/2/75
Out of Plane Distance (in)
0.3
0.25
0.2
0.15
0.1
0.05
0
0
2
4
6
8
10
12
14
16
18
20
22
24
Weld Distance (in)

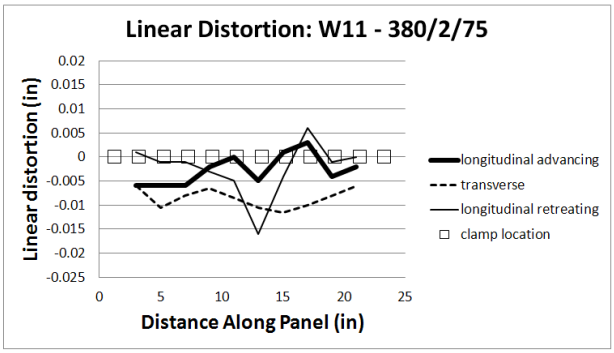
Linear Distortion: W11 - 380/2/75
Linear distortion (in)
0.02
0.015
0.01
0.005
0
-0.005
-0.01
-0.015
-0.02
-0.025
0
5
10
15
20
25
Distance Along Panel (in)
longitudinal advancing
transverse
longitudinal retreating
clamp location

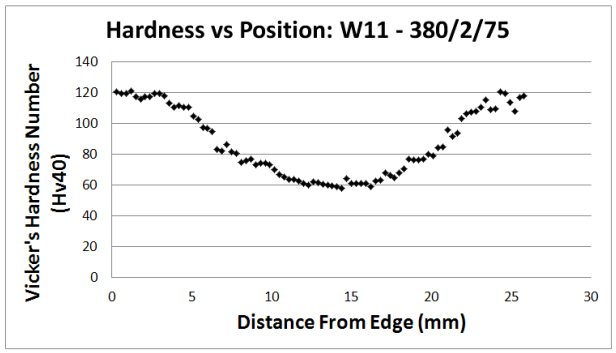
Hardness vs Position: W11 - 380/2/75
Vicker's Hardness Number (Hv40)
140
120
100
80
60
40
20
0
0
5
10
15
20
25
30
Distance From Edge (mm)

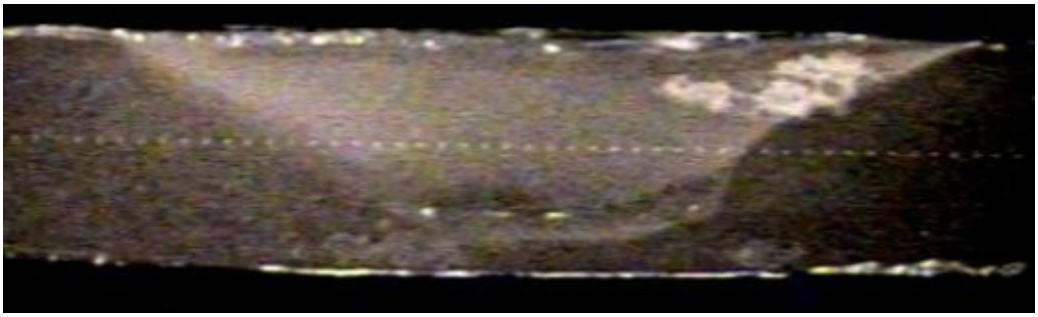

W12 – 360/4/50

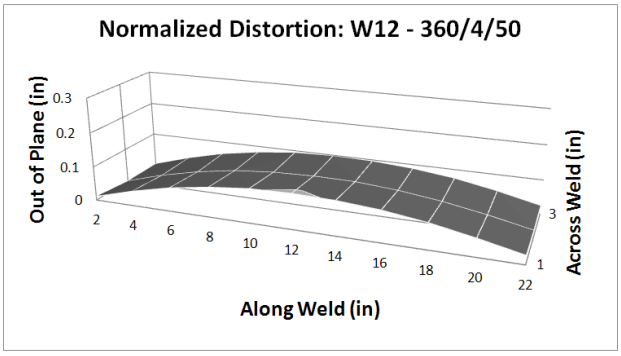
Normalized Distortion: W12 - 360/4/50
Out of Plane (in)
0.3
0.2
0.1
0
2
4
6
8
10
12
14
16
18
20
22
Along Weld (in)
1
3
Across Weld (in)

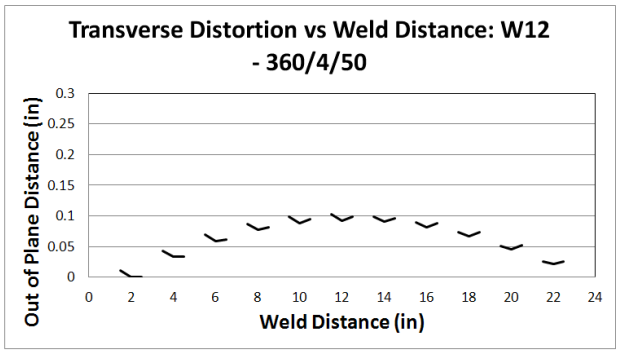
Transverse Distortion vs Weld Distance: W12 - 360/4/50
Out of Plane Distance (in)
0.3
0.25
0.2
0.15
0.1
0.05
0
0
2
4
6
8
10
12
14
16
18
20
22
24
Weld Distance (in)

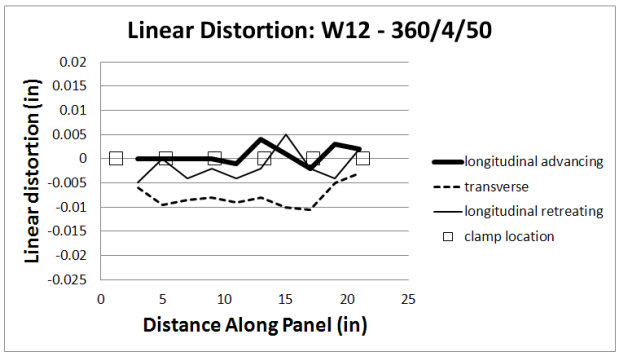
Linear Distortion: W12 - 360/4/50
Linear distortion (in)
0.02
0.015
0.01
0.005
0
-0.005
-0.01
-0.015
-0.02
-0.025
0
5
10
15
20
25
Distance Along Panel (in)
longitudinal advancing
transverse
longitudinal retreating
clamp location

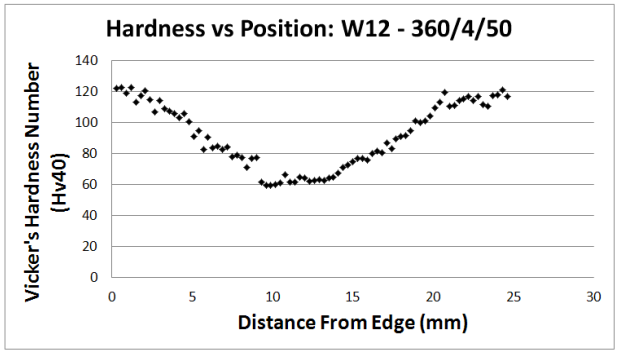
Hardness vs Position: W12 - 360/4/50
Vicker's Hardness Number (Hv40)
140
120
100
80
60
40
20
0
0
5
10
15
20
25
30
Distance From Edge (mm)

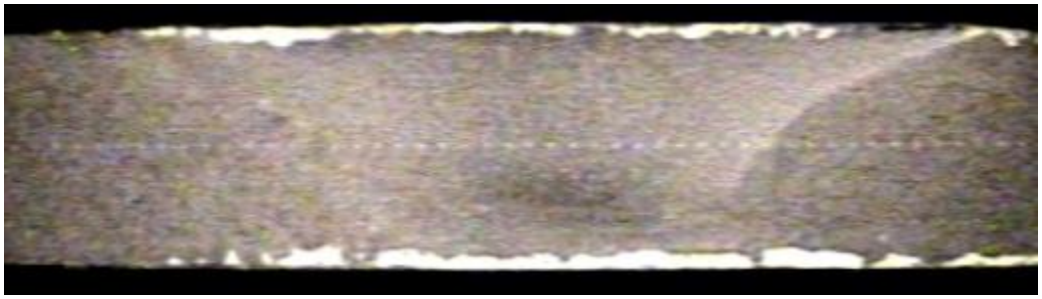

W13 – 380/2/25

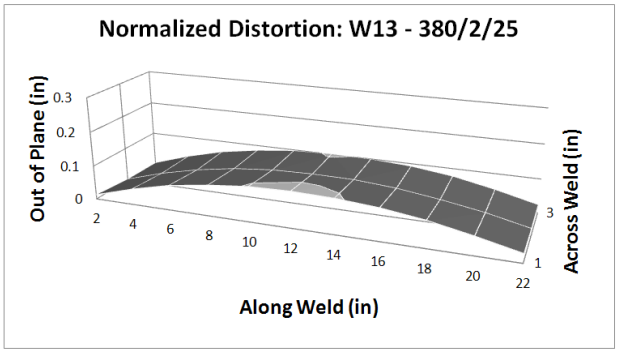
Normalized Distortion: W13 - 380/2/25
Out of Plane (in)
0.3
0.2
0.1
0
2
4
6
8
10
12
14
16
18
20
22
Along Weld (in)
1
3
Across Weld (in)

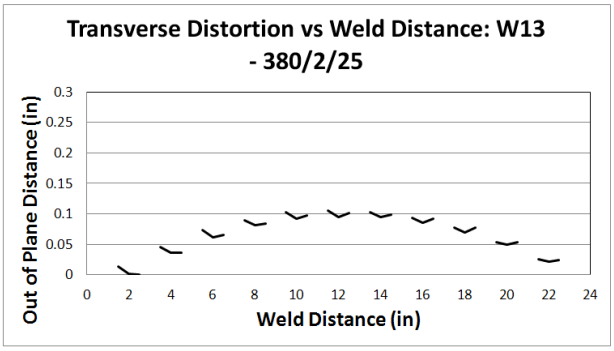
Transverse Distortion vs Weld Distance: W13 - 380/2/25
Out of Plane Distance (in)
0.3
0.25
0.2
0.15
0.1
0.05
0
0
2
4
6
8
10
12
14
16
18
20
22
24
Weld Distance (in)

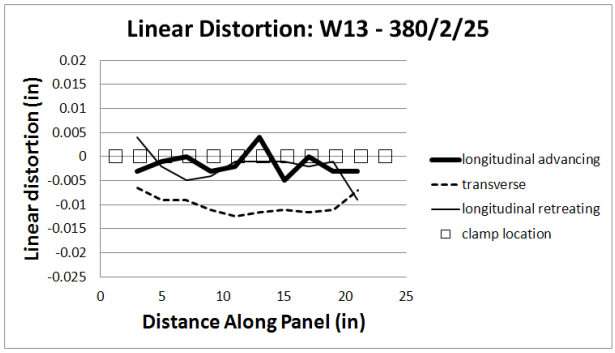
Linear Distortion: W13 - 380/2/25
Linear distortion (in)
0.02
0.015
0.01
0.005
0
-0.005
-0.01
-0.015
-0.02
-0.025
0
5
10
15
20
25
Distance Along Panel (in)
longitudinal advancing
transverse
longitudinal retreating
clamp location

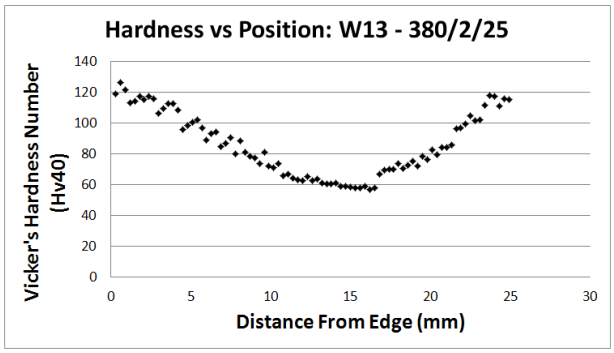
Hardness vs Position: W13 - 380/2/25
Vicker's Hardness Number (Hv40)
140
120
100
80
60
40
20
0
0
5
10
15
20
25
30
Distance From Edge (mm)

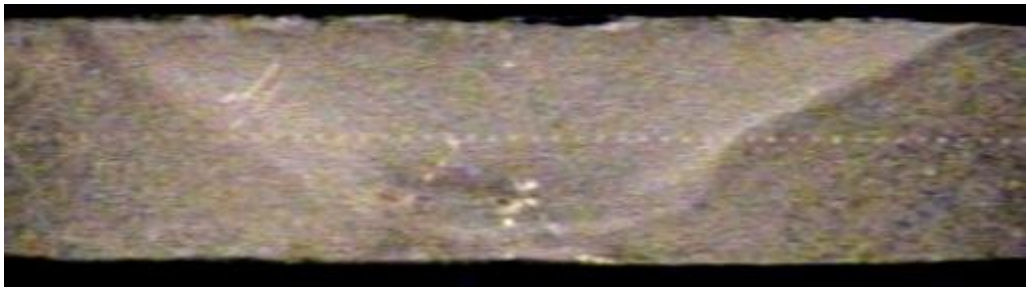

W14 – 380/4/50

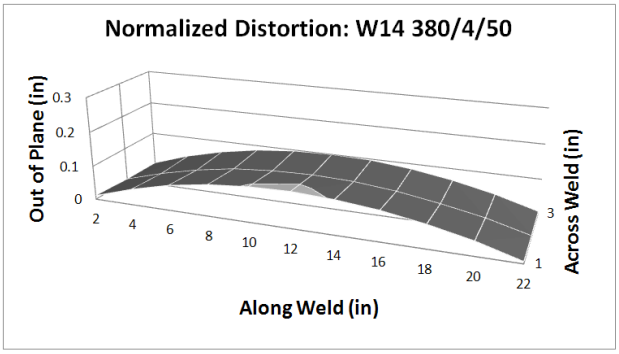
Normalized Distortion: W14 380/4/50
Out of Plane (in)
0.3
0.2
0.1
0
2
4
6
8
10
12
14
16
18
20
22
Along Weld (in)
1
3
Across Weld (in)

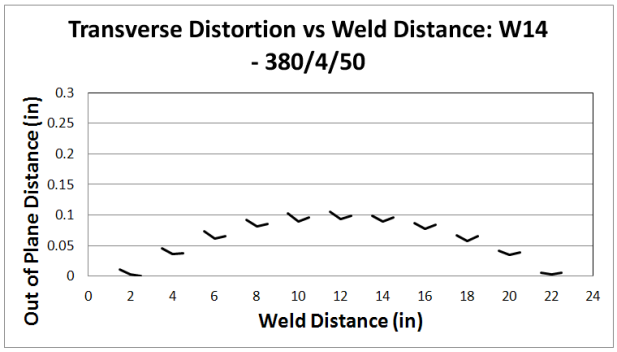
Transverse Distortion vs Weld Distance: W14 - 380/4/50
Out of Plane Distance (in)
0.3
0.25
0.2
0.15
0.1
0.05
0
0
2
4
6
8
10
12
14
16
18
20
22
24
Weld Distance (in)

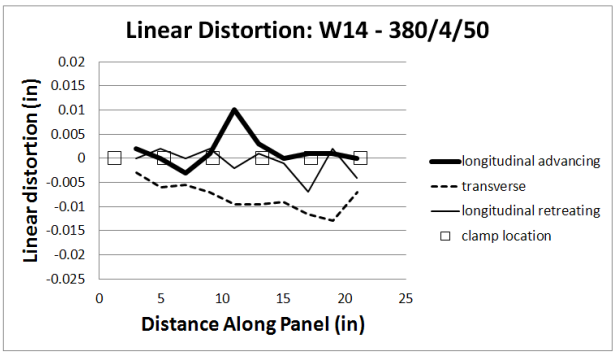
Linear Distortion: W14 - 380/4/50
Linear distortion (in)
0.02
0.015
0.01
0.005
0
-0.005
-0.01
-0.015
-0.02
-0.025
0
5
10
15
20
25
Distance Along Panel (in)
longitudinal advancing
transverse
longitudinal retreating
clamp location

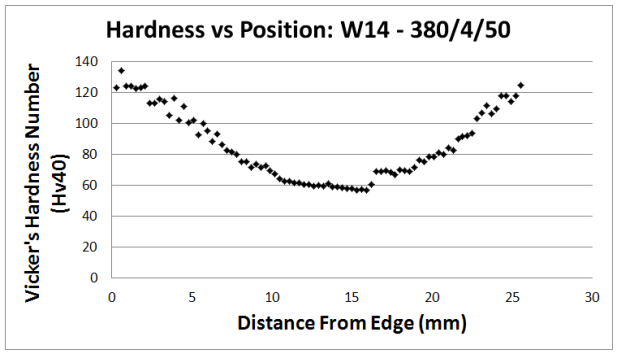
Hardness vs Position: W14 - 380/4/50
Vicker's Hardness Number (Hv40)
140
120
100
80
60
40
20
0
0
5
10
15
20
25
30
Distance From Edge (mm)

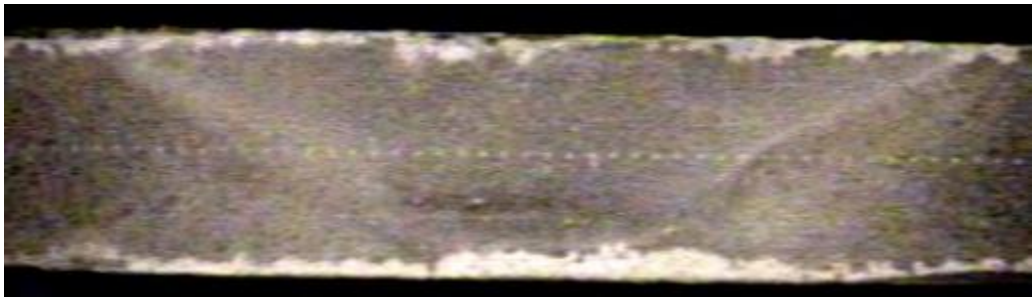

W15 – 340/2/25

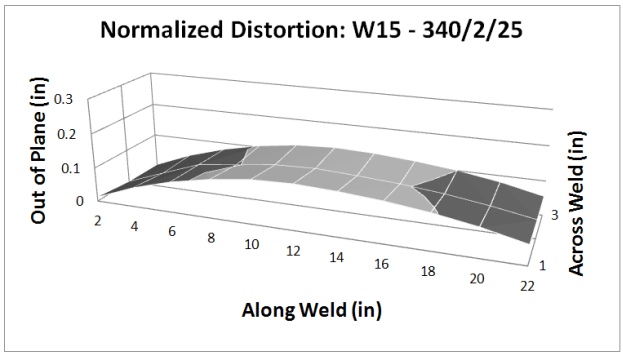
Normalized Distortion: W15 - 340/2/25
Out of Plane (in)
0.3
0.2
0.1
0
2
4
6
8
10
12
14
16
18
20
22
Along Weld (in)
1
3
Across Weld (in)

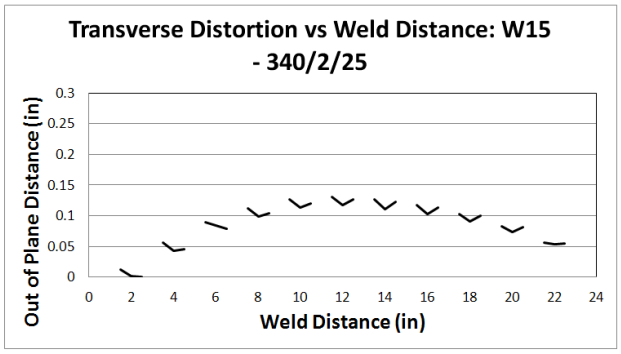
Transverse Distortion vs Weld Distance: W15 - 340/2/25
Out of Plane Distance (in)
0.3
0.25
0.2
0.15
0.1
0.05
0
0
2
4
6
8
10
12
14
16
18
20
22
24
Weld Distance (in)

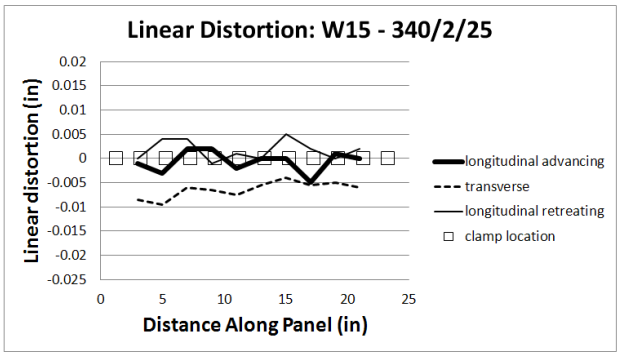
Linear Distortion: W15 - 340/2/25
Linear distortion (in)
0.02
0.015
0.01
0.005
0
-0.005
-0.01
-0.015
-0.02
-0.025
0
5
10
15
20
25
Distance Along Panel (in)
longitudinal advancing
transverse
longitudinal retreating
clamp location

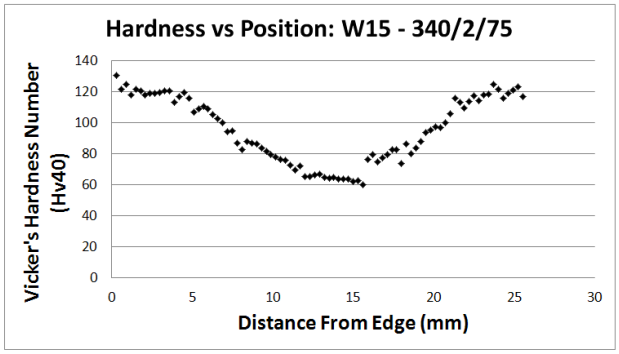
Hardness vs Position: W15 - 340/2/75
Vicker's Hardness Number (Hv40)
140
120
100
80
60
40
20
0
0
5
10
15
20
25
30
Distance From Edge (mm)

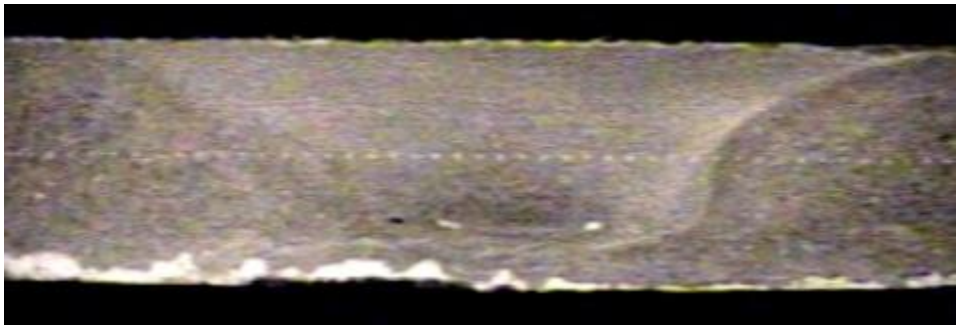

W16 – 340/8/75

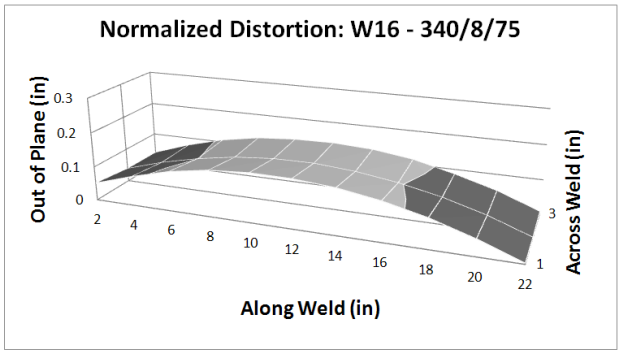
Normalized Distortion: W16 - 340/8/75
Out of Plane (in)
0.3
0.2
0.1
0
2
4
6
8
10
12
14
16
18
20
22
Along Weld (in)
1
3
Across Weld (in)

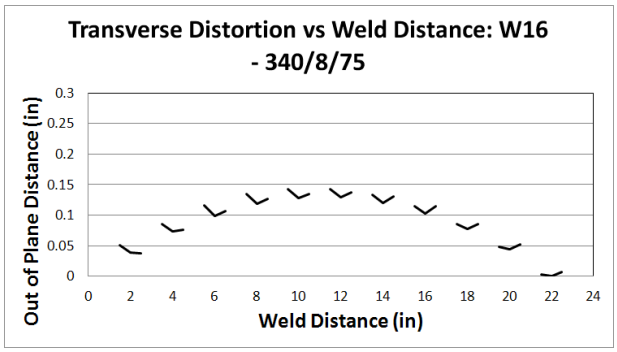
Transverse Distortion vs Weld Distance: W16 - 340/8/75
Out of Plane Distance (in)
0.3
0.25
0.2
0.15
0.1
0.05
0
0
2
4
6
8
10
12
14
16
18
20
22
24
Weld Distance (in)

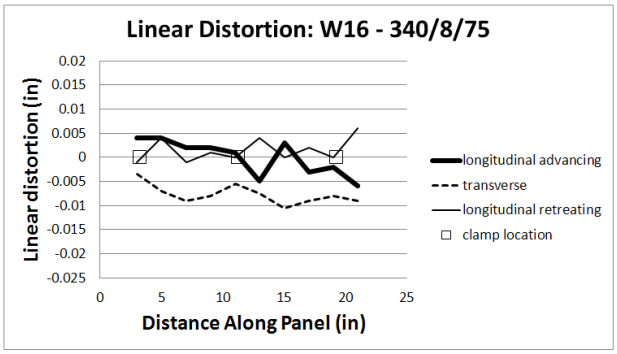
Linear Distortion: W16 - 340/8/75
Linear distortion (in)
0.02
0.015
0.01
0.005
0
-0.005
-0.01
-0.015
-0.02
-0.025
0
5
10
15
20
25
Distance Along Panel (in)
longitudinal advancing
transverse
longitudinal retreating
clamp location

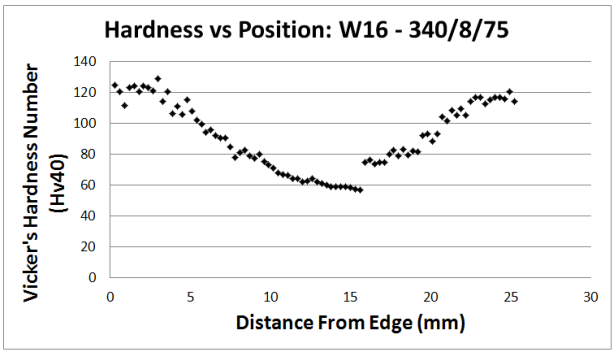
Hardness vs Position: W16 - 340/8/75
Vicker's Hardness Number (Hv40)
140
120
100
80
60
40
20
0
0
5
10
15
20
25
30
Distance From Edge (mm)

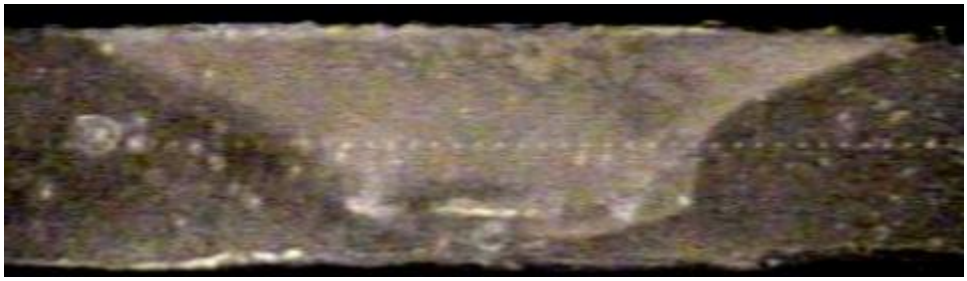

W17 – 340/2/75

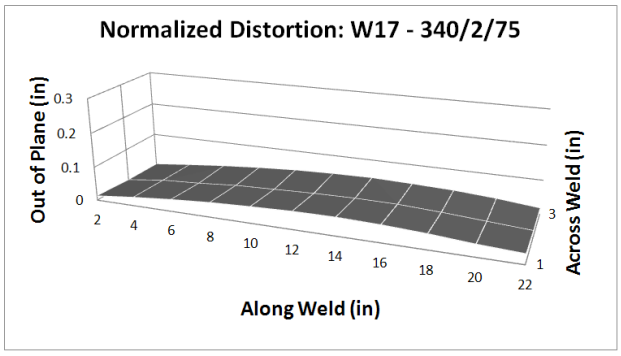

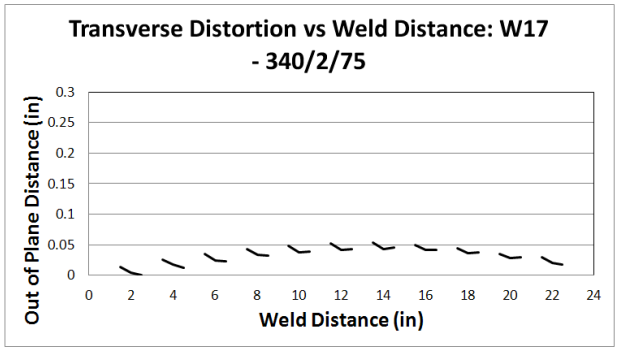

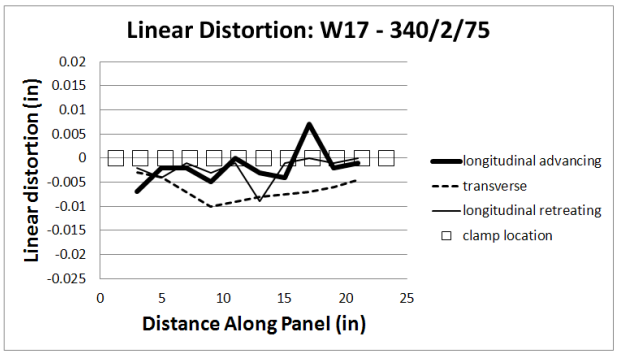

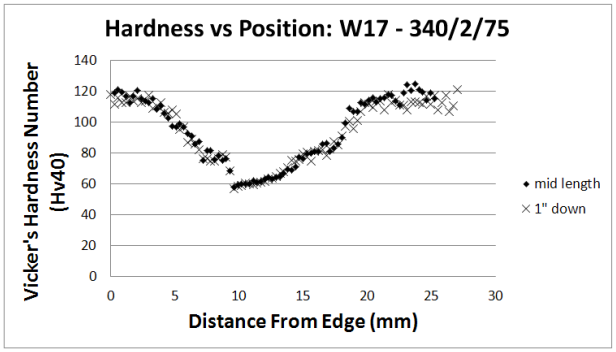

Mid Length:

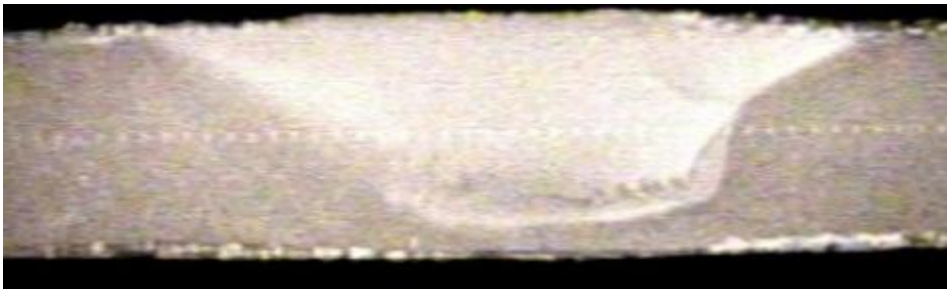

1” Down Weld:

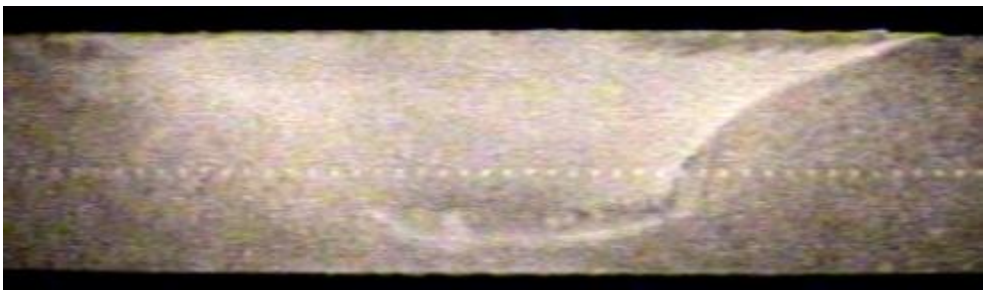

W18 – 340/2/25

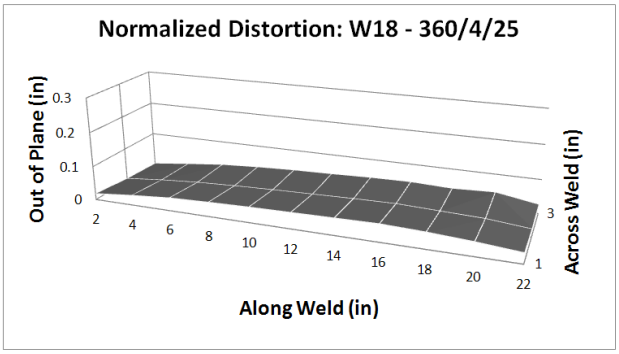
Normalized Distortion: W18 - 360/4/25
Out of Plane (in)
0.3
0.2
0.1
0
2
4
6
8
10
12
14
16
18
20
22
Along Weld (in)
1
3
Across Weld (in)

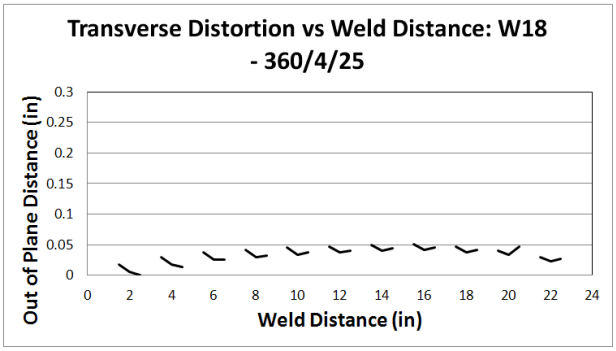
Transverse Distortion vs Weld Distance: W18 - 360/4/25
Out of Plane Distance (in)
0.3
0.25
0.2
0.15
0.1
0.05
0
0
2
4
6
8
10
12
14
16
18
20
22
24
Weld Distance (in)

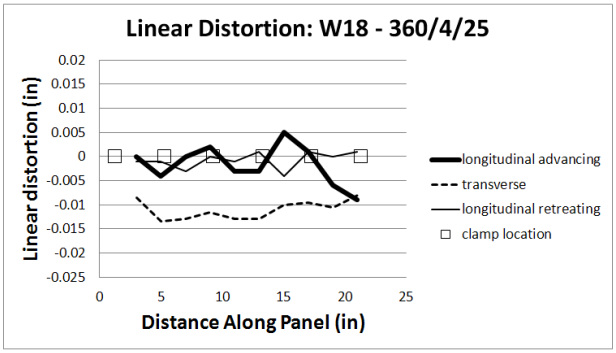
Linear Distortion: W18 - 360/4/25
Linear distortion (in)
0.02
0.015
0.01
0.005
0
-0.005
-0.01
-0.015
-0.02
-0.025
0
5
10
15
20
25
Distance Along Panel (in)
longitudinal advancing
transverse
longitudinal retreating
clamp location

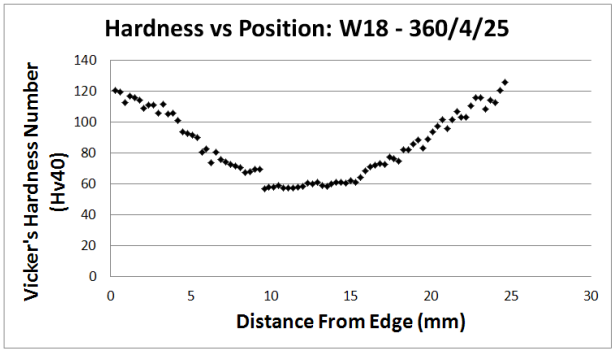
Hardness vs Position: W18 - 360/4/25
Vicker's Hardness Number (Hv40)
140
120
100
80
60
40
20
0
0
5
10
15
20
25
30
Distance From Edge (mm)

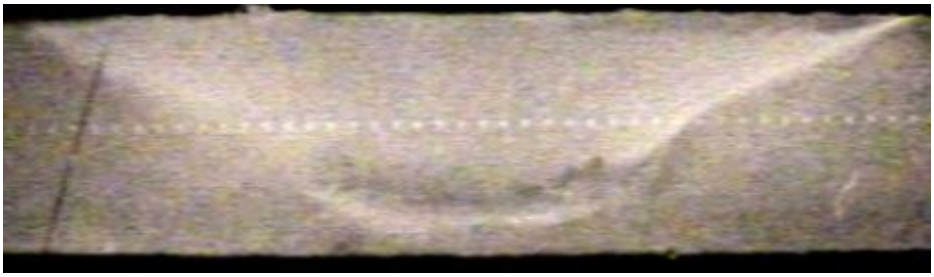

W19 – 340/4/50

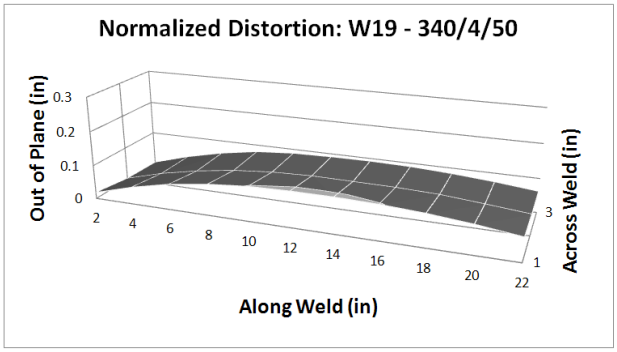
Normalized Distortion: W19 - 340/4/50
Out of Plane (in)
0.3
0.2
0.1
0
2
4
6
8
10
12
14
16
18
20
22
Along Weld (in)
1
3
Across Weld (in)

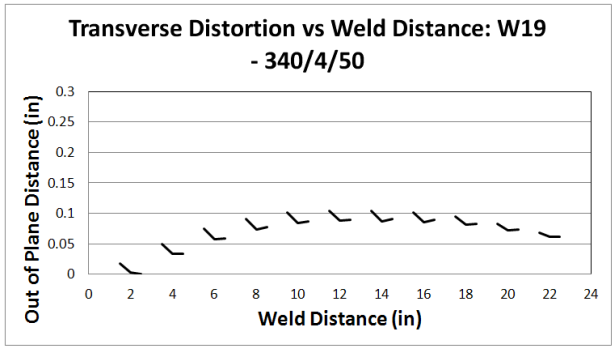
Transverse Distortion vs Weld Distance: W19 - 340/4/50
Out of Plane Distance (in)
0.3
0.25
0.2
0.15
0.1
0.05
0
0
2
4
6
8
10
12
14
16
18
20
22
24
Weld Distance (in)

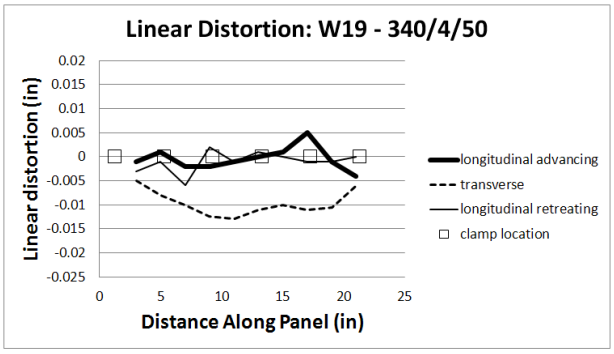
Linear Distortion: W19 - 340/4/50
Linear distortion (in)
0.02
0.015
0.01
0.005
0
-0.005
-0.01
-0.015
-0.02
-0.025
0
5
10
15
20
25
Distance Along Panel (in)
longitudinal advancing
transverse
longitudinal retreating
clamp location

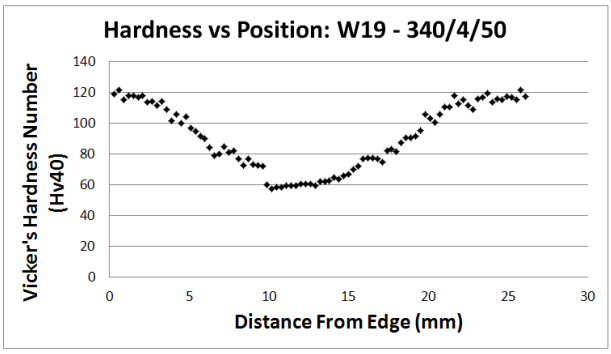
Hardness vs Position: W19 - 340/4/50
Vicker's Hardness Number (Hv40)
140
120
100
80
60
40
20
0
0
5
10
15
20
25
30
Distance From Edge (mm)

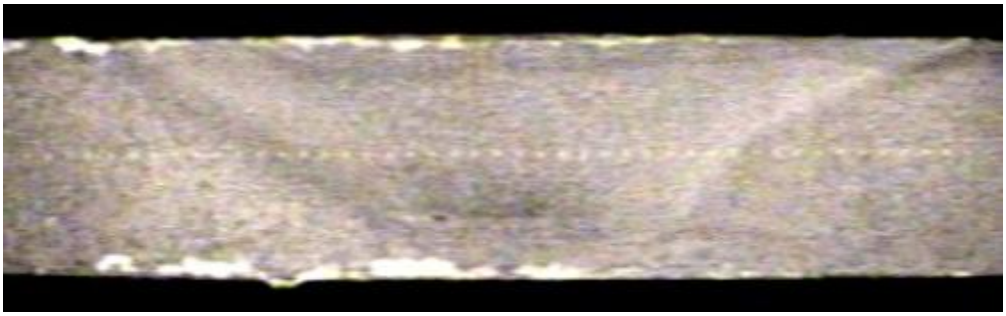

W20 – 360/2/50

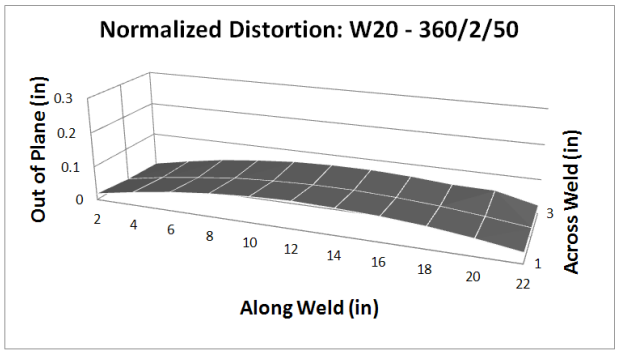
Normalized Distortion: W20 - 360/2/50
Out of Plane (in)
0.3
0.2
0.1
0
2
4
6
8
10
12
14
16
18
20
22
Along Weld (in)
1
3
Across Weld (in)

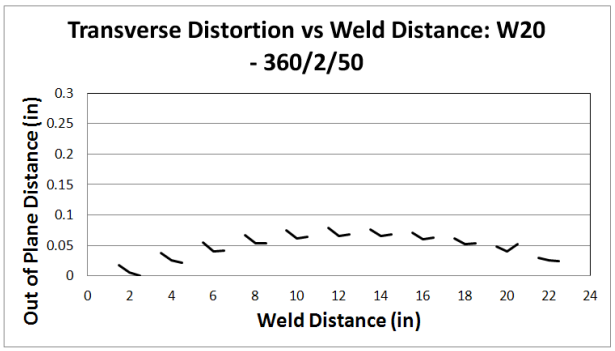
Transverse Distortion vs Weld Distance: W20 - 360/2/50
Out of Plane Distance (in)
0.3
0.25
0.2
0.15
0.1
0.05
0
0
2
4
6
8
10
12
14
16
18
20
22
24
Weld Distance (in)

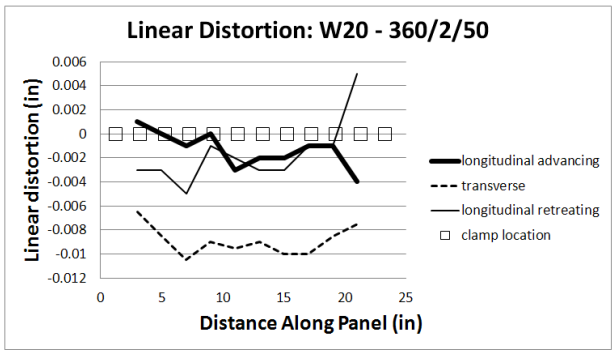
Linear Distortion: W20 - 360/2/50
Linear distortion (in)
0.006
0.004
0.002
0
-0.002
-0.004
-0.006
-0.008
-0.01
-0.012
0
5
10
15
20
25
Distance Along Panel (in)
longitudinal advancing
transverse
longitudinal retreating
clamp location

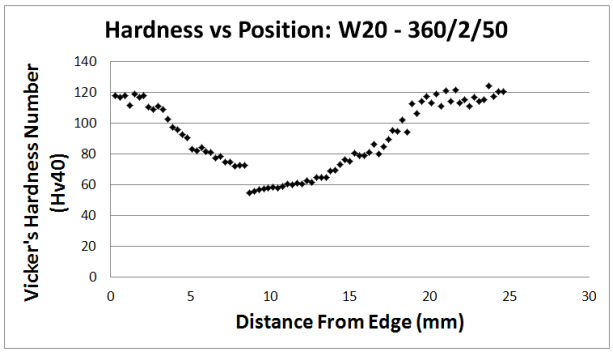
Hardness vs Position: W20 - 360/2/50
Vicker's Hardness Number (Hv40)
140
120
100
80
60
40
20
0
0
5
10
15
20
25
30
Distance From Edge (mm)

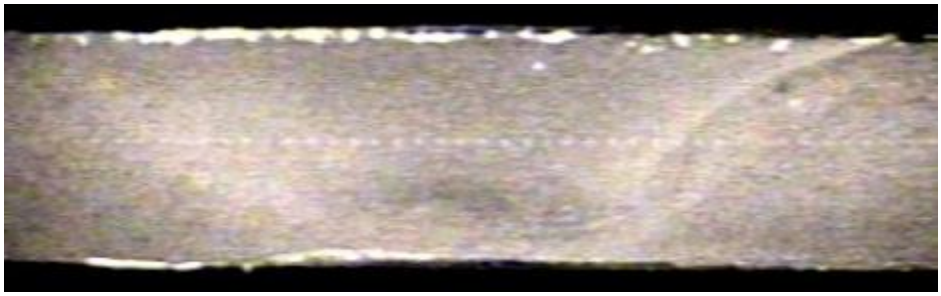

W21 – 360/4/75

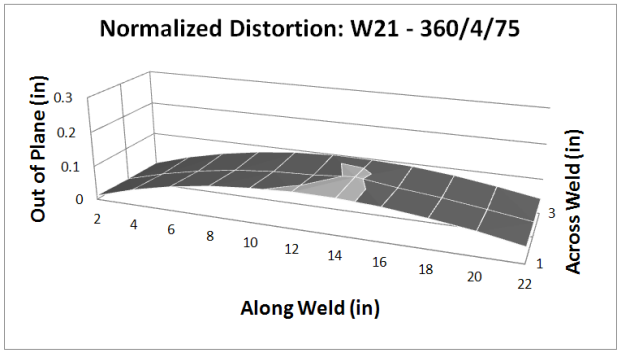
Normalized Distortion: W21 - 360/4/75
Out of Plane (in)
0.3
0.2
0.1
0
2
4
6
8
10
12
14
16
18
20
22
Along Weld (in)
1
3
Across Weld (in)

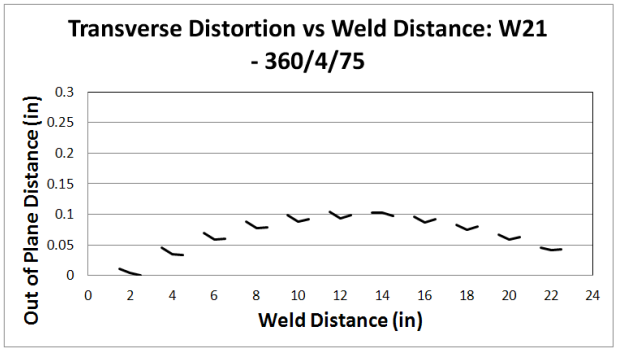
Transverse Distortion vs Weld Distance: W21 - 360/4/75
Out of Plane Distance (in)
0.3
0.25
0.2
0.15
0.1
0.05
0
0
2
4
6
8
10
12
14
16
18
20
22
24
Weld Distance (in)

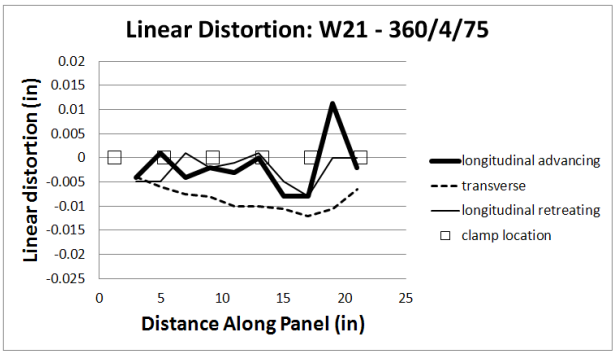
Linear Distortion: W21 - 360/4/75
Linear distortion (in)
0.02
0.015
0.01
0.005
0
-0.005
-0.01
-0.015
-0.02
-0.025
0
5
10
15
20
25
Distance Along Panel (in)
longitudinal advancing
transverse
longitudinal retreating
clamp location

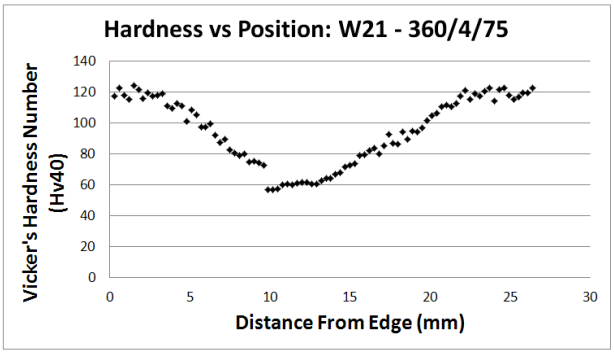
Hardness vs Position: W21 - 360/4/75
Vicker's Hardness Number (Hv40)
140
120
100
80
60
40
20
0
0
5
10
15
20
25
30
Distance From Edge (mm)

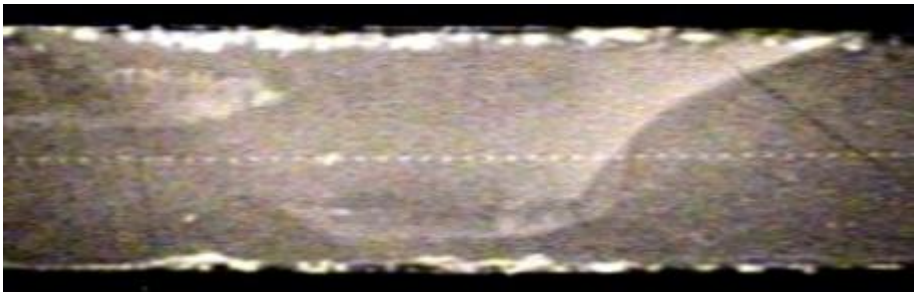

W22 – 340/8/25

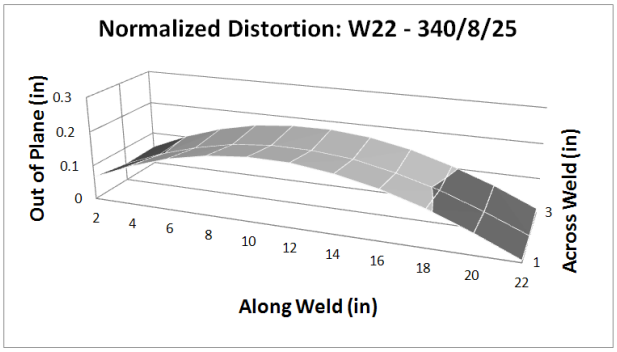
Normalized Distortion: W22 - 340/8/25
Out of Plane (in)
0.3
0.2
0.1
0
2
4
6
8
10
12
14
16
18
20
22
Along Weld (in)
1
3
Across Weld (in)

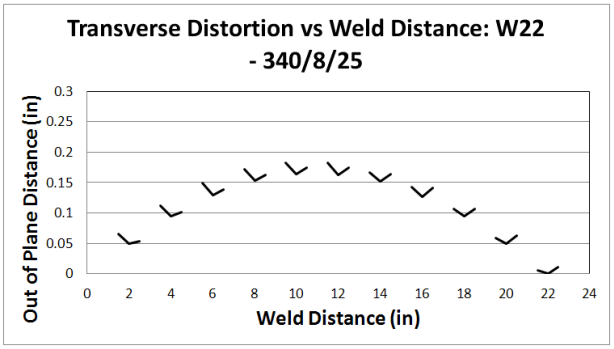
Transverse Distortion vs Weld Distance: W22 - 340/8/25
Out of Plane Distance (in)
0.3
0.25
0.2
0.15
0.1
0.05
0
0
2
4
6
8
10
12
14
16
18
20
22
24
Weld Distance (in)

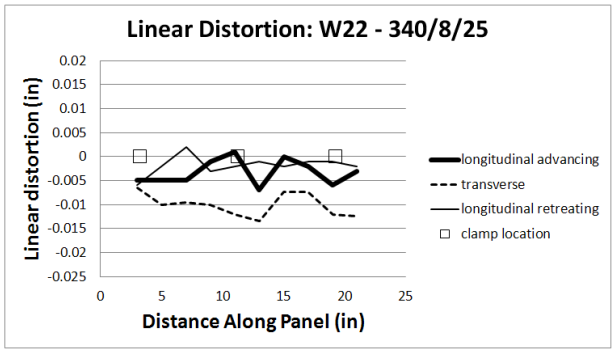
Linear Distortion: W22 - 340/8/25
Linear distortion (in)
0.02
0.015
0.01
0.005
0
-0.005
-0.01
-0.015
-0.02
-0.025
0
5
10
15
20
25
Distance Along Panel (in)
longitudinal advancing
transverse
longitudinal retreating
clamp location

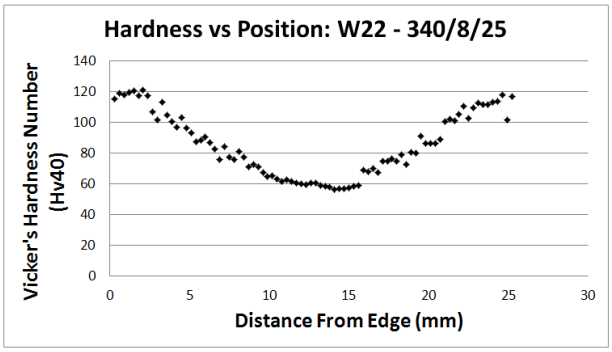
Hardness vs Position: W22 - 340/8/25
Vicker's Hardness Number (Hv40)
140
120
100
80
60
40
20
0
0
5
10
15
20
25
30
Distance From Edge (mm)

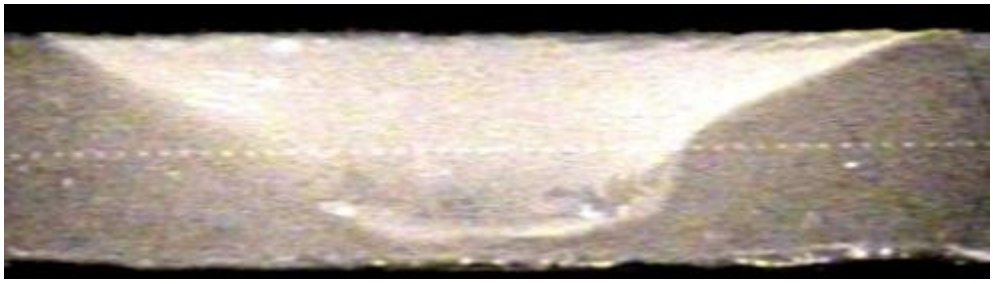

W23 – 340/2/25

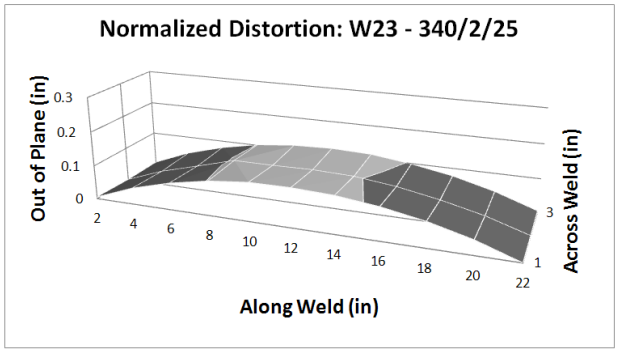
Normalized Distortion: W23 - 340/2/25
Out of Plane (in)
0.3
0.2
0.1
0
2
4
6
8
10
12
14
16
18
20
22
Along Weld (in)
1
3
Across Weld (in)

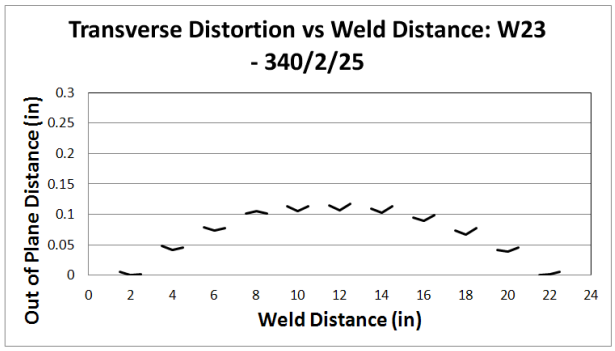
Transverse Distortion vs Weld Distance: W23 - 340/2/25
Out of Plane Distance (in)
0.3
0.25
0.2
0.15
0.1
0.05
0
0
2
4
6
8
10
12
14
16
18
20
22
24
Weld Distance (in)

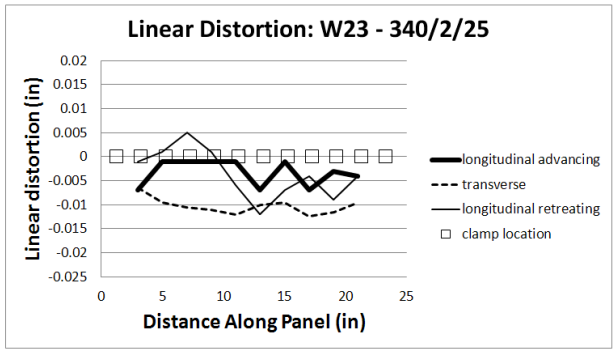
Linear Distortion: W23 - 340/2/25
Linear distortion (in)
0.02
0.015
0.01
0.005
0
-0.005
-0.01
-0.015
-0.02
-0.025
0
5
10
15
20
25
Distance Along Panel (in)
longitudinal advancing
transverse
longitudinal retreating
clamp location

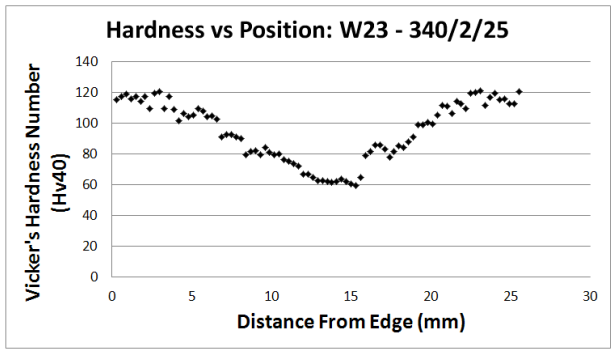
Hardness vs Position: W23 - 340/2/25
Vicker's Hardness Number (Hv40)
140
120
100
80
60
40
20
0
0
5
10
15
20
25
30
Distance From Edge (mm)

W24 – 360/4/50

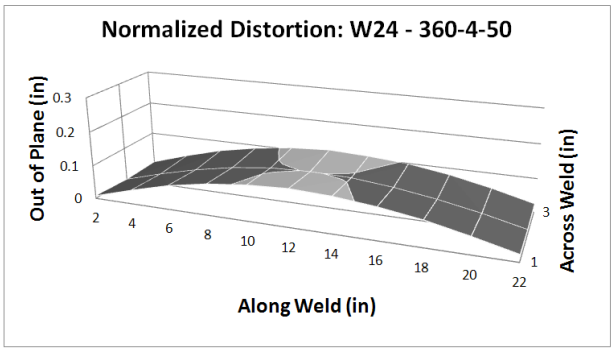
Normalized Distortion: W24 - 360-4-50
Out of Plane (in)
0.3
0.2
0.1
0
2
4
6
8
10
12
14
16
18
20
22
Along Weld (in)
1
3
Across Weld (in)

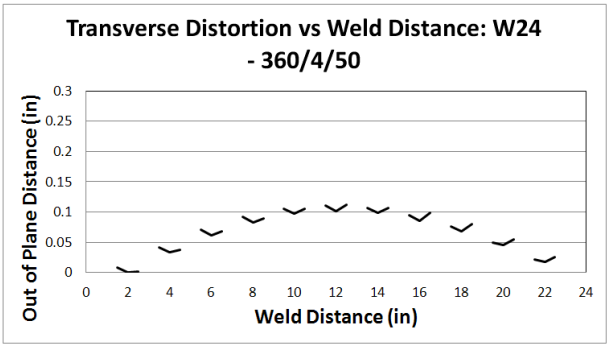
Transverse Distortion vs Weld Distance: W24 - 360/4/50
Out of Plane Distance (in)
0.3
0.25
0.2
0.15
0.1
0.05
0
0
2
4
6
8
10
12
14
16
18
20
22
24
Weld Distance (in)

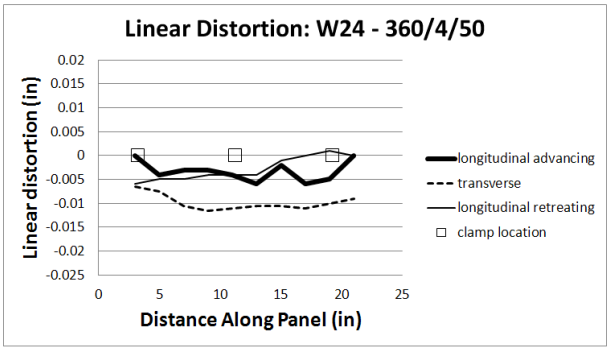
Linear Distortion: W24 - 360/4/50
Linear distortion (in)
0.02
0.015
0.01
0.005
0
-0.005
-0.01
-0.015
-0.02
-0.025
0
5
10
15
20
25
Distance Along Panel (in)
longitudinal advancing
transverse
longitudinal retreating
clamp location

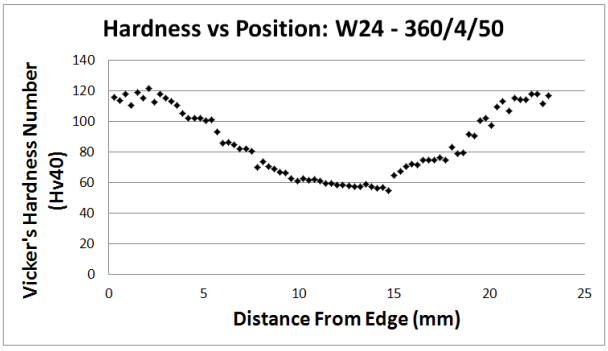
Hardness vs Position: W24 - 360/4/50
Vicker's Hardness Number (Hv40)
140
120
100
80
60
40
20
0
0
5
10
15
20
25
Distance From Edge (mm)

W25 – 360/4/50

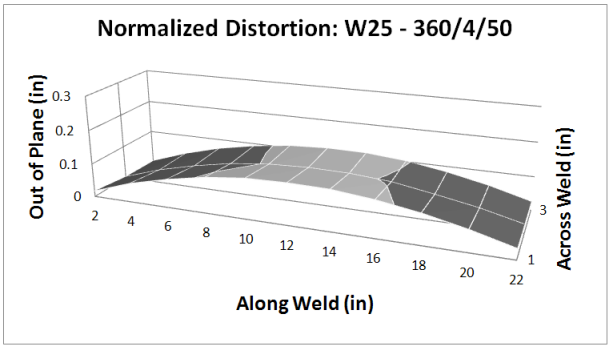
Normalized Distortion: W25 - 360/4/50
Out of Plane (in)
0.3
0.2
0.1
0
2
4
6
8
10
12
14
16
18
20
22
Along Weld (in)
1
3
Across Weld (in)

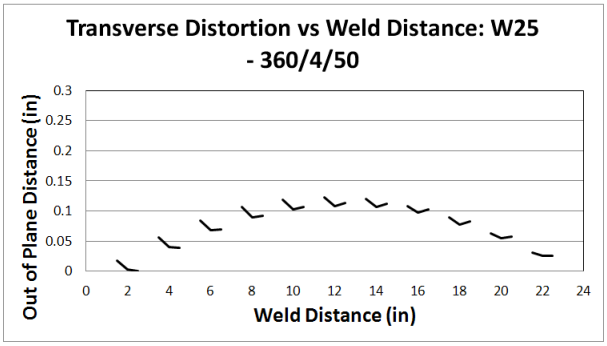
Transverse Distortion vs Weld Distance: W25 - 360/4/50
Out of Plane Distance (in)
0.3
0.25
0.2
0.15
0.1
0.05
0
0
2
4
6
8
10
12
14
16
18
20
22
24
Weld Distance (in)

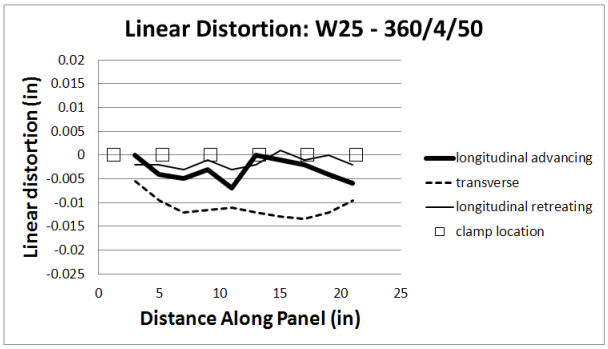
Linear Distortion: W25 - 360/4/50
Linear distortion (in)
0.02
0.015
0.01
0.005
0
-0.005
-0.01
-0.015
-0.02
-0.025
0
5
10
15
20
25
Distance Along Panel (in)
longitudinal advancing
transverse
longitudinal retreating
clamp location

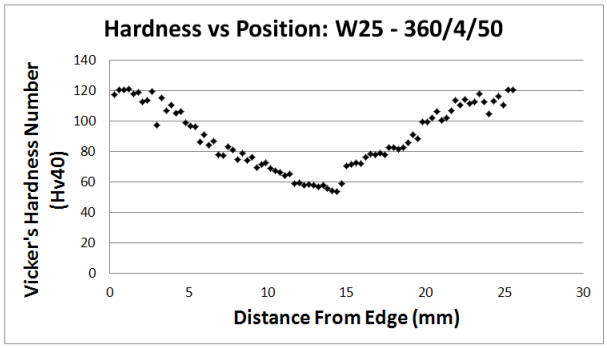
Hardness vs Position: W25 - 360/4/50
Vicker's Hardness Number (Hv40)
140
120
100
80
60
40
20
0
0
5
10
15
20
25
30
Distance From Edge (mm)

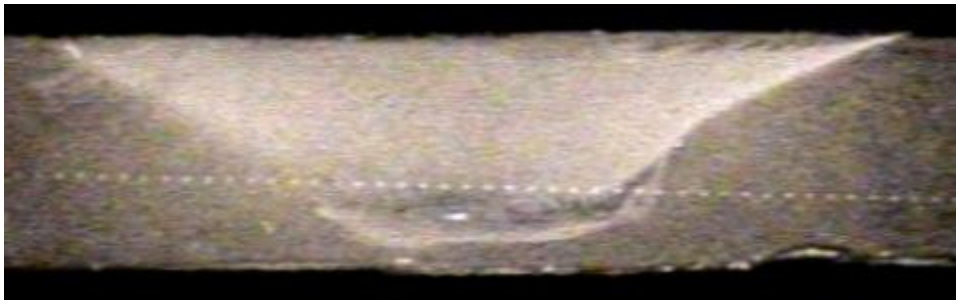

W26 – 380/4/50

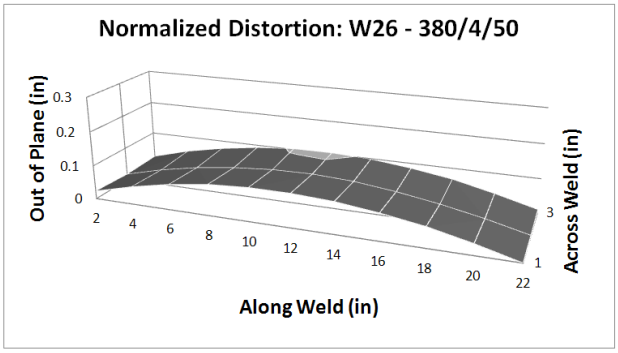
Normalized Distortion: W26 - 380/4/50
Out of Plane (in)
0.3
0.2
0.1
0
2
4
6
8
10
12
14
16
18
20
22
Along Weld (in)
1
3
Across Weld (in)

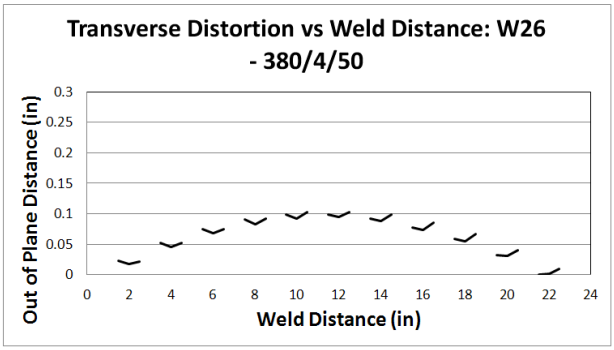
Transverse Distortion vs Weld Distance: W26 - 380/4/50
Out of Plane Distance (in)
0.3
0.25
0.2
0.15
0.1
0.05
0
0
2
4
6
8
10
12
14
16
18
20
22
24
Weld Distance (in)

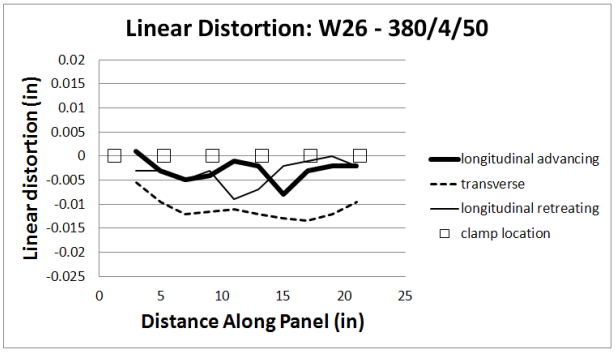
Linear Distortion: W26 - 380/4/50
Linear distortion (in)
0.02
0.015
0.01
0.005
0
-0.005
-0.01
-0.015
-0.02
-0.025
0
5
10
15
20
25
Distance Along Panel (in)
longitudinal advancing
transverse
longitudinal retreating
clamp location

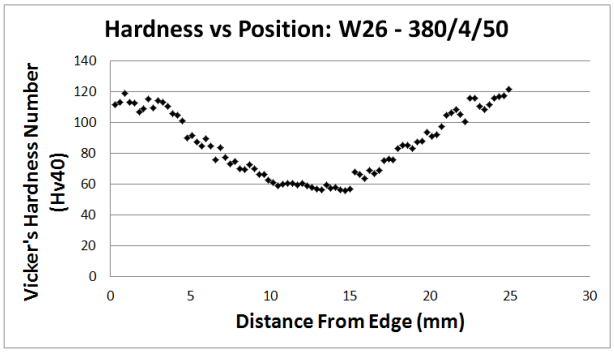
Hardness vs Position: W26 - 380/4/50
Vicker's Hardness Number (Hv40)
140
120
100
80
60
40
20
0
0
5
10
15
20
25
30
Distance From Edge (mm)

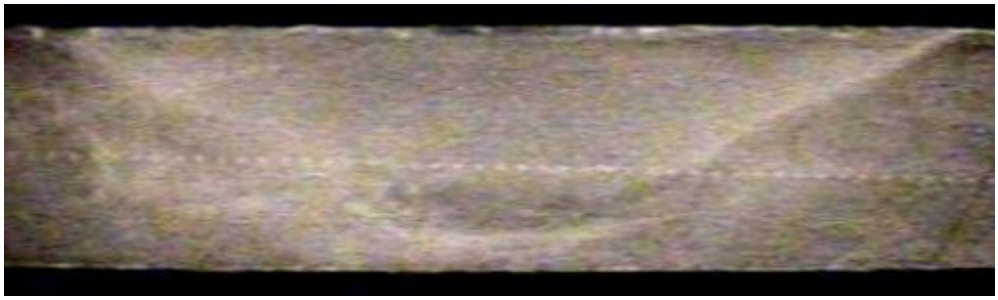

W27 – 380/8/75

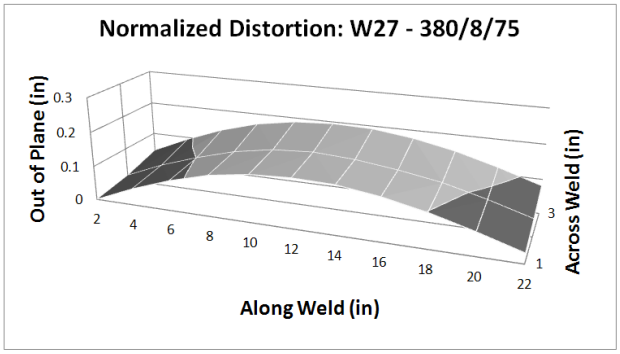
Normalized Distortion: W27 - 380/8/75
Out of Plane (in)
0.3
0.2
0.1
0
2
4
6
8
10
12
14
16
18
20
22
Along Weld (in)
1
3
Across Weld (in)

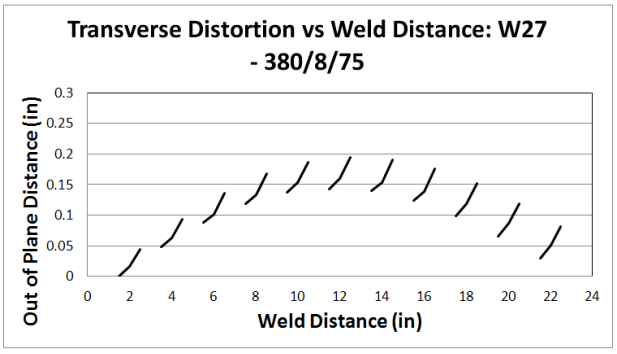
Transverse Distortion vs Weld Distance: W27 - 380/8/75
Out of Plane Distance (in)
0.3
0.25
0.2
0.15
0.1
0.05
0
0
2
4
6
8
10
12
14
16
18
20
22
24
Weld Distance (in)

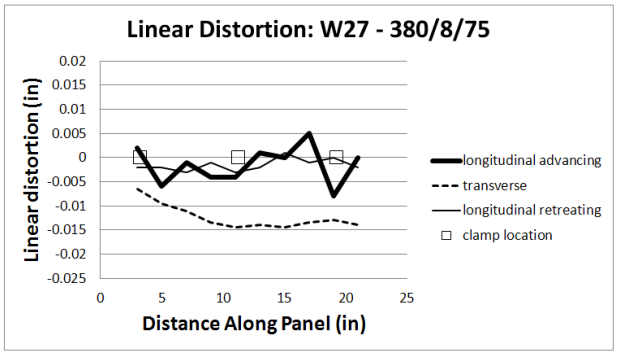
Linear Distortion: W27 - 380/8/75
Linear distortion (in)
0.02
0.015
0.01
0.005
0
-0.005
-0.01
-0.015
-0.02
-0.025
0
5
10
15
20
25
Distance Along Panel (in)
longitudinal advancing
transverse
longitudinal retreating
clamp location

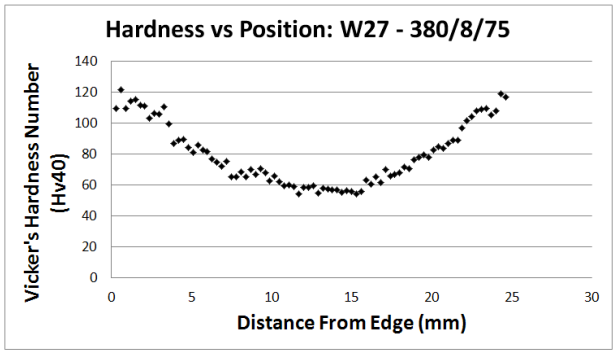
Hardness vs Position: W27 - 380/8/75
Vicker's Hardness Number (Hv40)
140
120
100
80
60
40
20
0
0
5
10
15
20
25
30
Distance From Edge (mm)

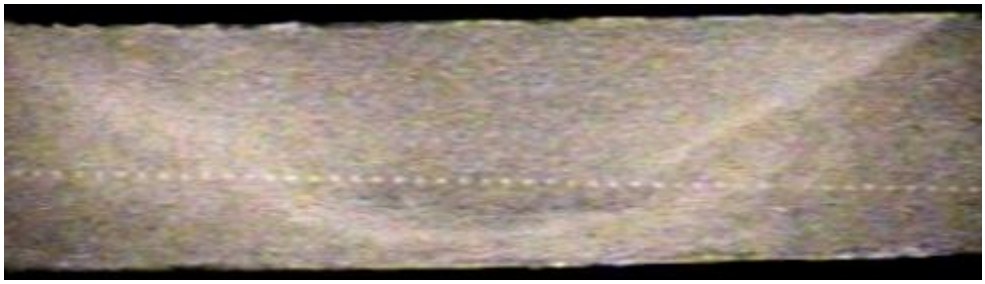

W28 – 340/8/75

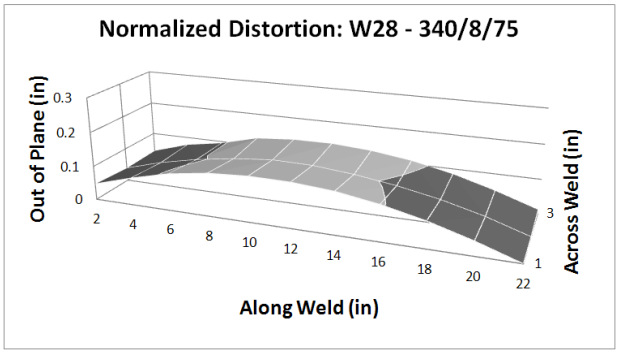
Normalized Distortion: W28 - 340/8/75
Out of Plane (in)
0.3
0.2
0.1
0
2
4
6
8
10
12
14
16
18
20
22
Along Weld (in)
1
3
Across Weld (in)

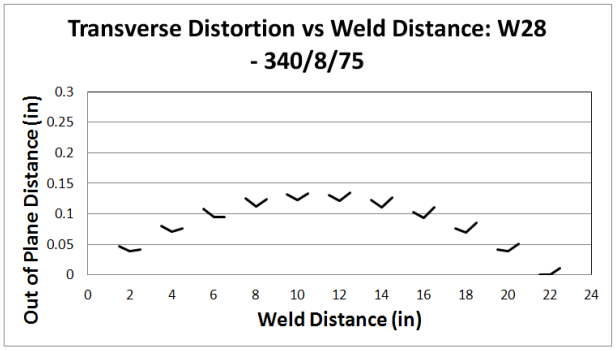
Transverse Distortion vs Weld Distance: W28 - 340/8/75
Out of Plane Distance (in)
0.3
0.25
0.2
0.15
0.1
0.05
0
0
2
4
6
8
10
12
14
16
18
20
22
24
Weld Distance (in)

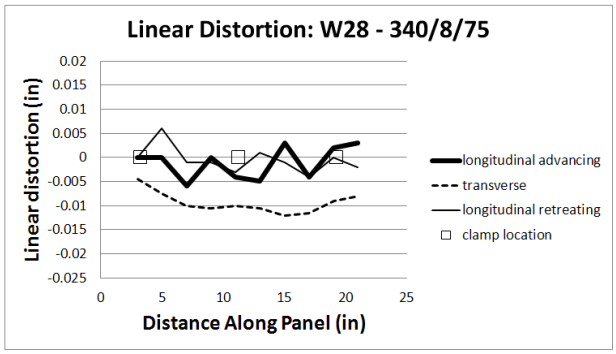
Linear Distortion: W28 - 340/8/75
Linear distortion (in)
0.02
0.015
0.01
0.005
0
-0.005
-0.01
-0.015
-0.02
-0.025
0
5
10
15
20
25
Distance Along Panel (in)
longitudinal advancing
transverse
longitudinal retreating
clamp location

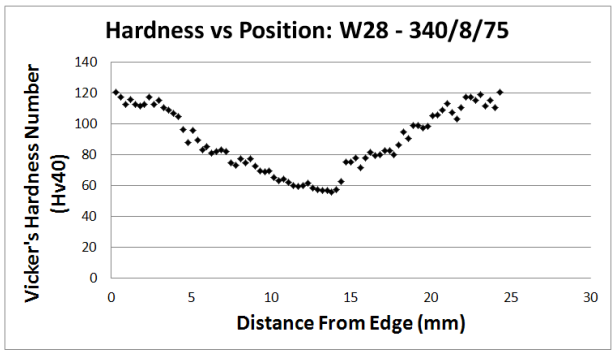
Hardness vs Position: W28 - 340/8/75
Vicker's Hardness Number (Hv40)
140
120
100
80
60
40
20
0
0
5
10
15
20
25
30
Distance From Edge (mm)

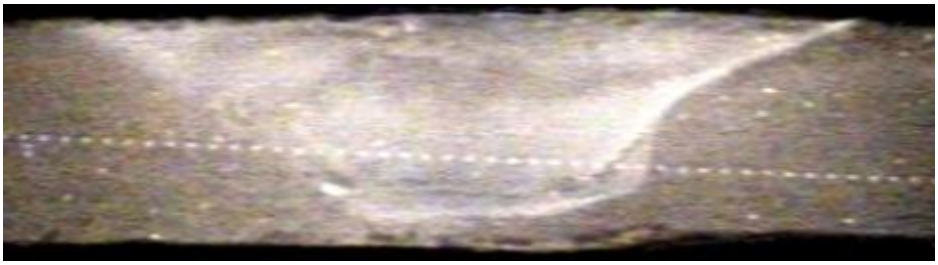

W29 – 380/2/75

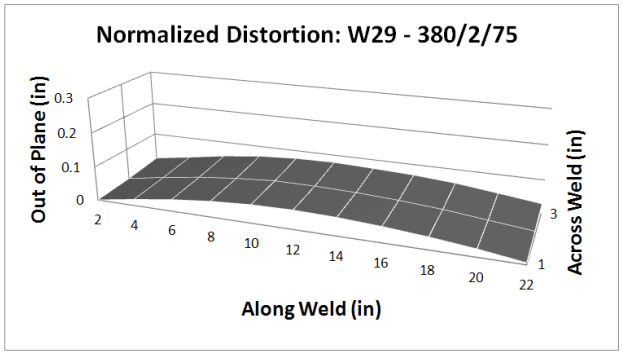
Normalized Distortion: W29 - 380/2/75
Out of Plane (in)
0.3
0.2
0.1
0
2
4
6
8
10
12
14
16
18
20
22
Along Weld (in)
1
3
Across Weld (in)

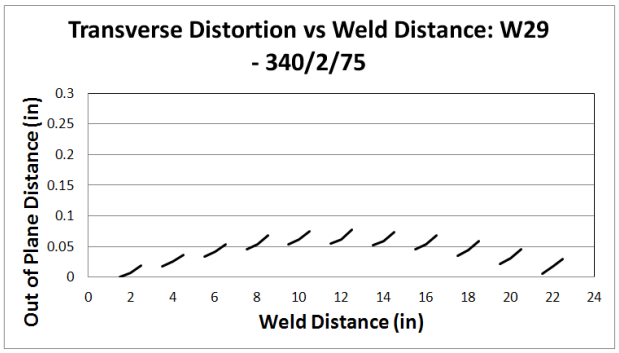
Transverse Distortion vs Weld Distance: W29 - 340/2/75
Out of Plane Distance (in)
0.3
0.25
0.2
0.15
0.1
0.05
0
0
2
4
6
8
10
12
14
16
18
20
22
24
Weld Distance (in)

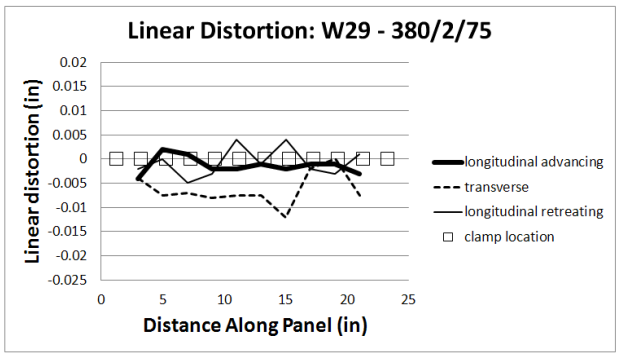
Linear Distortion: W29 - 380/2/75
Linear distortion (in)
0.02
0.015
0.01
0.005
0
-0.005
-0.01
-0.015
-0.02
-0.025
0
5
10
15
20
25
Distance Along Panel (in)
longitudinal advancing
transverse
longitudinal retreating
clamp location

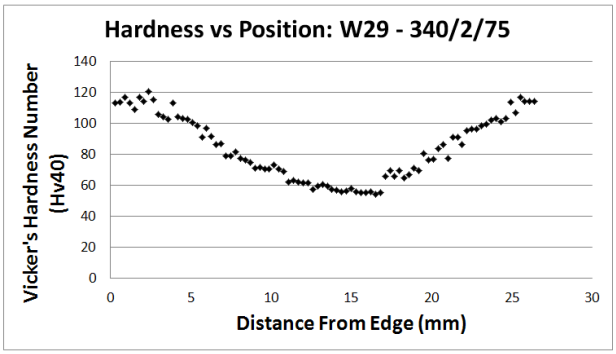
Hardness vs Position: W29 - 340/2/75
Vicker's Hardness Number (Hv40)
140
120
100
80
60
40
20
0
0
5
10
15
20
25
30
Distance From Edge (mm)

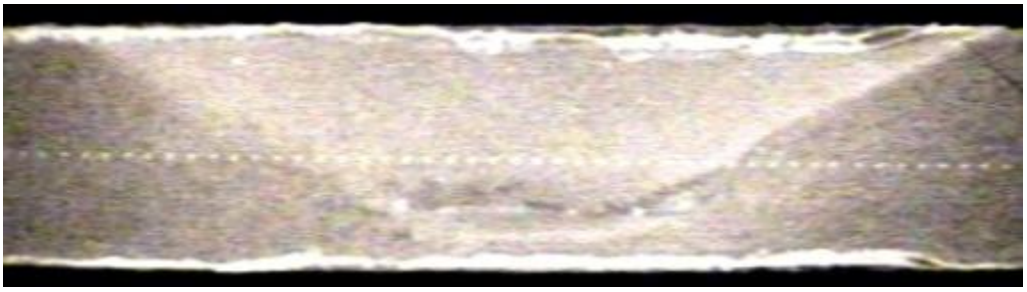

W30 – 380/2/25

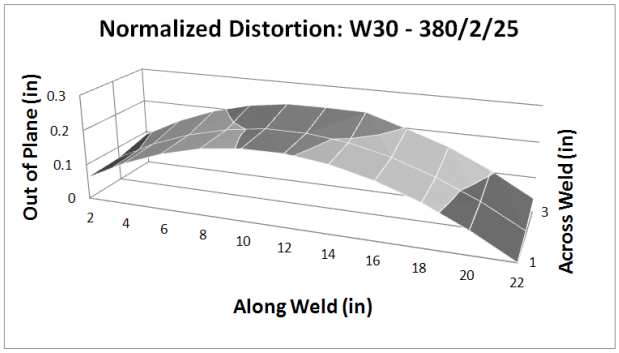
Normalized Distortion: W30 - 380/2/25
Out of Plane (in)
0.3
0.2
0.1
0
2
4
6
8
10
12
14
16
18
20
22
Along Weld (in)
1
3
Across Weld (in)

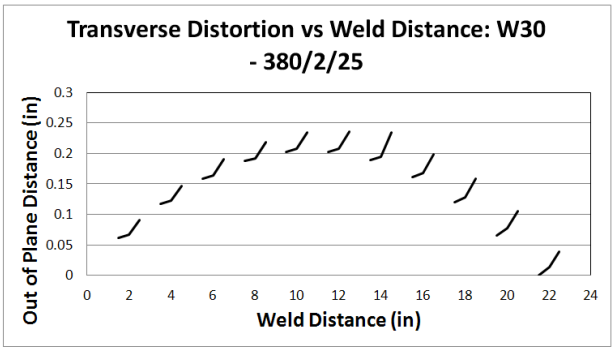
Transverse Distortion vs Weld Distance: W30 - 380/2/25
Out of Plane Distance (in)
0.3
0.25
0.2
0.15
0.1
0.05
0
0
2
4
6
8
10
12
14
16
18
20
22
24
Weld Distance (in)

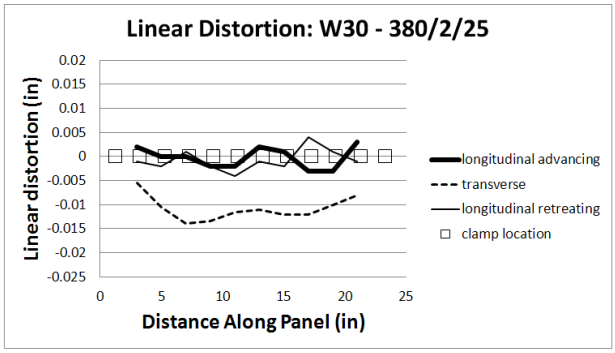
Linear Distortion: W30 - 380/2/25
Linear distortion (in)
0.02
0.015
0.01
0.005
0
-0.005
-0.01
-0.015
-0.02
-0.025
0
5
10
15
20
25
Distance Along Panel (in)
longitudinal advancing
transverse
longitudinal retreating
clamp location

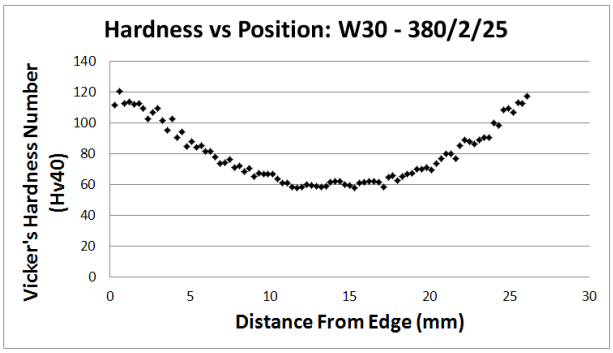
Hardness vs Position: W30 - 380/2/25
Vicker's Hardness Number (Hv40)
140
120
100
80
60
40
20
0
0
5
10
15
20
25
30
Distance From Edge (mm)

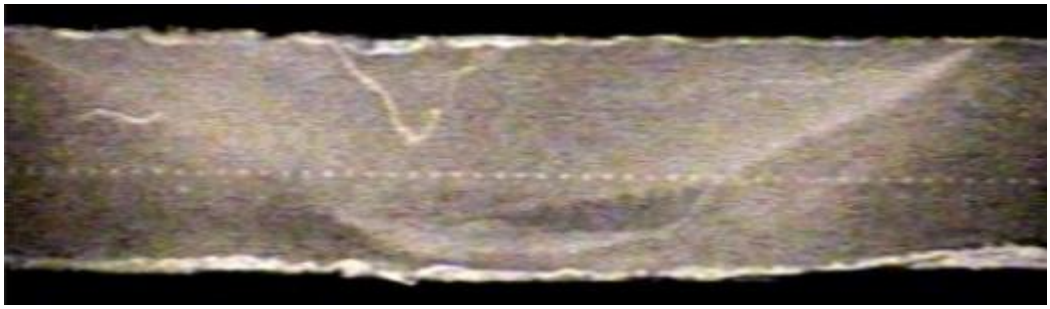

W31 – 380/8/25

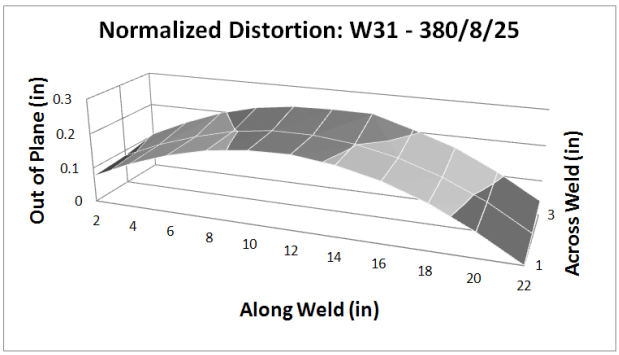

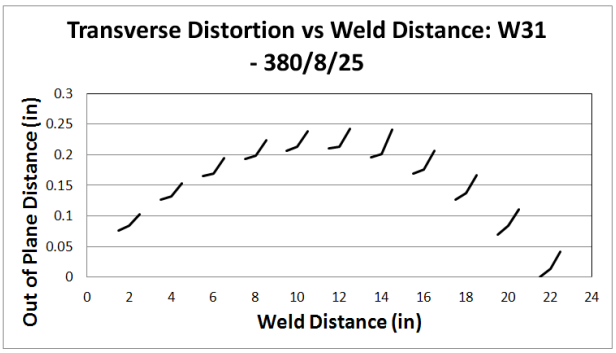

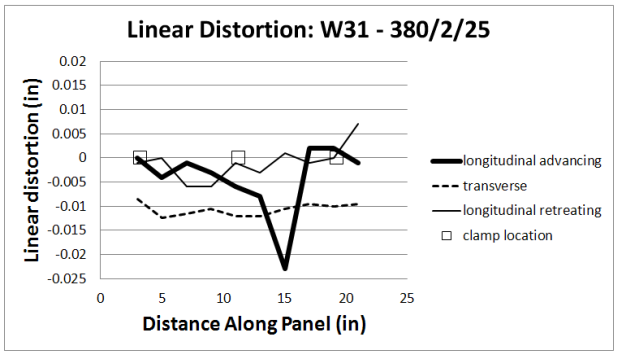

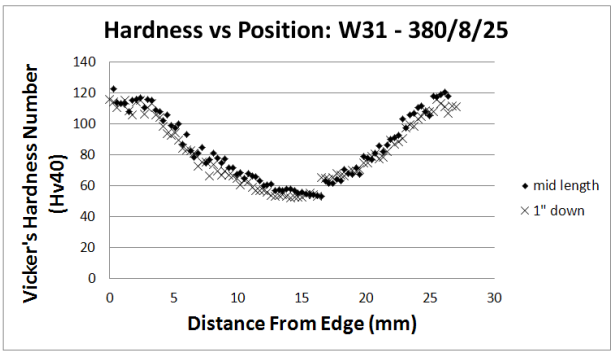

Mid Length:

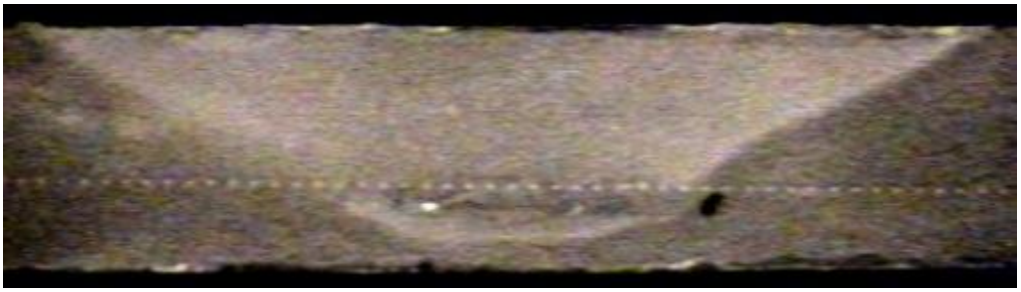

1" Down Weld:

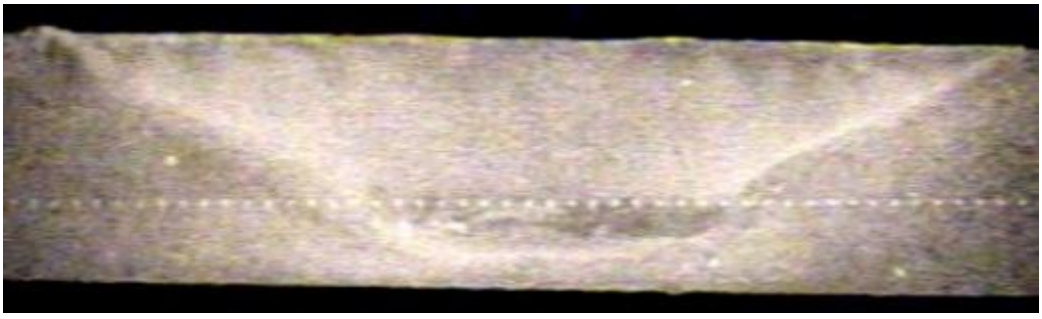

W32 – 360/8/50

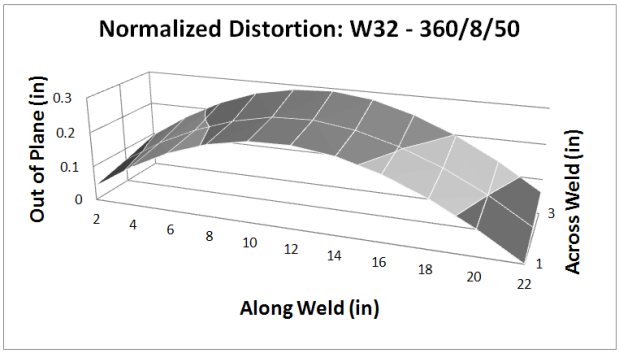
Normalized Distortion: W32 - 360/8/50
Out of Plane (in)
0.3
0.2
0.1
0
2
4
6
8
10
12
14
16
18
20
22
Along Weld (in)
1
3
Across Weld (in)

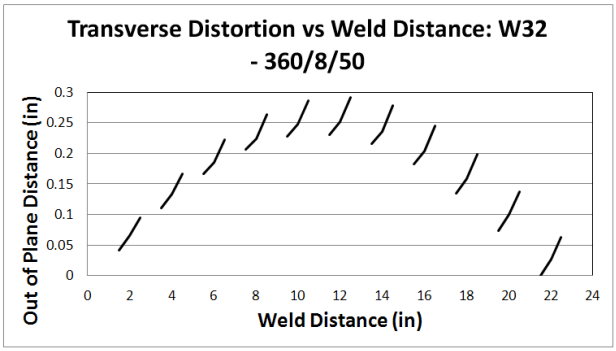
Transverse Distortion vs Weld Distance: W32 - 360/8/50
Out of Plane Distance (in)
0.3
0.25
0.2
0.15
0.1
0.05
0
0
2
4
6
8
10
12
14
16
18
20
22
24
Weld Distance (in)

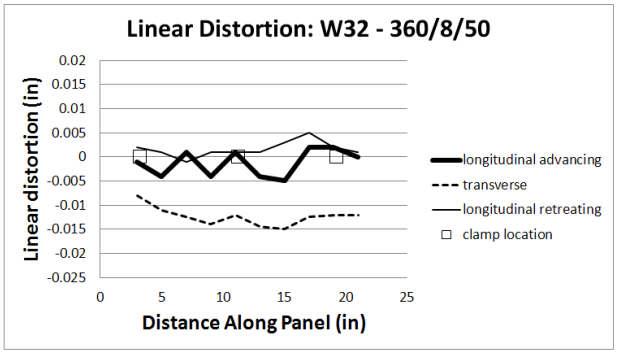
Linear Distortion: W32 - 360/8/50
Linear distortion (in)
0.02
0.015
0.01
0.005
0
-0.005
-0.01
-0.015
-0.02
-0.025
0
5
10
15
20
25
Distance Along Panel (in)
longitudinal advancing
transverse
longitudinal retreating
clamp location

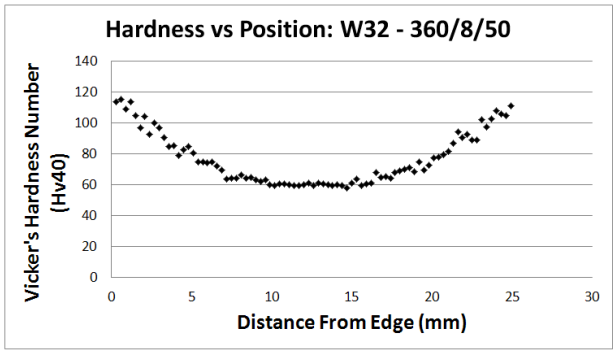
Hardness vs Position: W32 - 360/8/50
Vicker's Hardness Number (Hv40)
140
120
100
80
60
40
20
0
0
5
10
15
20
25
30
Distance From Edge (mm)

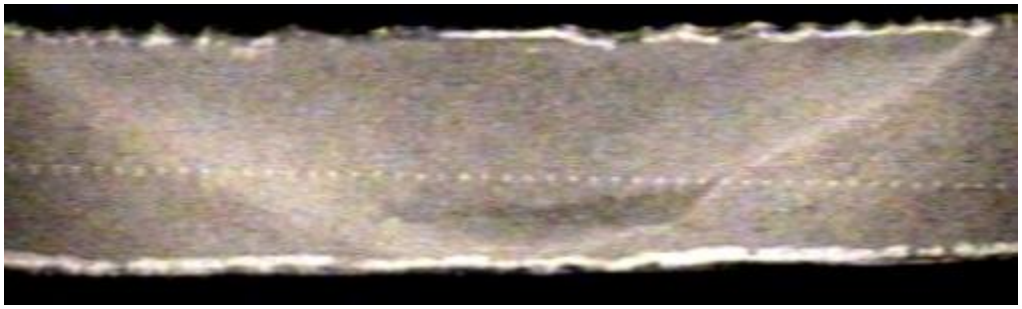

8.0 Vita

Travis Smith graduated from UC Berkeley in 2003 with a BS in chemical engineering. Since then he has worked for Lockheed Martin, most recently in the FSW research group.